Acta Universitatis Szegediensis

Acta Biologica Szegediensis

Volume 63,
Number 1,
2019

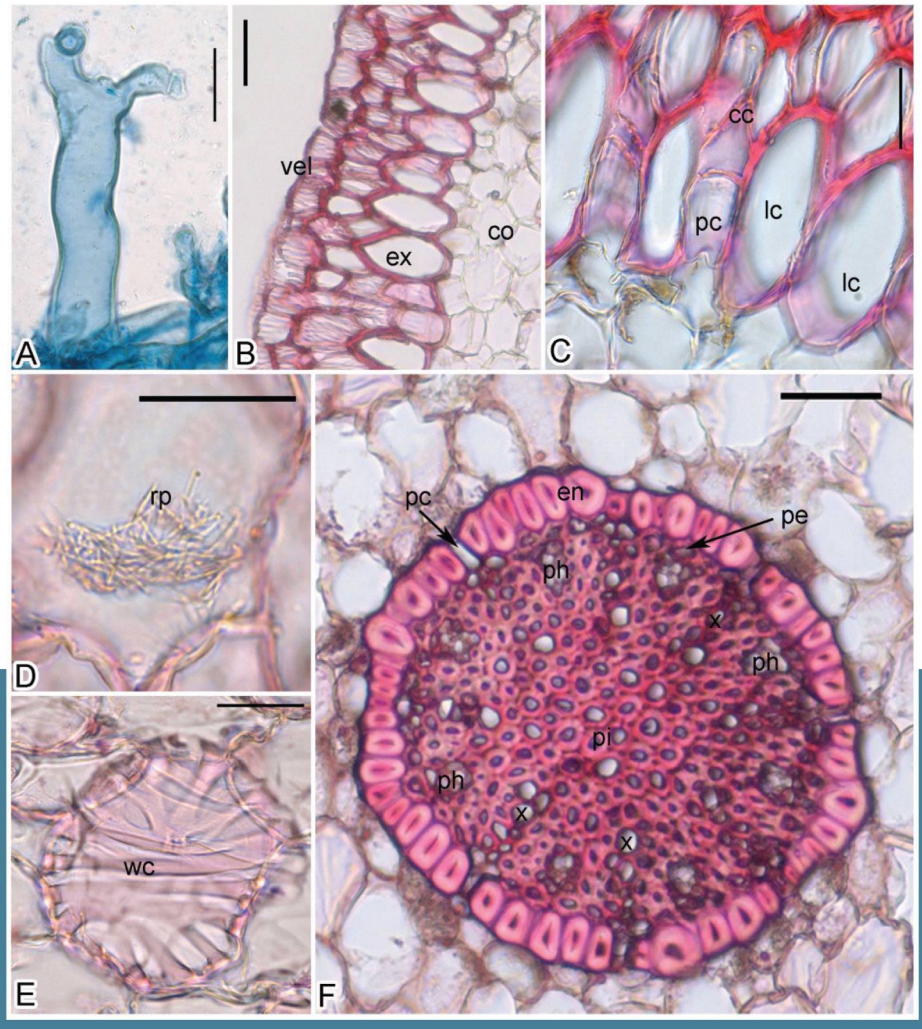

University of Szeged, Szeged, Hungary

http://abs.bibl.u-szeged.hu/index.php/abs

Acta Biologica Szegediensis

Volume 63(1):1-13, 2019
Acta Biologica Szegediensis
http://abs.bibl.u-szeged.hu/index.php/abs
DOI:10.14232/abs.2019.1.1-13

ARTICLE

Vegetative anatomy and mycorrhizal morphology of *Schoenorchis nivea* (Lindl.) Schltr., (Orchidaceae) and their adaptive significance

Mayakrishnan Balachandar*, Ravichandran Koshila Ravi, Kandhasamy Nagaraj, Thangavelu Muthukumar

Root and Soil Biology Laboratory, Department of Botany, Bharathiar University, Coimbatore 641 046, Tamilnadu, India

ABSTRACT The anatomical description of the vegetative parts (leaf, leaf sheath, stem and root) and mycorrhizal morphology of *Schoenorchis nivea* (Lindl.) Schltr., belonging to the subfamily Epidendroideae of Orchidaceae was investigated. Leaves were amphistomatic covered by 10-12 µm thick cuticle, stomata paracytic with small and irregular substomatal chambers. Mesophyll homogenous, composed of thin-walled chlorenchymatous cells. Banded water-storage cells abundant in the mesophyll and the largest vascular bundle occurred at the centre of the leaf. The leaf sheath has both adaxial and abaxial epidermis covered with cuticle, homogenous mesophyll, water-storage cells, raphides and vascular bundles. The stem is surrounded by a uniseriate epidermis, cortex consisting of thick-walled fibers and collateral vascular bundles scattered in the ground tissue. Cortical proliferation was evident in *S. nivea* stem. Root hairs present in root regions were in contact with the substratum. Root hairs frequently branched at their tips. Root possess 2-3 layered velamen, ∩-thickened exodermal cells, O-thickened uniseriate endodermis, and cortex of thin-walled parenchymatous cells containing raphides and water-storage cells. Cover cells present. Xylem arches are 9-11, with vascular tissues embedded in sclerenchymatous cells. Pith composed of thick-walled sclerenchymatous cells with intercellular space. The stomatal characteristics in leaf, the size of water-storage cells and vascular bundles exhibited significant variation in different plant parts. Intact and degenerating pelotons of orchid mycorrhizal fungi were observed in the root cortical cells. The observations of the present study clearly indicate that *S. nivea* possesses several anatomical adaptations to thrive in epiphytic habitats.

Acta Biol Szeged 63(1):1-13 (2019)

KEY WORDS
anatomical characteristics
cortical proliferation
orchid mycorrhiza
root hairs
stomata
water-storage cells

ARTICLE INFORMATION
Submitted
28 February 2019.
Accepted
3 May 2019
***Corresponding author**
E-mail: mbalachandar241055@gmail.com

Introduction

The plant family Orchidaceae with approximately 25000 species distributed in 780 genera is one among the largest plant families in angiosperms (Pridgeon et al. 2009). Orchids occur in a wide range of habitats with different life forms like terrestrial, epiphytes or lithophytes (Dearnaley 2012). Generally, epiphytic habitats are stressful due to the lack of substrate that can sufficiently hold moisture and provide nutrient essential for plant growth (Adhikari et al. 2012). Nevertheless, plant species belonging to different families have adopted several strategies to tolerate and thrive in the harsh epiphytic habitats. One such adaptation of the orchids to the epiphytic conditions is the development of multi-layered dead tissue covering the roots called velamen that helps in the acquisition and storage of water under limiting conditions (Benzing 2000).

Another unique characteristic of orchids is the mutualistic association with mycorrhizal fungi. Orchids, unlike other graminaceous members, are obligately mycorrhizal either throughout or part of their lifecycle. The dependence of orchids on mycorrhizal symbiosis arises from the fact that orchids produce minute seeds that have minimal or lack seed reserves (Arditti and Ghani 2000). Mycorrhizal fungi provide essential nutrients to the orchids from the soil or substrates needed for their growth (Smith and Read 2008, Nurfadilah et al. 2013). Orchid mycorrhiza is unique by the production of highly coiled fungal hyphal structures in the root cortical cells called pelotons. These pelotons enlarge the contact surface area between fungus and the cells, but are short-lived, senesce and collapse within the host cells (Smith and Read 2008). It is presumed that green orchids during their adult stage are less mycorrhizal dependent than during their earlier stages. However, this claim was refuted in many recent

studies where several mature green orchids were shown to adopt a mixotrophic mode of nutrition (Bertolini et al. 2014; Selosse and Martos 2014; Lallemand et al. 2019). Mycorrhizal morphology in roots of epiphytic orchids is not well studied than those of terrestrial forms despite more than 70% of orchids have an epiphytic life-form (Atwood 1986; Sathiyadash et al. 2012).

Commonly known as flea orchids, *Schoenorchis* belongs to the subtribe Aeridinae of tribe Vandeae, subfamily Epidendroideae of the plant family Orchidaceae. At present, there are 25 species of this genus distributed specifically in the subtropical and tropical Asia and the Western Pacific. In India, *Schoenorchis* is represented by five species of which *Schoenorchis nivea* (Lindl.) Schltr., is a small (up to 15 cm tall) epiphytic monopodial orchid distributed in peninsular India and Sri Lanka (Kumar and Sequiera 2000; Mathew and George 2015). Although *S. nivea* has no recorded economic importance, it is listed in the CITES Appendix II where trade on this species is stringently regulated to prevent utilization irreconcilable with its survival (Mathew and George 2015; ENVIS Centre on Floral Diversity 2019).

Anatomical investigations of orchids assist in resolving the problems related to the identification of plants in their vegetative stage (Kowsalya et al. 2017; Balachandar et al. 2019). Anatomy also helps to overcome the systematic problems and is a useful tool in the precise identification of plants in same genera sharing similar morphological characteristics (Kowsalya et al. 2017). Though detailed observation of vegetative anatomy of Aeridineae taxa like *Acampe*, *Amesiella*, *Chiloschista*, *Microtatorchis*, *Neofinetia*, *Phalaenopsis*, *Taeniophyllum*, *Trichoglottis*, and *Vanda* are available (Carlsward et al. 2006; Carlsward 2014; Kowsalya et al. 2017) the vegetative anatomy of members belonging to *Schoenorchis* are unknown except for a couple of studies involving foliar and nectary anatomical investigations (Stpiczyńska et al. 2011; Angela et al. 2015). The leaf anatomy of *Schoenorchis gemmata* (Lindl.) J. J. Sm., along with five other terete-leaved orchids was examined by Angela et al. (2015) to see if these orchids exhibited any xeromorphic characters. The leaves of *S. gemmata* were amphistomatic and the stomata were of a paracytic type. Moreover, the leaves were broadly V-shaped, cuticle ridged, adaxial cuticle thicker than the abaxial, presence of cuticular papillae, epidermal cells spherical to polygonal, presence of specialized water-storage cells with banded thickenings, small and large vascular bundles distributed together, and sclerenchymatous tissue covering both xylem and phloem. From these results, it was concluded that *S. gemmata* like all other terete-leaved orchids examined exhibited xeromorphic characters that were directed towards efficient use of water for survival in water stressed environments (Angela et al. 2015). A study on the anatomy of the nectary spurs in the entomophilous flowers of *S. gemmata* pollinated by hymenoptera indicated the absence of secretary trichomes, and a very short and saccate spurs with glabrous to a minutely papillose inner surface (Stpiczyńska et al. 2011).

As there is paucity of information on the anatomy of *Schoenorchis* in general we examined the anatomy of the vegetative structures of *S. nivea* growing in the Western Ghats region of southern India. Moreover, we also determined the various adaptive characters exhibited by *S. nivea* and recorded the extent of variation in similar structures occurring in different parts of the plant. In addition, the mycorrhizal morphology and the extent of mycorrhizal association were also studied in *S. nivea*.

Materials and method

Plant samples of *S. nivea* were collected during October 2018 from Indian Cardamom Research Institute campus (09°05′N and 77°09′E) located at the Myladumpara of Idukki district under Kerala state, peninsular India. The campus located at an altitude of 1050–1060 m a.s.l., spreads over an area of 64.60 ha with undulating terrain consisting of hills and valleys covered by lush evergreen forests (Balan and Harikrishnan 2017). This region is characterized by a cool and humid climate with an average maximum and minimum temperature of 25.70 °C and 17.05 °C, respectively. The hottest days occur during April-May and the coolest days occur between December-January. The relative humidity ranges from 90% to 96% and the average annual precipitation is 2153 mm. The rainfall data for 2007–2016 indicate that the amount of rainfall received consistently decline in the alternate years (Balan and Harikrishnan 2017). The floristic diversity of the site indicates the presence of 392 angiospermic taxa in 303 genera under 94 families consisting of both indigenous and naturalized flora. This angiospermic diversity also includes 15 orchids belonging to *Aerides*, *Bulbophyllum*, *Cottonia*, *Dendrobium*, *Disperis*, *Eria*, *Liparis*, *Luisia*, *Oberonia*, *Papilionanthe*, *Polystachya*, *Schoenorchis*, *Sirhookera*, *Thelasis* and *Trias* (Balan and Harikrishnan 2017).

Four mature plants of *S. nivea* were collected of which one plant was in late flowering phase. The specimen in flowering was used for authentication. The specimens were authenticated by the Botanical Survey of India, Southern Circle, Coimbatore, India and a voucher was deposited in the Bharati Herbarium, Department of Botany, Bharathiar University, Coimbatore, India (accession number: 007740). The plant samples were placed in an icebox and transported to the laboratory. In the lab, plants were washed thoroughly free of dirt and attached debris prior to sectioning. For uniformity, fully opened fourth

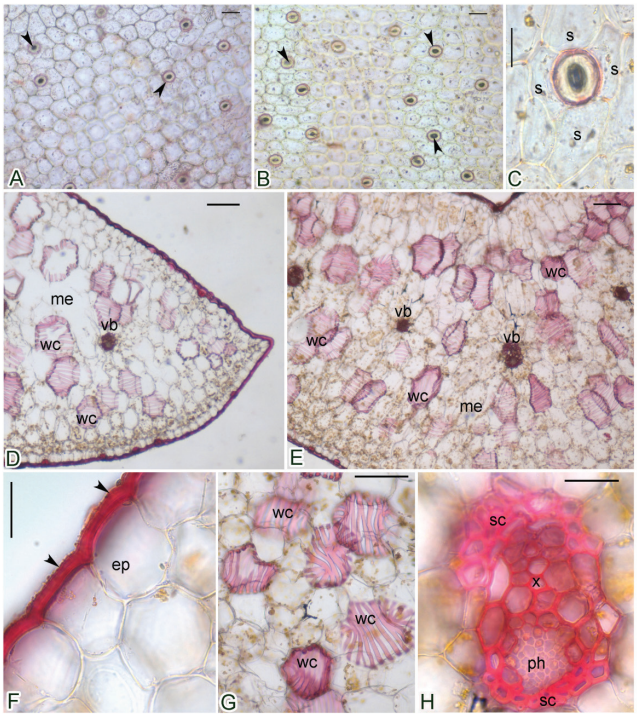

Figure 1. Leaf anatomy of *Schoenorchis nivea* (A,B) Epidermal peeling of leaf showing stomata (black arrow heads) on the adaxial (A) and abaxial (B) surface (C) stomata with guard cells and subsidiary cells; (D–E) cross section of leaf showing epidermis, mesophyll , vascular bundle and water- storage cells; (F) epidermis with cuticle (black arrow heads); (G) banded water-storage cells; (H) vascular bundle with phloem and xylem capped by sclerenchymatous cells.
ep = epidermis, me = mesophyll, ph = phloem, s = subsidiary cells, sc = sclerenchymatous cells, vb = vascular bundle, wc = water-storage cells, x = xylem. Scale bars = 50 µm (A, B, D, E, G) and 30 µm (C, F, H).

leaf from the tip, 1-cm stem or root from 3 cm below the shoot or root tip was used in the study. The transverse sections for histological observations were prepared by freehand sectioning (Lux et al. 2005). The sections of desired plant parts were made using smooth strokes with a sharp razor blade and transferred onto a drop of water on a microscopic slide. The water was later removed using a filter paper and various types of stains such as safranin, Iodine-Potassium iodide, Phloroglucinol-HCl, and Toludine Blue O were used for identifying cell inclusions and other compounds such as cutin, lignin, starch grains, and polysaccharides (Johanson 1940). For the observation of epidermal surface, 1 cm square leaf pieces were placed in Jeffrey's maceration solution for 72 hours at 35 °C (Kigkr 1971). The specimens were later washed, stained with safranin and examined under an Olympus BX51 light microscope (Olympus, Tokyo, Japan). Cellular details like the cuticle thickness, length and width of different types of cells, and vascular bundles were measured using a calibrated ocular micrometer. The stomatal index (SI %) was calculated by using the formula (S/S+E) × 100 according to Salisbury (1927) where S and E denote the number of stomata and epidermal cells. The stomatal type was determined according to Van Cotthem (1970).

For estimation of mycorrhizal colonization, the roots were cut into 1 cm long bits, cleared by boiling in 2.5% KOH at 100 °C for 60 minutes. The cleared roots were washed and treated with 5 N HCl for 30 minutes. The acidified roots were stained by placing them in trypan blue (0.05%, w/v) solution overnight (Koske and Gemma 1989). Squashes of stained root bits were prepared and observed for the presence orchid mycorrhizal fungal structures. McGonigle et al. (1990) magnified intersection method was used to calculate the percentage of total root length colonization and root length containing intact and degenerating pelotons. The pelotons were considered intact when the fungal hyphae were undamaged and degenerating when the hyphae were damaged or were a crumbling mass.

To determine the extent of variation in structures occurring in different plant parts we performed statistical analysis [t-test or Analysis of Variance (ANOVA)] using SPSS version 9.0 for windows (SPSS Inc., Chicago, USA). The data were examined for homogeneity prior to statistical analysis (Levene's test) and Post Hoc analysis (Duncan's Multiple Range Test) was performed when the Fishers values were found significant. Box plot analysis was performed for assessing the extent of mycorrhizal colonization. The values presented in tables as mean.

Results

Leaf

Leaves are fleshy and succulent. Stomata are of paracytic type observed on both the leaf surfaces with two subsidiary cells parallel to the guard cells (Fig. 1 A-C) The abaxial leaf surface had significantly more stomata (19-21 mm^{-2}) than the abaxial surface (42-47 mm^{-2}). The stomatal index (SI %) on the abaxial surface (8.62%) was significantly higher than the adaxial surface (5.51%). Similarly, the length and width of guard cells (0.87% and 18.92%) and stomatal pores (47.05% and 43.05%) were significantly greater on the adaxial surface than abaxial leaf surface (Table 1). Cuticle ridged, 10-12 µm thick, present on both adaxial and abaxial surfaces (Fig. 1D). The thickness of the cuticle was 11.59% higher on the adaxial than the abaxial surface. Cells of adaxial and abaxial epidermis were compactly arranged. Cell wall on the outer tangential surface much thicker than the other walls. The epidermal cells on the adaxial surface were 25.03% longer and 27.77% wider respectively when compared to the abaxial

surface of the leaf (Table 1). Substomatal chambers small and irregular. Hypodermis and fiber bundles absent. Mesophyll cells: homogenous, chlorenchymatous, and composed of thin-walled, elongated to oval-shaped cells (Fig. 1D-E). Banded water-storage cells present in the mesophyll (Fig. 1G). Bundle sheath indistinct. Vascular bundles oriented towards the upper epidermis. Largest vascular bundle present in the centre of the leaf. Xylem and phloem are covered by sclerenchymatous cells (Fig. 1H). The walls of sclerenchymatous cells enclosing the phloem tissues are more thickened than those enclosing the xylem. Stegmata absent in the sclerenchyma cells of the xylem and phloem poles.

Table 1. Cell dimensions in transverse section of *Schoenorchis nivea* leaf and leaf sheath.

Variables	Leaf (L)	Leaf sheath (LS)
Stomata number (mm^2)		
Adaxial	21.76 ± 1.52	--
Abaxial	47.06 ± 1.37	--
Guard cell (adaxial) (µm)		
Length	37.67 ± 0.17	--
Width	9.67 ± 0.33	--
Guard cell (abaxial) (µm)		
Length	38.00 ± 0.50	--
Width	11.50 ± 0.41	--
Stomatal pore length (µm)		
Adaxial	17.00 ± 0.27	--
Abaxial	13.17 ± 0.30	--
Stomatal pore width (µm)		
Adaxial	9.00 ± 0.48	--
Abaxial	7.50 ± 0.42	--
Cuticle thickness (µm)		
Adaxial	12.25 ±0.51	8.58 ± 0.23
Abaxial	10.83 ± 0.64	19.17 ± 0.78
Epidermis (adaxial) (µm)		
Cell Length	53.25 ± 1.19	16.67 ± 0.77
Cell Width	51.92 ± 1.56	33.50 ± 1.25
Epidermis (abaxial) (µm)		
Cell length	39.92 ± 0.62	47.33 ± 1.09
Cell width	37.50 ± 1.35	46.00 ± 0.88
Mesophyll (µm)		
Cell length	135.42 ± 5.60	42.83 ± 1.02
Cell width	76.58 ± 2.27	59.92 ± 1.46
Water-storage cell (µm)		
Length	168.25 ± 6.60	39.42 ± 0.84
Width	127.00 ± 3.77	99.33 ± 4.24
Vascular bundle (µm)		
Length	99.50 ± 5.22	98.67 ± 2.93
Width	69.00 ± 3.09	87.08 ± 3.67
Vascular bundle (No. per L/LS)	9.13 ± 0.83	11.40 ±0.21

Leaf sheath

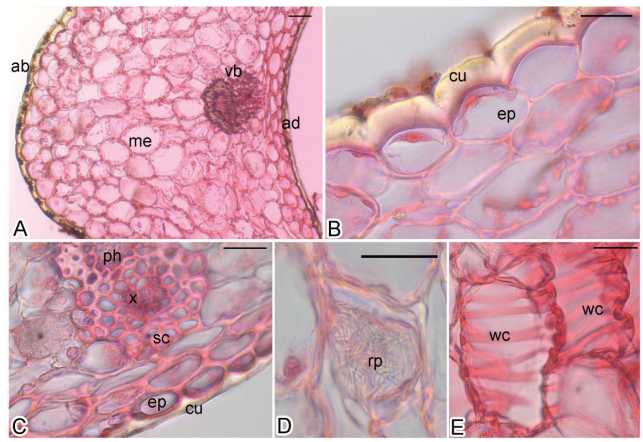

Figure 2. Leaf sheath anatomy of *Schoenorchis nivea* (A) cross section of leaf sheath showing adaxial and abaxial epidermis, mesophyll and vascular bundle; (B) epidermis with thick cuticle on the abaxial side; (C) epidermis and cuticle on the adaxial side and vascular bundle with phloem and xylem capped by sclerenchymatous cells; (D) raphides present in the mesophyll cell; (E) water-storage cell with banded thickening.
ab = abaxial, ad = adaxial, cu =cuticle, ep = epidermis, ep = epidermis, me = mesophyll, ph = phloem, rp = raphides, sc = sclerenchymatous cells, vb = vascular bundle, wc = water-storage cell, x = xylem. Scale bars = 50 µm (A) and 30 µm (B–E).

Stomata absent. Cuticle present on both adaxial and abaxial surfaces. Cuticle heavily ridged along the contours and is twice more thickened on the abaxial side when compared to the adaxial surface (Table 1). Adaxial epidermis uniseriate, compactly arranged with thick-walled rectangular cells. Abaxial epidermis single layered, composed of thin-walled round to oval-shaped cells (Fig. 2A, B). Both radial and tangential walls of the adaxial epidermal cells are much thicker than those on the abaxial side of the leaf sheath. The dimension including length (64.53%) and width (27.17%) of the abaxial epidermal cell is significantly larger than the adaxial epidermis (Table 1). Hypodermis absent. Mesophyll undifferentiated into palisade and spongy parenchyma, chlorenchymatous. Mesophyll cells are periclinally oriented, smaller and compactly arranged towards the adaxial surface. Idioblasts containing raphides and banded water-storage cells are present in the mesophyll (Fig. 2D, E). Vascular bundles oriented towards the adaxial surface. Xylem and phloem tissues are surrounded by sclerenchymatous cells. The phloem tissue is covered by thickened sclerenchymatous cells (Fig. 2C).

Stem

Stem consists of cuticle, epidermis, cortex, ground tissue containing vascular bundles (Fig. 3A). Stem circular in shape and covered by cuticle of 10-13 µm thickness (Table

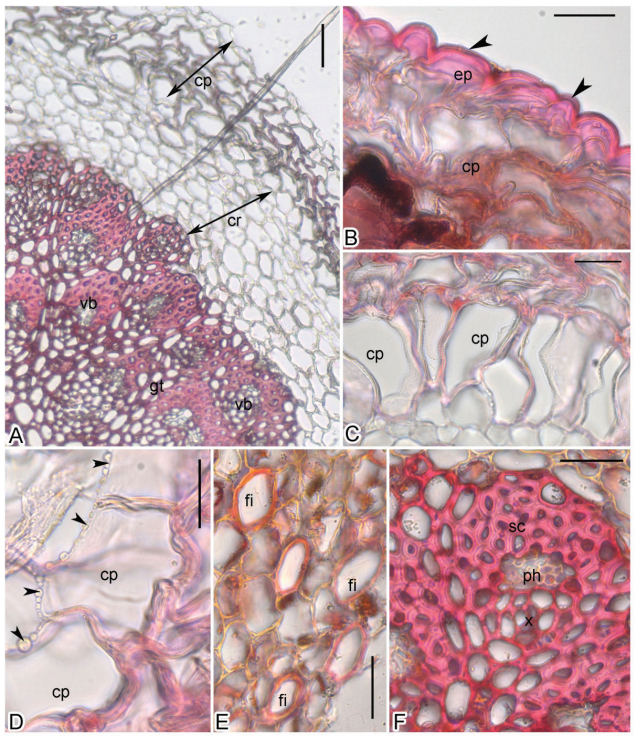

Figure 3. Stem anatomy of *Schoenorchis nivea* (A) transverse section of stem showing cortical proliferation, cortex and vascular bundle embedded in ground tissue; (B) epidermis covered by cuticle (black arrow heads) and cortical proliferation; (C) elongated cortical cells during cortical proliferation; (D) vesicles (black arrow heads) arranged close to the expanding cortical cell walls in cortical proliferation; (E) fibers in the cortical region; (F) vascular bundle with phloem and xylem capped by sclerenchymatous tissue .
cp = cortical proliferation, cr =cortex, ep = epidermis, fi = fibers, gt = ground tissue, ph = phloem; sc = sclerenchymatous cell, vb = vascular bundle, x = xylem. Scale bars = 50 µm (A), 30 µm (B-F).

2). Epidermis single layered, consisting of compactly arranged parenchymatous cells (Fig. 3B). Cortex subtending the epidermis is 6-9 layered and composed of thin-walled parenchymatous cells. Thick-walled fibers are present in the cortex (Fig. 3E). This region is characterized by the absence of vascular bundles. Ground tissue: comprising of circular to angular, thick-walled sclerenchymatous cells enclosing triangular intercellular air spaces. Cortical proliferation is evident during the process of stem thickening (Fig. 3B-D). The outer most cells of the cortical region expand radially which is later on followed by tangential expansion. During the cortical proliferation, small vesicle-like structures are formed which could help in lignifications (Fig. 3D). The cell walls of expanding cells get isolated from the primary cortical cells and buckles up providing thickness to the stem. Vascular bundles are collateral and scattered in the ground tissue. Larger vascular bundles are present at the central portion and smaller ones are oriented towards the peripheral region of the ground tissue. Xylem and phloem tissues are enclosed by thick-walled sclerenchymatous tissues (Fig. 3F).

Table 2. Cell dimensions in transverse section of *Schoenorchis nivea* stem.

Variables	Measurements (µm)
Cuticle thickening	13.17 ± 0.27
Epidermis	
Cell length	19.83 ± 0.87
Cell width	17.33 ± 0.75
Hypodermis	
Cell length	31.08 ± 1.05
Cell width	32.58 ± 0.99
Ground tissue	
Cell length	26.42 ± 0.99
Cell width	25.67 ± 1.31
Vascular bundle	
length	95.75 ± 2.37
width	80.17 ± 2.02

Root

Roots are mostly attached to the substratum. Circular in outline when aerial and the region attached to the substratum is not much flattened. Root hairs present in the portions of the roots that were in contact with the substratum. Root hairs are frequently branched at their tips (Fig. 4A). Velamen: 2-3 layered, differentiated into exovelamen and endovelamen. The cells of both exovelamen and endovelamen possess striations and both the radial as well as the tangential walls are thicker (Fig. 4B). The cells of endovelamen are longer when compared to exovelamen whereas; the exovelamen cells were wider than those of endovelamen (Table 3). Exodermis: Uniseriate, dimorphic and ∩-thickened and composed of both long and short cells. Long-cells of exodermis are thick-walled. Thin-walled short passage cells are present in-between the long exodermal cells (Fig. 4C). Tilosomes absent. Cover cells present above the passage cells. Cortex is 6-8 layered and composed of thin-walled parenchymatous cells (Fig. 4B). Raphides and water-storage cells are abundant in the cortex (Fig. 4D, E). Endodermis is O-thickened and present opposite to the phloem tissue and interrupted by thin-walled passage cells oriented opposite to the xylem. Pericycle located opposite to the xylem is thin-walled and thick-walled pericycle is oriented opposite to the phloem. Xylem and phloem elements are embedded in sclerenchymatous tissues. Pith consists of thick-walled cells with intercellular space of varied shapes (Fig. 4F).

Table 3. Cell dimensions in transverse section of *Schoenorchis nivea* root.

Variables	Measurements (µm)
Root hair	
Length	146.17 ± 5.34
Width	47.92 ± 1.41
Exovelamen	
Cell length	29.25 ± 1.09
Cell width	30.33 ± 1.03
Endovelamen	
Cell length	50.25 ± 1.68
Cell width	23.67 ± 0.65
Exodermis	
Cell length	54.67 ± 1.97
Cell width	33.42 ± 1.19
Cortex	
Cell length	53.50 ± 2.68
Cell width	45.50 ± 1.29
Water cell	
Length	97.42 ± 2.84
Width	68.50 ± 2.46
Endodermis	
Cell length	26.00 ± 0.68
Cell width	20.00 ± 0.74
Passage cell	
Length	15.75 ± 0.71
Width	10.08 ± 0.46
Meta xylem	
Cell length	13.50 ± 0.23
Cell width	12.50 ± 0.24
Phloem patch	
Length	24.08 ± 0.53
Width	13.08 ± 0.57
Pith	
Cell length	15.08 ± 0.58
Cell width	14.50 ± 0.57

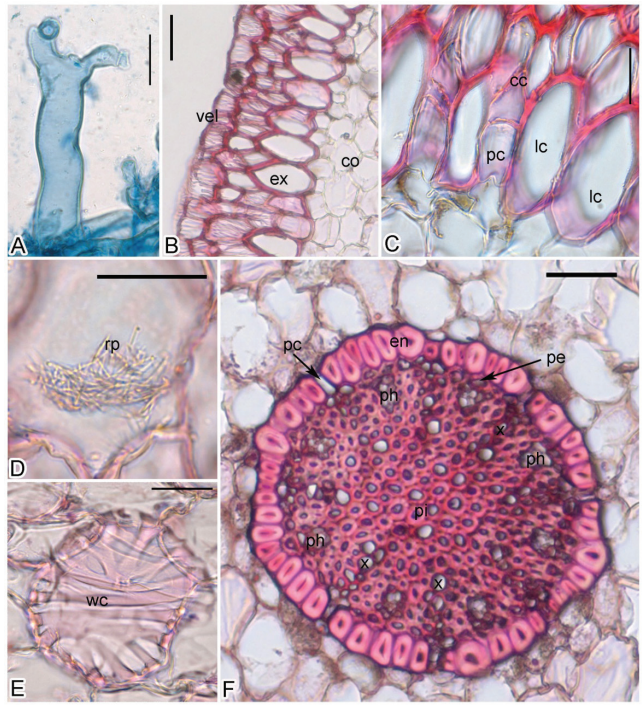

Figure 4. Root anatomy of *Schoenorchis nivea* (A) branched root hair; (B) transverse section of root showing velamen, exodermis and cortex; (C) exodermis long cell, cover cell and passage cell; (D) raphides in cortical cell; (E) banded water-storage cell; (F) stele showing O- thickened endodermis, thin-walled passage cell, pericycle, phloem, xylem, and thick-walled pith.
cc = cover cell, co = cortex, en = endodermis, ex = exodermis, lc = long cell, pc = passage cell; pe = pericycle, ph = phloem, pi = pith, rp = raphides, vel = velamen, wc = water-storage cell, x = xylem. Scale bars = 50 µm (B, F) and 30 µm (A, C-E).

Mycorrhizal morphology and extent of colonization

Mycorrhizal colonization was observed in the roots that were attached to the substrate. The fungal hyphae entered the roots through the root hairs and transacted through the velamen and the passage cells of the exodermis into the cortex (Fig. 5A, B). Regularly septate hyphae, hyphal coils, microsclerotia and moniliform cells were observed in the velamen tissue (Fig. 5C, F). Both intact and degenerating pelotons were present in the root cortical cells (Fig. 5D, E). The proportion of root length with degeneration pelotons was several folds higher than the root length with intact pelotons (Fig. 6). Root infection by nematodes was occasionally seen (Fig. 5G). Nevertheless, no distortion or damage was visible in roots containing nematodes.

The orchid mycorrhizal fungal structures including intact pelotons and degenerating pelotons varied significantly ($F_{2,8} = 72.756$; $P < 0.001$) in *S. nivea*. The percentage of root length colonization with degenerating pelotons was higher than the percentage of root length colonization with intact pelotons. The percentage of total root length colonization was 50.15% (Fig. 6).

Comparison of common structures in plant parts

The stomatal characteristics including the width of the guard cell, size of the stomatal pore and the number of stomata were significantly different on both adaxial and abaxial surface of the leaf except for guard cell length. The cell dimension of epidermal cells, cuticle thickening, number and width of vascular bundles on adaxial and abaxial surfaces had significant variation between leaf and leaf sheath except for the length of vascular bundles (Table 4). Similarly, the size of the water-storage cells and width of the vascular bundles also exhibited significant variation except for the length of the vascular bundles

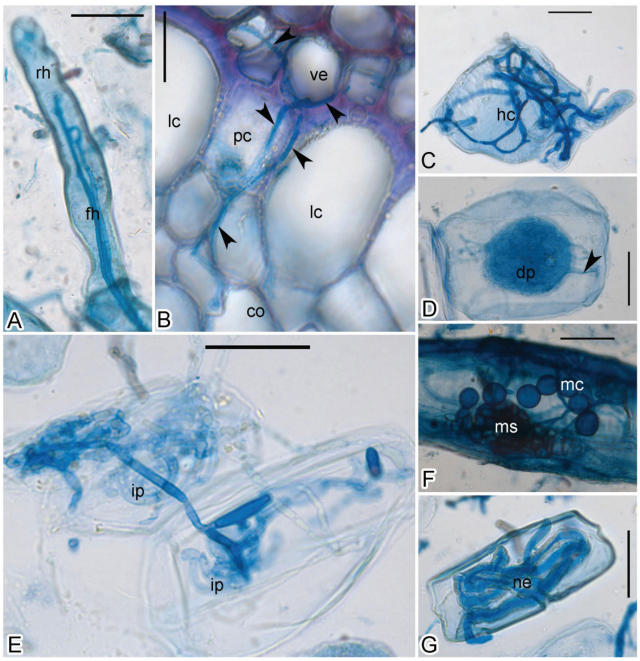

Figure 5. Mycorrhizal morphology of *Schoenorchis nivea* root. (A) fungal hyphae within root hair; (B) fungal hyphae (black arrow heads) traversing the velamen into the cortex through the passage cell of the exodermis; (C) hyphal coil in velamen cell; (D) degenerating peloton with hyphal remnants (black arrow head); (E) intact pelotons in cortical cells; (F) moniliform cells and microsclerotia; (G) nematode in cortical cell. co = cortex, dp = degenerating peloton, fh = fungal hyphae, hc = hyphal coil, ip = intact pelotons, lc = long cell, mc = moniliform cells, ms = microsclerotia, ne = nematode, pc = passage cell, rh = root hair, ve = velamen. Scale bars = 50 µm (B) and 30 µm (A, C–F).

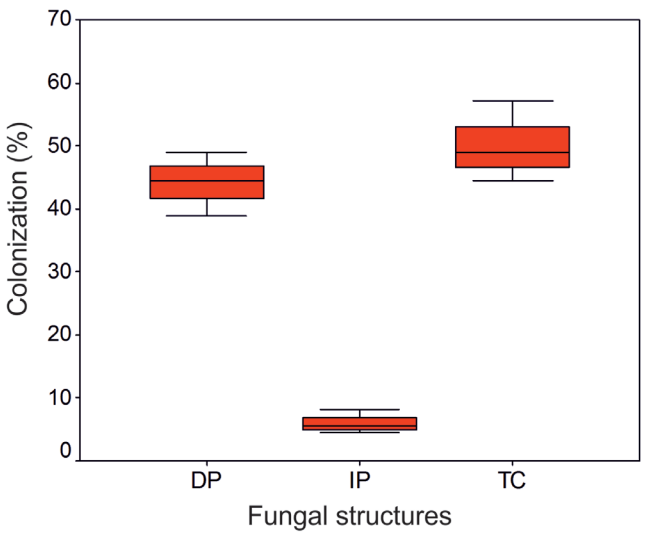

Figure 6. Box plots showing the distribution of total mycorrhizal colonization (TC) and root length with degenerating (DP) and intact (IP) pelotons in *Schoenorchis nivea* root.

Table 4. Comparison of stomata, epidermis and cuticle characteristics using student's t-test.

Stomata (adaxial and abaxial)			
Variables	**t-value**	**df**	**Significance (2-tailed)**
Guard cell			
Length	-0.695	14	0.499
Width	-3.556	14	0.003
Stomata pore			
Length	11.500	14	0.001
Width	2.806	14	0.014
Stomata number	-21.767	14	0.001
Stomatal index (%)	9.953	14	0.001
Leaf and Leaf sheath			
Upper epidermis			
Cell length	-7.891	29	0.001
Cell width	28.039	29	0.001
Lower epidermis			
Cell length	-5.877	29	0.001
Cell width	9.062	29	0.001
Cuticle thickening			
Lower side	-8.118	29	0.001
Upper side	6.279	29	0.001
Vascular bundle			
Length	0.141	29	0.889
Width	-3.935	29	0.001
Number	-2.639	14	0.019

among plant parts (Table 5). A three-way ANOVA involving cuticle thickness, length and breadth of cells (cell dimension) of adaxial and abaxial surfaces (sides) of leaf and leaf sheath (plant parts) indicated a significant variation among these variables (Table 6). In addition, the two-way and three-way interactions among these factors were also highly significant.

Discussion

Schoenorchis nivea exhibited several adaptive characteristics to thrive in the harsh epiphytic habitats. Cuticle, the key barrier between the comparable dry atmosphere and the hydrated aerial parts of plants covered all the airy parts of *S. nivea*. Cuticular thickness covering the leaves can substantially vary among plant species in spite of environmental influence on this anatomical trait (Zhong et al. 2018). This is clearly evident in the present study where the cuticle covering the adaxial and abaxial surfaces of the leaves in *S. nivea* were respectively 9.26% and 8.96% thinner those of *S. gemmata* examined from Tamenglong, Manipur, India (Angela et al. 2015). The altitudes and temperature ranges of Myladumpara, Kerala and Tamenglong, Mani-

Table 5. Characteristics of water-storage cells and vascular bundle in different parts of *Schoenorchis nivea*.

Plant organs	Water-storage cell (µm)		Vascular bundle (µm)	
	Length	Width	Length	Width
Leaf	168.25 ± 6.59a	127.00 ± 3.77a	99.50 ± 5.22a	69.0 0 ± 3.09a
Leaf sheath	39.42 ± 0.83c	99.33 ± 4.23b	98.67 ± 2.92a	87.08 ± 3.67b
Stem	-	-	95.75 ± 2.37a	80.17 ± 2.02b
Root	97.42 ± 2.84b	68.50 ±2.45c	-	-
df- 29	238.793***	67.226***	0.281ns	9.214***

Means ± S.E., in a row followed by a same letter(s) are not significantly (P > 0.05) different according to Duncan's Multiple Range Test.
*** significant at 0.01%, ns- not significant

pur are almost similar except for Tamenglong receiving twice the average rainfall of Myladumpara. Moreover, the cuticle in *Schoenorchis* is several times thicker than those reported for other epiphytic orchids like *Ascochilus*, *Bulbophyllum*, *Epidendrum*, *Dendrobium*, *Thrixspermum* and *Vanda* (Yang et al. 2016; Kowsalya et al. 2017; Muthukumar and Shenbagam 2017, 2018; Rindyastuti et al. 2018). The cuticle is a hydrophobic covering made up of cutin and solvent soluble cuticular waxes. This covering plays an important role in effectively controlling the loss of water from the cell interior, protects against radiation and biotic stresses (Mill and Stark Schilling 2009; Hen-Avivi et al. 2014). In addition, cuticle development has been shown to be closely related to cell patterning and organ development (Shi et al. 2013). According to Haworth and McElwain (2008), the occurrence of cuticle on the leaf surface is an indication of aridity. The thick cuticle on *S. nivea* aerial parts prevents water loss and improves the efficiency of water when it is scarce (Guan et al. 2011). Yang et al. (2016) also suggested that the presence of thick cuticle is one of the strategies adopted by epiphytic orchids to maintain the water balance. In the present study, the cuticle was thickest on the abaxial surface of the leaf sheath which was 56.49% and 77.01% thicker than the cuticle covering the adaxial and abaxial surface of the leaves respectively and 45.56% thicker than those covering the stem. Some of the leaf anatomical characters *S. nivea* shares with *S. gemmata* include paracytic stomata, water-storage cells with banded thickenings, and fibrous caps bordering xylem and phloem. However, cuticle papillae, conjunct vascular bundles, and cuticularized guard cells reported in leaves of *S. gemmata* was absent in *S. nivea* (Angela et al. 2015). Similarly, the absence of hypodermis and fiber bundles, homogenous mesophyll and sclerenchymatous caps bordering xylem and phloem resembles the leaves of Vandeae members. However, *S. nivea* differs from other Vandean taxa in amphistomatous condition and absence of glandular hairs, distinct bundle sheath, and stegmata associated with the vascular tissue (Carlsward et al. 2006).

Table 6. F-values from three-way ANOVA for epidermis cell length, width and cuticle thickening in both sides of S*choenorchis nivea* leaf and leaf sheath. Numerator and denomenator difference is presented as subscripts in paranthesis.

Source	*F*-value
Plant parts$_{(1,348)}$	102.990***
Surface$_{(1,348)}$	597.779***
Cell dimension$_{(1,348)}$	1104.3***
Plant parts × Surface$_{(1,348)}$	52.546***
Plant parts × Cell dimension$_{(1,348)}$	75.120***
Surface × Cell dimension$_{(1,348)}$	66.878***
Plant parts × Surface × Cell dimension$_{(1,348)}$	24.350***

Plant parts- Leaf and Leaf sheath, Sides- adaxial and abaxial Cell dimension- Length, Width, cuticle thickening. *** significant at P< 0.001

Despite the widespread occurrence of hypostomatic in many orchids, *S. nivea* had an amphistomatal leaves. Amphistomatal condition is also reported in other epiphytic orchids like *Acampe*, *Aerides*, *Bulbophyllum*, *Rhynchostylis*, and *Vanda* (Muthukumar and Shenbagam 2017; Mulgaonkar 2005a,b; Sonowal and Baruah 2010). Richardson et al. (2017) suggested that the existence of amphistomatic condition has a strong relationship with the environment based on their commonality in high light and/or dry environments. In addition, amphistomatic leaves have an advantage of increased CO_2 conductance for photosynthesis and efficient supply water to both the surfaces of the leaves (Buckley et al. 2015). The stomata in *S. nivea* were smaller and less dense than some of the epiphytic orchids. For example, the stomatal aperture dimensions in *S. nivea* were several folds smaller than those reported for some Vandoideae members. The stomatal index of 7.06% in *S. nivea* is higher than *S. gemmata* (5%) reported by Angela et al. (2015). Zhang et al. (2016) indicated that plants with small and dense stomata respond more rapidly to changes in the environment or to the reduction in leaf water potential than those with larger stomata.

Moreover, the results of that study also indicated that evergreen epiphytic orchids were better adapted to cope with water limitations during the growing season than the deciduous conspecifics (Zhang et al. 2016). This condition is generally advantageous for evergreen orchids like *S. nivea* occurring in monsoonal dry environments.

Limited studies have examined the stem anatomy of orchids than root and leaves (Kowsalya et al. 2017; Balachandar et al. 2019). Stems of *S. nivea* possess a thick cuticle which is in accordance with the observation of Kowsalya et al. (2017) in Vandas growing in south India. The hardy stem of *S. nivea* was completely covered by the leaf sheath as in *Luisia*, where, the leaf sheath covered almost the entire internode (Balachandar et al. 2019). Further, Muthukumar and Shenbagam (2017) suggested that leaf sheath aids in adding stiffness to the stem based on the difference in the thickness of the cuticle on the stems that were covered and uncovered by leaf sheath. The hard woody nature of the stem in *S. nivea* arises through progressive cortical proliferation and lignification as reported in *Luisia* (Balachandar et al. 2019). The uniseriate epidermis in *S. nivea* also provides mechanical support in addition to the lignified cortical proliferation. The stem cortex composed of parenchymatous cells was devoid of vascular bundles as observed in *Luisia* species (Balachandar et al. 2019). The sclerenchymatous ground tissue comprising of vascular bundles in *S. nivea* were similar to the stems of *Vanda spathulata* Spr. and *Vanda wightii* Rchb.f. reported by Kowsalya et al. (2017). These sclerenchymatous ground tissues provide additional mechanical support to the stems (Balachandar et al. 2019). Unlike the stems of some Vandae members, the ground tissue in *S. nivea* was characterized by the absence of idioblasts containing raphides, water-storage cells and aeration units (Carlsward et al. 2006; Kowsalya et al. 2017; Balachandar et al. 2019). The vascular bundles were scattered in the ground tissue and embedded in sclerenchymatous cells. The xylem and phloem were capped by sclerenchyma cells and the size of vascular bundles tended to be larger in the centre as reported in several species of *Luisia*, *Vanda* and *Epidendrum radicans* Pav. ex Lindl. (Muthukumar and Shenbagam 2017; Kowsalya et al. 2017; Balachandar et al. 2019).

Roots of *S. nivea* are mostly attached to the substratum. These roots were cylindrical and not much flattened in regions that were attached to the substratum. The substrate roots bear root hairs that were often branched. This is in line with the observations of Balachandar et al. (2019) where the roots of epiphytic orchid *Luisia tenuifolia* Blume were branched. The branched root hairs could be the result of stress experienced by the root hairs (Medeiros 2006) or mutation in genes involved in the root hair formation (Schiefelbein 2000).

The size of the velamen tissue and the number of cell layers could suggest the condition in which the orchid occurs. The 2-3 layered velamen of *S. nivea* resembles those of *V. spathulata* and *Luisia tristis* Hook.f. of the tribe Aeridinae (Kowsalya et al. 2017; Balachandar et al. 2019). The few layered velamen tissue may be the result of humid conditions in which *S. nivea* occurs. All the cells of the exovelamen and endovelamen in *S. nivea* possessed striations and wall thickenings. The striations were of type IIA according to Sanford and Adanlawo (1973) classification of velamen striations. The thickened walls render mechanical support to the velamen cells by preventing cell collapse during dehydration (Oliveira and Sajo 1999).

The uniseriate exodermis in *S. nivea* was dimorphic comprising of long and short cells. Similarly, Muthukumar and Kowsalya (2017) also observed long and short exodermal cells in substrate roots of *Acampe praemorsa* (Rox.) Blatt. & McCann. Although the importance of long exodermal cells is unknown, Pridgeon (1982) reported that long cells give rise to secondary wall thickenings during maturity and die. Further, the long cells of exodermis in plants could be helpful to tolerate drought (Chimungu et al. 2014). The exodermal cells were larger than the velamen cells in *S. nivea* which resembles with the *Vanda*-type of velamen according to Porembski and Barthlott (1988) classification of velamen radicum. The exodermal proliferations unlike reported in some of members of Aeridinae subtribe, (Carlsward et al. 2006, Muthukumar and Kowsalya 2017) was not observed in any of the *S. nivea* roots examined. The exodermal cell thickenings in *S. nivea* may prevent the loss of water through transpiration (Benzing et al.1982). The exodermis is interrupted by thin-walled passage cells in *S. nivea* as observed in the roots of *Luisia* species and other members of Vandeae tribe (Balachandar et al. 2019). The nutrients and water transferred into the cortical cells through the thin-walled exodermal passage cells (Benzing et al. 1982, Bercu et al. 2011). Moreover, Chomichi et al. (2014) suggested that the distribution and frequency of passage cells in the exodermis might be a strategy adopted by orchids to localize and control fungal invasion. Tilosomes are absent in the roots of *S. nivea* as reported for some of the orchid species in Aeridinae (Carlsward et al. 2006). However, Leitgeb (1864) observed tilosomes in some members of Vandaceous taxa. The cover cells are present above the exodermal layer which is similar to the observations of Carlsward et al. (2006) and Kowsalya et al. (2017) in roots of some *Vanda* species. These cover cells are associated with the condensation of gases and water (Pridgeon 1987).

The cortex in *S. nivea* is parenchymatous (Kowsalya et al. 2017; Balachandar et al. 2019). The water-storage cells with banded thickening in *S. nivea* are similar to those observed by Carlsward et al. (2006) and Balachandar et

al. (2019) in the roots of Vandeae members. The water-storage cells with uniformly thickened walls can enhance the apoplastic movement of substance in the vascular tissues (Kowsalya et al. 2017). In epiphytic habitats, the rooting zones are limited to small patches of organic matter accumulating on the branches. These patches get soaked with water during rain and then quickly dry off. So epiphytic plants like orchids that are able to maintain constant water content in their tissues independent of fluctuating water content of the rooted medium have a selective advantage (Tulyananda and Nilsen 2017). The cortical cells are thin-walled in *S. nivea*. Nevertheless, wall thickenings in the root cortical cells were recorded in species of Aeridinae subtribe (Carlsward et al. 2006, Kowsalya et al. 2017) which contradicts with the results of the present study. Idioblasts comprising of raphides are present in the root cortex of *S. nivea*. The function of raphides in roots is yet to be ascertained (Balachandar et al. 2019). Nevertheless, their function in leaves and stem are well documented (Paiva and Machado 2005; Moreira et al. 2013).

The endodermis was uniseriate and O-thickened in *S. nivea* as observed in the endodermal cells of roots in other species of Vandeae (Carlsward et al. 2006; Kowsalya et al. 2017; Balachandar et al. 2019). The endodermal cell walls were heavily thickened in *S. nivea*. This is in accordance with Balachandar et al. (2019), who also revealed the presence of thick-walled endodermal cells in *Luisia pulniana Vatsala* roots. Nevertheless, most of the Vandeae taxa exhibit thin to slightly thick endodermal cell walls, and endodermis interrupted by thin-walled passage cells oriented towards the xylem. Similarly, cells of the pericycle are thick-walled opposite to the phloem tissue. The arrangement and orientation of cells in endodermis and pericycle in *S. nivea* are similar to other epiphytic orchid species of Vandeae taxa (Kowsalya et al. 2017; Balachandar et al. 2019). The thickenings in the endodermal cell walls act as an apoplastic barrier for water and nutrient transport and protect vascular bundles from pathogens (Moreira and Isaias 2008; Muthukumar and Kowsalya 2017).

The number of xylem arches (9-11) in *S. nivea* is in line with the observations of Carlsward et al. (2006) who also reported 9-12 xylem arches in *Neofinetia* of Aeridinae. Like in other Vandeae members, the vascular tissues in *S. nivea* were embedded in the sclerenchymatous cells. The sclerenchymatous cells enclosing the phloem patches were heavily thickened than those cells around the xylem (Kowsalya et al. 2017; Balachandar et al. 2019). In most of the epiphytic orchids, the occurrence of vascular elements in the sclerenchyma cells is considered as an anatomical feature that is related with drought tolerance (Nawaz et al. 2013; Muthukumar and Shenbagam 2017). Pith in *S. nivea* was of sclerenchymatous enclosing intercellular spaces as observed in the Vandeae taxa (Carlsward et al. 2006). However, parenchymatous pith was reported in *L. tenuifolia* (Balachandar et al. 2019). Cell inclusions such as silica bodies and starch grains are absent in pith of *S. nivea*. In contrast, many members of Vandeae are characterized by the presence of such cell inclusions (Carlsward et al 2006; Balachandar et al. 2019).

Mycorrhizal colonization in *S. nivea* was evident in the root portions that were attached to the substrate which is in line with the observations of Sathiyadash et al. (2012) and Muthukumar and Kowsalya (2017) in various epiphytic and terrestrial roots. The fungal hyphae entered *S. nivea* roots through root hairs and traversed the velamen tissue and passage cells of exodermis and then moved into cortical cells where the fungal hyphae formed highly coiled structures called pelotons. Both degenerating and intact pelotons was observed in the root cortex. This is in accordance with the observations reported for epiphytic orchids (Sathiyadash et al. 2012; Kowsalya et al. 2017). It is well known that intact pelotons act as a reservoir for the exchange of nutrient between the orchid and fungus (Dearnalay et al. 2012). The total root length colonization was 50% in *S. nivea* with a high proportion of degenerating pelotons when compared to the intact pelotons. This suggests that *S. nivea* could have adopted mixotrophic mode of nutrition as it occurs in shady regions as observed for *L. tenuifolia* and *L. tristis*. This could have been the reason for the higher percentage of degenerating pelotons in *S. nivea* as suggested by Balachandar et al. (2019).

Conclusion

Schoenorchis nivea exhibited anatomical traits in all the vegetative parts that enable it to survive in the epiphytic habitats. These include thick-walled cuticle covering the entire surface of the leaves, leaf sheath, and the stem, abundant water-storage cells in all the vegetative parts except stem, well developed velamen tissue, presence of cover cells and thick-walled exodermis and endodermis in the roots. All the anatomical characteristics directed towards the acquisition and prevention of water loss could be attributed to the adaptation of *S. nivea* to the xeromorphic conditions of the epiphytic habitat. Moreover, the results of the study clearly revealed that the dimensions of the same structures occurring in different plant parts could vary significantly. In addition, the presence of mycorrhizal association along with the large proportion of degenerating pelotons in the roots suggests that *S. nivea* could adopt a mixotrophic mode of nutrition. Further anatomical and mycorrhizal investigations of other spe-

cies of the *Schoenorchis* could help in the understanding of the precise adaptation of these taxa to epiphytic habitats and resource acquiring strategies.

Acknowledgments

We thank the Director, Indian Cardamom Research Institute (ICRI) Myladumpara, Idukki district, Kerala for permitting to collect the plants in ICRI campus. We also like to thank Dr. K. Dhanapal and Mr. P. Karthi for assisting during the plant collection. We thank Dr. R. Manigandan, Scientist D, i/c, Botanical Survey of India, Southern circle, Coimbatore, India for authenticating the orchid specimen.

References

Adhikari YP, Fischer HS, Fischer A (2012) Host tree utilization by epiphytic orchids in different land-use intensities in Kathmandu valley, Nepal. Plant Ecol 213:393-1412.

Angela N, Chowlu K, Sharma BH, Rao NA, Vij SP (2015) Anatomy of some terete-leaved orchid species. Kasetsart J Nat Sci 49:13-21.

Arditti J, Ghani A (2000) Tansley Review No. 110. Numerical and physical properties of orchid seeds and their biological implications. New Phytol 145:367-421.

Atwood JT (1986) The size of the Orchidaceae and the systematic distribution of epiphytic orchids. Selbyana 9:171-186.

Balachandar M, Koshila Ravi R, Ranjithamani A, Muthukumar T (2019) Comparative vegetative anatomy and mycorrhizal morphology of three South Indian *Luisia* species (Orchidaceae) with the note on their epiphytic adaptations. Flora 251:39-61.

Balan AP, Harikrishnan S (2017) Floristic diversity of the Indian Cardamom Research Institute campus, Myladumpara, Western Ghats, India. J Threat Taxa 9:10804-10822.

Benzing DH, Ott DW, Friedman WE (1982) Roots of *Sobralia macrantha* (Orchidaceae): Structure and function of the velamen-exodermis complex. Am J Bot 69:608-614.

Benzing DH (2000) Bromeliaceae: profile of an adaptive radiation. Cambridge, UK: Cambridge University Press.

Bercu R, Livia A, Broască B (2011) Anatomical aspects of *Phalaenopsis amabilis* (L.) Blume. Ann Rom Soc Cell Biol 16:102-109.

Bertolini V, Cruz-Blasi J, Damon A, Mora JV (2014) Seasonality and mycorrhizal colonization in three species of epiphytic orchids in southeast Mexico. Acta Bot Bras 28:512-518.

Buckley TN, John GP, Scoffoni C, Sack L (2015) How does leaf anatomy influence water transport outside the xylem? Plant Physiol 168:1616-1635.

Carlsward BS (2014) *Campylocentrum*. In: Pridgeon AM, Cribb PJ, Chase MW, Rasmussen FN (Eds.) Genera Orchidacearum. Vol. 6. Oxford University Press, Oxford. pp. 370-372.

Carlsward BS, Stern WL, Bytebier B (2006) Comparative vegetative anatomy and systematics of the angraecoids (Vandeae, Orchidaceae) with an emphasis on the leafless habit. Bot J Linn Soc 151:165-218.

Chimungu JG, Brown KM, Lynch JP (2014) Large root cortical cell size improves drought tolerance in maize. Plant Physiol 166:2166-2178.

Chomicki G, Bidel LPR, Jay-Allemand C (2014) Exodermis structure controls fungal invasion in the leafless epiphytic orchid *Dendrophylax lindenii* Lindl. Benth. ex Rolfe. Flora 209:88-94.

Dearnaley JDW, Martos F, Selosse MA (2012) Orchid mycorrhizas: molecular ecology, physiology, evolution and conservation aspects. In Esser K (Ed.), The Mycota, Vol. IX –Fungal Associations, 2nd ed. Springer-Verlag, Berlin, Germany, pp. 207-230.

ENVIS Centre on Floral Diversity (2019) CITES Plants. Botanical Survey of India, Kolkata, West Bengal, India (http://www.bsienvis.nic.in/Database/bsi_3949.aspx) accessed on 16th January 2019.

Guan ZJ, Zhang SB, Guan KY, Li SY, Hu H (2011) Leaf anatomical structures of *Paphiopedilum* and *Cypripedium* and their adaptive significance. J Plant Res 124:289-298.

Haworth M, McElwain J (2008) Hot, dry, wet, cold or toxic? Revisiting the ecological significance of leaf and cuticular micromorphology. Palaeogeogr Palaeoclimatol Palaeoecol 262:79-90.

Hen-Avivi S, Lashbrooke J, Costa F, Aharoni A (2014) Scratching the surface: genetic regulation of cuticle assembly in fleshy fruit. J Exp Bot 65:4653-4664.

Johanson DA (1940) Plant microtechnique. McGrew Hill Book, New York and London, pp.523.

Kigkr RW (1971) Epidermal and cuticular mounts of plant material obtained by maceration. Stain Technol 46:71-75.

Koske RE, Gemma JN (1989) A modified procedure for staining roots to detect VA mycorrhizas. Mycol Res 92:486-505.

Kowsalya A, Rojamala K, Muthukumar T (2017) Comparative vegetative anatomy of South Indian Vandas, Orchidaceae. Flora 235:59-75.

Kumar M, Sequiera S (2000) A new species of *Schoenorchis* (Orchidaceae) from India. Kew Bulletin 55:241-244.

Lallemand F, Figura T, Damesin C, Fresneau C, Griveau C, Fontaine N, Zeller B, Selosse M (2019) Mixotrophic orchids do not use photosynthates for perennial underground organs. New Phytol 221:12-17.

Leitgeb H (1864) Die Luftwurzeln der Orchideen: Denk-

schriften der KaiserlichenAkademie der Wissenschaften. Math Naturwiss Kl 24:179-222.
Lux A, Morita S, Abe J, Ito K (2005) Improved method for clearing and staining free-hand sections and whole-mount samples. Ann Bot 96:989-996.
Mathew J, George KV (2015) Checklist of orchids of Kottavasal Hills in Achancoil Forests, Southern Western Ghats, (Kollam, Kerala), India. Threat Taxa 7:7691-7696.
McGonigle TP, Miller MH, Evans DG, Fairchild GL, Swan JA (1990) A new method which gives an objective measure of colonization of roots by vesicular-arbuscular mycorrhizal fungi. New Phytol 115:495-501.
Medeiros JD (2006) Branched root hairs in *Miconia albicans* (Sw.) Triana (Melastomaceae). Insula 35: 85-94.
Mill RR, Stark Schilling DM (2009) Cuticle micromorphology of *Saxegothaea* (Podocarpaceae). Bot J Linn Soc 159:58-67.
Moreira AS, Isaias RM (2008) Comparative anatomy of the absorption roots of terrestrial and epiphytic orchids. Braz Arch Biol Technol 51:83-93.
Moreira AS, Filho JP, Isaias RM (2013) Structural adaptations of two sympatric epiphytic orchids (Orchidaceae) to a cloudy forest environment in rocky outcrops of Southeast Brazil. Rev Biol Trop 61:1053-1065.
Mulgaonkar MS (2005a) Studies on dermal anatomy of three corticolous orchids from India. Int J Mendel 22:105-106.
Mulgaonkar MS (2005b) Dermal anatomy of some species of genus *Aerides* Lour. from Maharashtra. Int J Mendel 22:107-108.
Muthukumar T, Kowsalya A (2017) Comparative anatomy of aerial and substrate roots of *Acampe praemorsa* Rox Blatt and MC Cann. Flora 266:17-28.
Muthukumar T, Shenbagam M (2017). Vegetative anatomical adaptations of *Epidendrum radicans* (Epidendroideae, Orchidaceae) to epiphytic conditions of growth. Mod Phytomorphol 11:117-130.
Muthukumar T, Shenbagam M (2018) Vegetative anatomy of the orchid *Bulbophyllum Sterile* (Orchidaceae: Epidendroideae). Lankesteriana 18:13-22.
Nawaz A, Farooq M, Cheema SA, Wahid A (2013) Differential response of wheat cultivars to terminal heat stress. Int J Agric Biol 15:1354-1358.
Nurfadilah S, Swarts ND, Dixon KW, Lambers H, Merritt DJ (2013) Variation in nutrient-acquisition patterns by mycorrhizal fungi of rare and common orchids explains diversification in a global biodiversity hotspot. Ann Bot 111:1233-1241.
Oliveira VC, Sajo MG (1999) Root anatomy of nine Orchidaceae species. Braz Arch Biol Technol 42:405-413.
Paiva EA, Machado SR (2005) Role of intermediary cells in *Peltodon radicans* (Lamiaceae) in the transfer of calcium and formation of calcium oxalate crystals. Braz Arch Biol Technol 48:147-153.
Porembski S, Barthlott W (1988) Velamen radicum micromorphology and classification of Orchidaceae. Nord J Bot 8:117-137.
Pridgeon AM (1982) Diagnostic anatomical characters in the Pleurothallidinae (Orchidaceae). Am J Bot 69:921-38.
Pridgeon AM (1987) The velamen and exodermis of orchid roots. In: Arditti, J. (Ed.), Orchid Biology–Reviews and Perspectives. Cornell University Press, Ithaca, NY, pp. 139-192.
Pridgeon AM, Cribb PJ, Chase MW, Rasmussen FN, (Eds). (2009) Genera Orchidacearum, vol. 5: Epidendroideae (part 2). Oxford University Press, Oxford. p.585.
Richardson F, Brodribb TJ, Jordan GJ (2017) Amphistomatic leaf surfaces independently regulate gas exchange in response to variations in evaporative demand. Tree Physiol 37:869-878.
Rindyastuti R., Nurfadilah S, Rahadiantoro A, Hapsari L, Abywijaya IK (2018) Leaf anatomical characters of four epiphytic orchids of Sempu Island, East Java, Indonesia: The importance in identification and ecological adaptation. Biodiversitas 19:1906-1918.
Salisbury EJ (1927) On the causes and ecological significance of stomatal frequency, with special reference to the woodland flora. Philos Trans Royal Soc B 216:1-65.
Sanford WW, Adanlawo I (1973) Velamen and exodermis characters of West African epiphytic orchids in relation to taxonomic grouping and habitat tolerance. Bot J Linn Soc 66:307-321.
Sathiyadash K, Muthukumar T, Uma E, Pandey RR (2012) Mycorrhizal association and morphology in orchids. J Plant Interact 7:238-247.
Schiefelbein JW (2000) Constructing a plant cell. The genetic control of root hair development. Plant Physiol 124:1525-1531.
Selosse MA, Martos F (2014) Do chlorophyllous orchids heterotrophically use mycorrhizal fungal carbon? Trends Plant Sci 19:683-685.
Shi JX, Adato A, Alkan N, He Y, Lashbrooke J, Matas AJ, Meir S, Malitsky S, Isaacson T, Prusky D, Leshkowitz D, Schreiber L, Granell AR, Widemann E, Grausem B, Pinot F, Rose JKC, Rogachev I, Rothan C, Aharoni A (2013) The tomato SlSHINE3 transcription factor regulates fruit cuticle formation and epidermal patterning. New Phytol 197:468-480.
Smith S, Read D (2008) Mycorrhizal Symbiosis. Academic press, London, pp. 800.
Sonowal J, Baruah A (2010) Foliar epidermis of twenty orchid species from Northeast India with emphasis to their taxonomy. Pleione 4:163-171.
Stpiczyńska M, Davies KL, Kaminska M, (2011) Comparative anatomy of the nectary spur in selected species of Aeridinae (Orchidaceae). Ann Bot 107:327-345.
Tulyananda T, Nilsen ET (2017) The role of idioblasts in

leaf water relations of tropical *Rhododendron*. Am J Bot 104 :828-39.

Van Cotthem WRJ (1970) A classification of stomatal types. Bot J Linn Soc 63:235-246.

Yang SJ, Sun M,Yang QY, Ma RY, Zhang JL, Zhang SB (2016) Two strategies by epiphytic orchids for maintaining water balance: thick cuticles in leaves and water storage in pseudobulbs. AoB Plants 8: plw046.

Zhang W, Hu H, Zhang SB (2016) Divergent adaptive strategies by two co-occurring epiphytic orchids to water stress: escape or avoidance? Front Plant Sci 7:1-11.

Zhong M, Shao X, Wu R, Wei X, Van L, Richard SP, Cornelissen, Johannes HC (2018) Contrasting altitudinal trends in leaf anatomy between three dominant species in an alpine meadow. Aus J Bot 66:448-458.

Acta Biologica Szegediensis

Volume 63(1):15-24, 2019
Acta Biologica Szegediensis
http://abs.bibl.u-szeged.hu/index.php/abs
DOI:10.14232/abs.2019.1.15-24

ARTICLE

Molecular characterization of sesame germplasms of West Bengal, India using RAPD markers

Soumen Saha[1,2], Tarak Nath Dhar[1], Parthadeb Ghosh[1], Tulsi Dey[1,3*]

[1]Cytogenetics and Plant Biotechnology Research Unit, Department of Botany, University of Kalyani, Kalyani-741235, Nadia, West Bengal, India
[2]Cytogenetics and Plant Breeding Section, Department of Sericulture, Raiganj University, Raiganj-733134, Uttar Dinajpur, West Bengal, India
[3]Department of Botany, Kalyani Mahavidyalaya, Kalyani-741235, Nadia, West Bengal, India

ABSTRACT The aim of this research was to assess the genetic diversity of sesame (*Sesamum indicum* L.) and also to reveal the genetic relationships using the Random Amplified Polymorphic DNA (RAPD) markers. Fifteen sesame germplasms were collected from seven districts or four zones of West Bengal, India. A high genetic diversity was revealed by ten RAPD primers within and among the fifteen germplasms. The value of Jaccard's similarity coefficients among and within the fifteen germplasms ranged from 0.287 to 0.725 which indicated high degree of genetic variability. Cluster analysis using Unweighted Pair Group Method with Arithmetic Mean (UPGMA) grouped all the germplasms into three main clusters. Analysis of various genetic diversity indices strongly indicated high level of genetic diversity among the populations of four different regions. UPGMA analysis of four populations resulted into two groups and the results of Principal Coordinates Analysis (PCoA) depicted a clear distinction among the germplasms.
Acta Biol Szeged 63(1):15-24 (2019)

KEY WORDS
genetic diversity
germplasm
molecular marker
Sesamum indicum
Random Amplified Polymorphic DNA

ARTICLE INFORMATION
Submitted
12 March 2019.
Accepted
3 July 2019.
***Corresponding author**
E-mail: deyugb2012@gmail.com

Introduction

Sesame (*Sesamum indicum* L., Pedaliaceae) is perhaps the oldest annual oilseed crop known to man. Based on its ancient history of cultivation, availability of diversity of forms of cultivated varieties and occurrence of the wild sesame (*S. indicum* var. *malabaricum*), India is considered to be the basic centre of origin of the crop (Brar et al. 1979). Sesame seeds are highly nutritive and are important source of oil (44-58%) and protein (25%) with lignan-type antioxidants such as sesamolin and sesamon (Bedigian et al. 1985). According to FAO (2016), about 10.57 million hectares were harvested worldwide in 2016, producing about 6.11 million tonnes. India leads the world in the sesame production and its contribution towards production quantity of sesame seeds in the world was 13.05% in the year 2016. Including India, other supreme sesame producers are China, Myanmar, Sudan, and Uganda covering about 75% of world production (Akbar et al. 2011). The yield of sesame in India was 4198 hg/ha compared to the world average of 5778 hg/ha in the year 2016 (FAO 2016). West Bengal is very rich in genetic diversity of sesame and is usually grown as a catch crop in the pre-*kharif* season (March-May to June-October). So far as West Bengal is concerned, this state produces only 0.17 million tonnes of sesame seeds in the year 2010-2011, covering only about 19.1% with respect to all India production (Economic Review-Finance Department, Govt. of West Bengal, 2011-2012). Thus, the production of sesame seed in West Bengal is not so significant compared to the all India production and despite economic importance of sesame for the West Bengal as well as Indian economy, big fluctuations occur in production and yield. An extensive review of literature regarding the performance and production of sesame in India as well as in other countries reveals that many factors can be held responsible for low yield of such an important oilseed and the factors are absence of non-shattering cultivars suited for mechanical harvest, indeterminate growth, uneven ripening of capsules and biotic and abiotic stresses such as disease, pest drought, etc. (Abdellatef et al. 2008; Bhat et al. 1999), use of conventional varieties (Hamid et al. 2003), and lack of enhanced cultivars (Akbar et al. 2011).

Therefore, it is urgent to study the genetic diversity among sesame germplasms present in different zones of West Bengal and identification and catalogue of the highly diverse germplasms for the purpose of broadening the genetic base. The genetic diversity assessment in sesame has been carried out using both agro-morphological char-

Table 1. List of sesame germplasm from the state West Bengal, India used in this study.

Germplasm number	Germplasm name	Zone of collection	Place of collection	Mean latitude	Mean longitude
Acc-1	VB-67	North Zone	Murshidabad	24°8'24'' N	88°15'36'' N
Acc-2	V-8-Sheera	North Zone	Murshidabad	24°8'24'' N	88°15'36'' N
Acc-3	V-SWB-18	North Zone	Murshidabad	24°8'24'' N	88°15'36'' N
Acc-4	Seklar	North Zone	Murshidabad	24°8'24'' N	88°15'36'' N
Acc-5	V-JTS-8	North Zone	Murshidabad	24°8'24'' N	88°15'36'' N
Acc-6	V-SWB-32-10-1	North Zone	Murshidabad	24°8'24'' N	88°15'36'' N
Acc-7	Rama	North Zone	Murshidabad	24°8'24'' N	88°15'36'' N
Acc-8	Til-2	East Zone	Burdwan	23°14'24'' N	87°51'36'' N
Acc-9	Til-1	East Zone	Hooghly	22°53'24'' N	88°24'00'' N
Acc-10	HT-1	East Zone	Howrah	22°35'24'' N	88°18'36'' N
Acc-11	Savitri	South Zone	South 24 Parganas	22°31'48'' N	88°19'48'' N
Acc-12	Tiloktama (B-67)	South Zone	South 24 Parganas	22°31'48'' N	88°19'48'' N
Acc-13	GT-2	West Zone	East Midnapore	22°18'00'' N	87°54'36'' N
Acc-14	GT-3	West Zone	East Midnapore	22°18'00'' N	87°54'36'' N
Acc-15	Prakash	West Zone	West Midnapore	22°25'48'' N	87°19'48'' N

acters (Bedigian 2010; Ercan et al. 2002; Furat et al. 2010; Pham et al. 2010) and molecular markers such as isozymes (Isshiki et al. 1997), Randomly Amplified Polymorphic DNA (RAPD; Akbar et al. 2011; Bhat et al. 1999; Ercan et al. 2004; Pham et al. 2009; Salazar et al. 2006), Inter Simple Sequence Repeat (ISSR; Kim et al. 2002; Kumar et al. 2012; Woldesenbet et al. 2015), Amplified Fragment Length Polymorphism (AFLP; Uzun et al. 2003), Simple Sequence Repeat (SSR; Dixit et al. 2005; Zhang et al. 2012; Pandey et al. 1015) and Sequence-related Amplified Polymorphism (SRAP; Ali et al. 2017). Among the various available molecular markers, we have selected RAPD for the assessment of genetic diversity (Williams et al. 1990) owing to its simplicity, speed and low cost. Being a fast and sensitive method, RAPD can be quickly and efficiently applied to identify polymorphisms (Doldi et al. 1997; Ko et al. 1998). Moreover, the resolving power of this tool is numerous folds superior than morphological or isozyme markers and is much simpler and technically less demanding than RFLP and other new generation markers. RAPD markers have successfully established their grandness for diversity analysis in many cultivated and wild plants such as *Morus alba* (Orhan et al. 2007), *Vigna unguiculata* (Malviya et al. 2012), *Linum usitatissimum* (Kumari et al. 2017) and also in *S. indicum* (Bhat et al. 1999; Ercan et al. 2004; Quenum and Yan 2017).

Figure 1. Sesame plants growing in the experimental plant garden.

This communication sets out to enumerate the results of our efforts pertaining to the evaluation of genetic variation among fifteen germplasms collected from seven districts of West Bengal and determination of relationship between genetic diversity of sesame population and their geographical distribution within four zones of the state.

Materials and methods

Plant materials

On the basis of diversity in vegetative and reproductive characters, the 15 indigenous germplasms (accessions) of West Bengal were used in this study (Table 1) and were grown in the experimental garden (Fig. 1) of Department of Botany, University of Kalyani, West Bengal, India which is located at 22°57′ N latitude, 88°22′ E longitude with an average altitude of 9.75 m above mean see level. Physicochemical properties of soil and meteorological information are provided in the Supplementary Table 1a and b.

DNA extraction

Fresh tender leaves were collected from ten plants of each germplasm and quickly frozen with liquid nitrogen. Total genomic DNA was extracted based on hexadecyltrimethylammonium bromide (CTAB) procedure (Murray et al. 1980) with minor modifications. The DNA concentration was quantified by spectrophotometry (Cecil, Germany). Thus, the estimated DNA concentrations were rechecked by ethidium bromide staining of the gels after electrophoresis in 0.8% agarose gel.

RAPD analysis

A set of 25 randomly selected oligonucleotide primers (Bangalore Genei, India) were used for RAPD assay. Each 50 µl RAPD polymerase chain reaction (PCR) mixture included 50 ng genomic DNA (template), 10 mM dNTPs, 5 µl of 10X Taq polymerase buffer, 1.0 mM $MgCl_2$, 3U of Taq DNA polymerase enzyme and 400 ng RAPD primers. The final volume of 50 µl was made up with PCR grade water (Genie, Bangalore, India). The reaction mixture was subjected to amplification using Perkin Elmer GeneAmp 2400 PCR system according to the following program: 5 min at 94 °C for initial denaturation, followed by 45 cycles of 1 min denaturation at 94 °C, 1 min annealing at 38 °C, and 2 min extension at 72 °C. The reaction mixture was further incubated at 72 °C for 5 min. Amplification products were separated in 1.5% agarose gel mixed in 1X TAE buffer at 70 V for 1.3 h and were visualised by staining with ethidium bromide. DNA ladder (2 kb) with fragment size 100 to 2000 bp was used as a molecular size marker. The gel was observed under ultraviolet light on a transilluminator and photographed using Gel Documentation System 1000 (Bio-Rad).

Data analysis

Since the RAPD markers are dominant, genetic data analysis was carried out on the assumption that each band represented the phenotype at a single biallelic locus. Amplification with each arbitrary primer was repeated three times and consistent bands were selected for data generation. The presence and absence of bands were scored as the presence (1) or absence (0), respectively. DNA fragment intensity was not taken into consideration and the bands with the same mobility were considered to be the same bands. Only main DNA fragments constantly amplified were scored and weak bands were not utilised for analysis. By comparing the banding patterns of genotypes (germplasms) for a specific primer, genotype-specific bands were identified. The binary data so generated was used to estimate the levels of polymorphism by dividing the polymorphic bands by the total number of scored bands. To analyze the suitability of RAPD markers for evaluating the genetic profiles of sesame performance of the markers was measured using three parameters: (i) polymorphic information content (PIC), (ii) marker index (MI) and (iii) resolving power (RP). The PIC value for each locus was calculated using the formula: PIC = 2fi (1-fi), where fi is the frequency of the amplified fragments (band present) and 1 - fi is the frequency of non-amplified fragments (band absent) (Roldán-Ruiz et al. 2000). The frequency was calculated as the ratio between the number of amplified bands at each locus and the total number of accessions (excluding missing data). The PIC of each primer was calculated using the average PIC value from all loci of each primer. MI was calculated applying the formula: MI = EMR × PIC, where EMR (effective multiplex ratio) is the product of the fraction of polymorphic loci and the number of polymorphic loci for an individual assay (Varshney et al. 2007). RP of each primer was calculated according to Prevost and Wilkinson (1999): RP = ΣIb, where Ib represents the informative fragments. The Ib can be represented on a scale of 0 to 1 by the following formula: Ib = 1 - [2 × (0.5 - p)], where p is the proportion of accessions containing the band. The genotype and allelic frequency data were used to compute the genetic diversity indices, that is, (i) percentage of polymorphic loci [P% = (polymorphic loci/total loci) × 100], (ii) observed (na) and effective number of alleles (ne), where ne is the number of equally frequent alleles that would be necessary to achieve the same degree of genetic diversity produced by na, (iii) Shannon's Information Index (I) (Shannon et al. 1949) calculated from I = (Σ pi log pi), where pi is the frequency of RAPD fragments amplified in the accessions and L is the total number of fragments and (iv) Nei's genetic diversity (h) (Nei 1973) derived from h = 1 - Σpi2, where pi is the frequency of the i^{th} allele at the locus, were calculated with the aid of the POPGENE program version 1.31 (Yeh et al. 1999). For each locus, the Nei's index produces values between 0 and 0.5, while the Shannon index varies from 0 to 0.73 according to a natural log scale (Lowe et al. 2004).

The binary data matrix was used to calculate Jaccard's similarity coefficient (Jaccard 1908) between pairs of accessions using the Simqual module of NTsys-PC (Numerical Taxonomy System, version 2.1) (Rohlf 1993). These distance coefficients were used to construct dendrogram using the Unweighted Pair Group Method with Arithmetic Mean (UPGMA) employing the Sequential Agglomerative Hierarchical and Nested (SAHN) algorithm for determining the genetic diversity and relationships among the accessions. In order to highlight the resolving power of the ordination, Principal Coordinates Analysis (PCoA) was performed using the EIGEN and PROJ modules of NTSYS Pc.

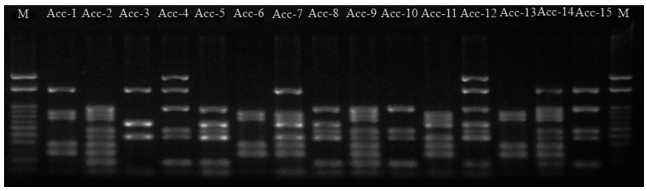

Figure 2. RAPD profile of the 15 accessions (Acc 1-15) of *Sesamum indicum* L. generated by primer OTD-01.

Results

To assess the genetic diversity and relationship among 15 germplasms, a total of 25 RAPD primers were screened, out of which ten primers revealed reproducible polymorphic patterns (Fig. 2) and were used for further study. Two main aspects of genetic diversity-marker informativeness (polymorphic and overall efficiency of informative fragment detection) and marker performance (overall efficacy of a primer set used in determining polymorphism level, genetic diversity, and discriminatory power) were estimated (Table 2).

Marker informativeness

Marker informativeness of ten RAPD primers was evaluated using different parameters (Table 2). A total of 116 clear, reproducible and scorable RAPD fragments ranging from 100 to 2000 bp were generated among all germplasms. Out of 116 scorable RAPD bands, 110 were polymorphic and 6 were monomorphic. Each primer was tried thrice, and the results were reproducible. In general, 10 to 12 amplified fragments were scored depending upon the primers. The number of polymorphic bands per primers ranged from nine (OTD4) to twelve (OTD1, OTD2, OTD5) with an average of eleven (Table 2). Selections of polymorphic alleles were carried out in a careful manner and only the clear, reproducible and polymorphic bands were scored and used for statistical analysis. The percentage of polymorphic bands ranged from 90% (OTD4, OTD6, and OTD7) to 100% (OTD1, OTD2, OTD3, and OTD5), with a high average value of 94.42% (Table 2). The ranges of frequencies of polymorphic fragments for a given primer across for all germplasms were 0.066 to 1 with an average of 0.55. A large proportion (55.17) had frequencies in the range 0.5 to 0.6 (Fig. 3).

Marker performance

Information on the genetic profile of each germplasm was used to assess the marker performance by evaluating the PIC, EMR, MI and RP (Table 2). The range of PIC for 110 polymorphic fragments obtained by using ten RAPD primers was 0.37 to 0.44 with an average of 0.40. Eighty-three of polymorphic fragments were highly informative (PIC ≥ 0.44), six had lower level of PIC (≥ 0.1) and the remaining twenty seven showed moderate values (≥ 0.1 to < 0.44) (Fig. 4). The highest PIC value (0.44) was observed for primer OTD1 and the lowest PIC value (0.37) was observed for OTD9 (Table 2).

The highest EMR (12) was observed for the primer OTD1, OTD2 and OTD5 and the mean EMR per primer was 11 (Table 2). To determine the overall utility of the maker system, the marker index was calculated for each RAPD primer. The marker index for the ten primers ranged from 1.91 (OTD4) to 2.88 (OTD2 and OTD5) with an average 2.416 (Table 2). The resolving power of RAPD primers is a feature that indicates a discriminatory potential of the primer ranged from 1.03 (OTD8) to 1.14 (OTD2, OTD5), averaging 1.095 (Table 2). No significant correlation was found between

Table 2. Polymorphism and marker attributes of RAPD primers.

Primer name	Sequence (5´- 3´)	Number of fragments			% Polymorphism	PIC	EMR	Marker index	Resolving power
		Total	Monomorphic	Polymorphic					
OTD-01	TTGGCGGCCT	12	0	12	100	0.44	12	2.87	1.09
OTD-02	ACCTCGCCAC	12	0	12	100	0.42	12	2.88	1.14
OTD-03	GAGGTCCACA	11	0	11	100	0.38	11	2.25	1.08
OTD-04	TGCCGAGCTG	10	1	9	90	0.39	9	1.91	1.09
OTD-05	AGTCAGCCAC	12	0	12	100	0.42	12	2.88	1.14
OTD-06	GGGTAACGCC	12	1	11	90	0.38	11	2.27	1.09
OTD-07	AGGTGACCGT	12	1	11	90	0.41	11	2.53	1.12
OTD-08	CTGGGCAACT	11	1	10	90.9	0.41	10	2.11	1.03
OTD-09	AGGCGGGAAC	12	1	11	91.66	0.37	11	2.21	1.09
OTD-10	AGGTCTTGGG	12	1	11	91.66	0.38	11	2.25	1.08
Total	-	116	6	110	-	-	-	-	-
Average	-	11.6	0.6	11	94.42	0.4	11	2.416	1.095

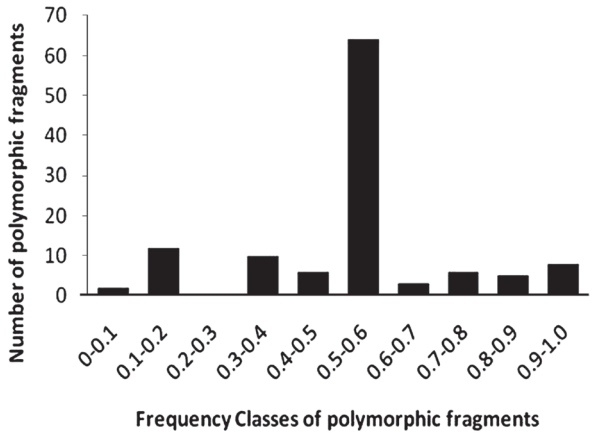

Figure 3. Frequency distribution of polymorphic RAPD fragment amplified in 15 sesame germplasms.

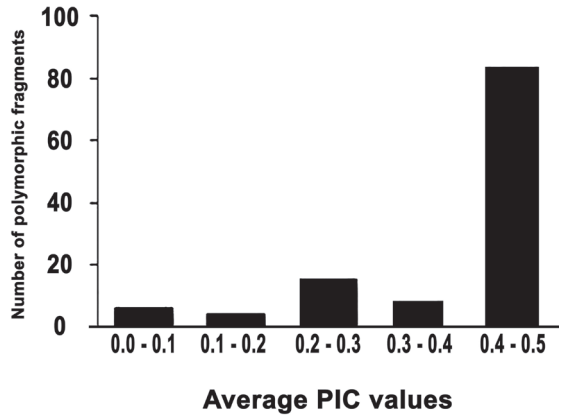

Figure 4. Average PIC values for polymorphic fragments generated by RAPD primers in 15 sesame germplasms.

the number of neither fingerprint nor lines with exclusive finger print with PIC, resolving power and marker index.

Genetic diversity at zone level

Using the RAPD amplification result, the genetic diversity of the four regions of West Bengal was analyzed (Table 3). The range of mean number of alleles (n_a) based on RAPD analysis was 1.55 to 1.92 and the effective number of alleles (n_e) was 1.53 to 1.73. The Shannon's information index (*I*) was 0.38 to 0.57 and the Nei's gene diversity index (*h*) was 0.27 to 0.39.

Analysis of RAPD data showed that north zone, west zone and east zone displayed more variation and the respective coefficients were 92.24, 77.59, and 67.24%. According to the number of polymorphic loci, the ranking of the regions was north zone › west zone › east zone › south zone. Table 3 shows that a general consistency is retained in different indexes of genetic diversity using RAPD marker and the polymorphic locus percentages was about more than 90%. These findings strongly indicated the high genetic variation among the sesame germplasms of four different regions and the RAPD marker approach was effective for the detection. For the level of gene flow (Nm), the number of migrating individuals among the population per generation was estimated to be 2.30 using RAPD marker which indicated that gene exchange between populations was rather high.

The genetic similarities were calculated following the Jaccard's coefficient (Jaccard 1908) method using the RAPD data. The similarity index ranged from 0.188 to 0.603 with an average of 0.276 (Table 4) indicating a close genetic relationship among the *Sesamum* germplasm of four different regions. The calculated similarity coefficient was utilized to prepare a tree for cluster analysis using UPGMA method (Fig. 5). The cluster analysis generated a sister group consisting of populations of east zone, west zone, and south zone. Moreover, results indicated that populations of east zone and west zone were found to be more similar (60%), while populations of north zone was outlier. The populations of north zone were separated from the other populations showing their maximum genetic dissimilarity.

Genetic diversity-phylogenetic relationship and PCoA analysis

The genetic similarities were calculated using the Jaccard's coefficient (Jaccard 1908) method for all the 15 germplasms of *S. indicum* according to RAPD data analysis. Based on

Table 3. Estimates of genetic diversity within four population/zones using RAPD markers.

Index	North Zone	East Zone	South Zone	West Zone	All
n_a	1.92	1.67	1.55	1.77	1.94
n_e	1.73	1.53	1.55	1.62	1.75
h	0.39	0.29	0.27	0.34	0.40
I	0.57	0.42	0.38	0.49	0.57
P%	92.24	67.24	55.17	77.59	94.83

na = average number of alleles; ne = effective number of alleles; h = heterozygosity; I = Shannon's index; P = percentage of polymorphic loci

Table 4. Similarity matrix based on Jaccard's coefficient revealed by RAPD marker within four populations/zones.

Index	North Zone	East Zone	South Zone	West Zone
North Zone	1.000			
East Zone	0.246	1.000		
South Zone	0.188	0.308	1.000	
West Zone	0.262	0.603	0.310	1.000

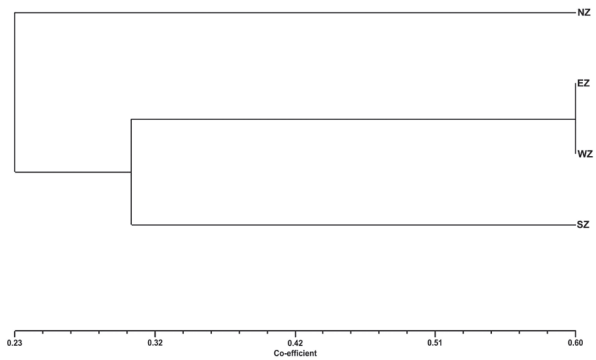

Figure 5. UPGMA dendrogram within four populations (zones) based on JACCARD's similarity coefficient calculated from RAPD data set.

the RAPD markers, the similarity index value ranged from 0.287 to 0.725 (Table 5) indicating a close genetic relationship within the varieties. The calculated similarity coefficients were utilized to construct a dendrogram using UPGMA. A dendrogram was prepared using UPGMA clustering algorithm based on RAPD data and fifteen varieties were grouped into three main cluster; cluster (I) containing three germplasms, cluster (II) containing a total of six germplasms and cluster (III) containing six germplasms (Fig. 6). By providing spatial representation of relative genetic distances among individuals, the PCoA analysis was performed to determine the consistency of the differentiation among the germplasms defined by the cluster analysis. The PCoA indicated that the effect of individual amplification products on the overall variation observed was lesser, hence a total of ten RAPD products were required to explain 94.83% of the variation among the fifteen sesame germplasms. The analysis indicated that, the first two principle coordinates accounted for 54.46% of the total variation, while the remaining coordinates individually were less than 5.00% each. Therefore, the biplot of only the first two coordinates are presented in Figure 7 and similar result was observed like that of three-dimensional representations (Fig. 8). The results from PCoA plot of the 15 sesame accessions reveal a clear distinction among the germplasms. The PCoA plot analysis was in congruence with the UPGMA cluster analysis.

Discussion

Accurate identification of germplasms of crop species and varieties by means of DNA fingerprints is important particularly when new crop varieties are to be released, different accessions of wild species are to be characterized and purity of germplasms is to be determined. RAPD markers were utilized in this study to evaluate the level of genetic variation among the 15 germplasms of *S. indicum* L. collected from different districts of West Bengal, India. The RAPD technique has been chosen as it does not require any previous knowledge on DNA sequence of this species, is an inexpensive and easy to use for evaluating the degree of genetic diversity in sesame and many other plant species (Akbar et al. 2011; Bhat et al. 1999; Ercan et al. 2004; Salazar et al. 2006; Sangwan et al. 2001; Sharma et al. 2009; Vieira et al. 2003; Singh et al. 2017; Dar et al. 2017).

Ten RAPD primers detected sufficient genetic variation within fifteen sesame germplasms to allow for complete

Table 5. Genetic similarity coefficients among fifteen sesame germplasm realized from RAPD markers.

Correlation	Acc-1	Acc-2	Acc-3	Acc-4	Acc-5	Acc-6	Acc-7	Acc-8	Acc-9	Acc-10	Acc-11	Acc-12	Acc-13	Acc-14	Acc-15
Acc-1	1.000														
Acc-2	0.347	1.000													
Acc-3	0.322	0.379	1.000												
Acc-4	0.378	0.388	0.352	1.000											
Acc-5	0.471	0.473	0.425	0.330	1.000										
Acc-6	0.526	0.376	0.353	0.379	0.287	1.000									
Acc-7	0.355	0.725	0.506	0.327	0.440	0.419	1.000								
Acc-8	0.444	0.495	0.593	0.523	0.452	0.482	0.402	1.000							
Acc-9	0.442	0.528	0.309	0.506	0.483	0.304	0.444	0.381	1.000						
Acc-10	0.481	0.344	0.487	0.458	0.544	0.345	0.309	0.494	0.391	1.000					
Acc-11	0.512	0.478	0.382	0.422	0.483	0.538	0.494	0.441	0.422	0.287	1.000				
Acc-12	0.438	0.538	0.396	0.404	0.446	0.459	0.576	0.533	0.361	0.404	0.347	1.000			
Acc-13	0.494	0.398	0.393	0.371	0.382	0.481	0.333	0.580	0.488	0.353	0.402	0.340	1.000		
Acc-14	0.506	0.571	0.398	0.484	0.495	0.351	0.522	0.500	0.688	0.376	0.484	0.418	0.372	1.000	
Acc-15	0.364	0.517	0.506	0.425	0.543	0.506	0.448	0.477	0.333	0.539	0.494	0.422	0.341	0.351	1.000

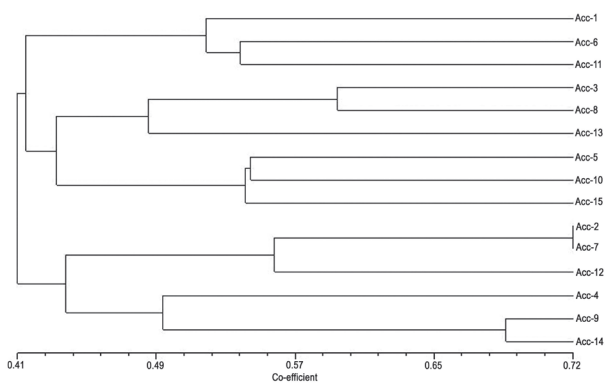

Figure 6. JACCARD's similarity dendrogram of the 15 germplasms (Acc1-Acc15) generated by UPGMA based on RAPD marker system.

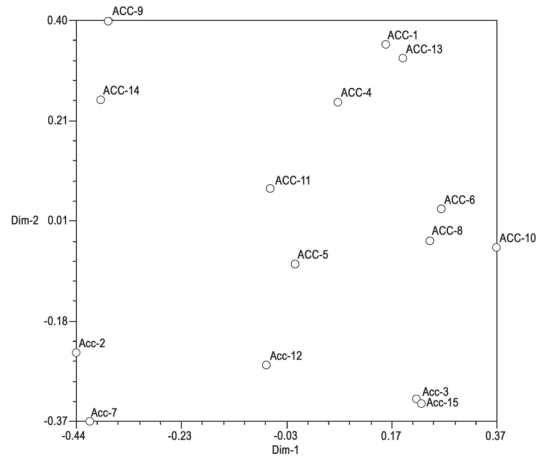

Figure 7. Two-dimensional plot obtained from Principal Coordinates Analysis (PCoA) of fifteen sesame germplasms using RAPD markers.

differentiation. According to Li and Midmore (1999) when the variation between genotype is high the use of few primers will be sufficient. For instance, Ercan et al. (2004) identified thirty-eight accessions only by using seven primers while twenty sesame genotypes were determined with ten primers by Akbar et al. (2011). Similarly, Millan et al. (1996) reported a high level of genetic diversity among rose genotypes using nearly ten RAPD primers. Schontz and Rether (1999) identified 37 lines of Foxtail millet employing just 4 RAPD primers.

A high level of genetic diversity was observed among the 15 germplasms of sesame. Although, sesame is generally followed by self-pollination, but cross pollination has been reported between 5 and 60% in this species

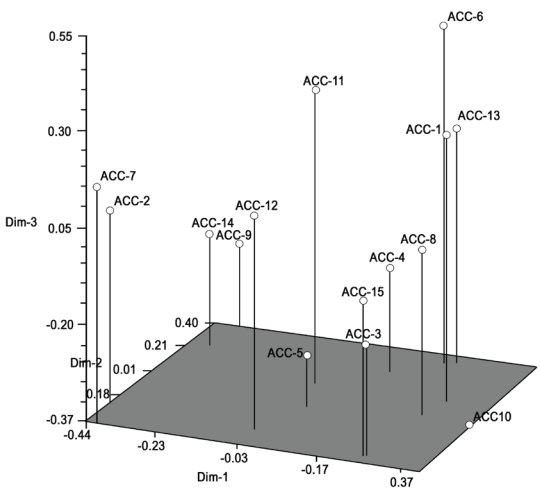

Figure 8. Three-dimensional plot obtained from Principal Coordinates Analysis (PCoA) of fifteen sesame germplasms using RAPD markers.

(Ashri 1989; Brar et al. 1979; Joshi 1961; Mazanni 1983; Yermanos 1980). Approximately 10 to 20% of the genetic diversity among the population is since out crossing could explicate the high genetic variability noticed in the present study. The present results are in conformity with the results of earlier workers based on RAPD and morpho-agronomic traits which have reported high genetic diversity in sesame germplasms (Akbar et al. 2011; Ashri 1998; Bhat et al. 1999; Ercan et al. 2004; Pham et al. 2009; Salazar et al. 2006).

Applying different methods would provide different results on the level of genetic diversity. Isshiki and Umezki (1997), reported little variation among 68 accessions of cultivated sesame employing isozymes. Laurentin and Karvilsky (2006) applied AFLP to clarify genetic relationship among 32 sesame accessions from the Venezuelan germplasms collections and reported a very low genetic relationship and diversity (0.14 to 0.21). ISSR polymorphism was used to determine the genetic relationship among 75 sesame accessions of Korea and other countries showed a low level of polymorphism with this particular marker and genetic distances ranged from 0 to 0.255 (Kim et al. 2002). However, it was shown that their method had low resolution.

In contrast, a very high level of genetic diversity among sesame accessions by means of RAPD molecular markers has been reported by Bhat et al. (1999), Ercan et al. (2004), Akbar et al. (2011), Dar et al. (2017) and Quenum and Yan (2017). The present study detected a high level of polymorphism for sesame between the different geographical areas of West Bengal. In the present study, a high level of polymorphism (94.42%) obtained is comparable to the 86.75% polymorphism noticed in a study of genetic diversity in Indian and exotic sesame germplasms by

Bhat et al. (1999) and also analogous to 82.99% observed in a study of genetic diversity of sesame of Vietnam and Cambodia (Pham et al. 2009). Salazar et al. (2006) also observed 100% of polymorphism in an analysis of genetic diversity of sesame of Venezuela. Ercan et al. (2004) also reported 78% polymorphism in an analysis of genetic diversity in Turkish sesame. Although, a considerable level of genetic diversity was noticed among diverse sesame germplasms collected from various geographical regions of West Bengal, it was found that some accessions situated geographically far apart were grouped together in the same cluster such as Acc-1 and Acc-6 (from north zone) and Acc-11 (from south zone) grouped together in cluster I (Fig. 6). Similarly, in the cluster II germplasms of north zone (Acc-3 and Acc-5), east zone (Acc-8 and Acc-10) and west zone (Acc-13 and Acc-15) were clustered together. Furthermore, cluster III germplasms collected from different regions of West Bengal appeared in the identical group such as north zone (Acc-2, Acc-4 and Acc-7), south zone (Acc-12), east zone (Acc-9) and west zone (Acc-14). This could be an outcome of large movement of West Bengal farmers to different regions of the state carrying sesame seeds for cultivation into their new geographical locations. According to Bhat et al. (1999), the cultivation practices and consumer preferences in respect to seed colour and seed texture and other quality attributes differ widely with the of cultivation. Stankiewicz et al. (2001) pointed out that human factor could be responsible for lack of association between genetic and geographical detachment in some cases. Germplasms collected from the same zone were found to have a close genetic relationship for example cluster I included germplasms Acc-1 and Acc-6 from North Zone and Acc-8, Acc-10 from East Zone in cluster II. Interestingly, all the three clusters included germplasms collected from north zone (Murshidabad district) which may be a consequence of largely substantial movement of farmers of Murshidabad district to different regions of West Bengal for collection of diverse germplasms of sesame for cultivation.

Using the RAPD results, attempts have been made to analyse the genetic diversity from the four different geographical zones of West Bengal. From the result it can be summarized that least gene diversity was among the germplasms collected from the south zone or South 24 Parganas district and the highest among germplasms of north zone or Murshidabad district. The same order of genetic heterogeneity was discerned to Shannon's information index (north zone > west zone > east zone > south zone) and the level of gene flow was 2.30. From the standpoint of population genetics, a value of gene flow (Nm) <1 (less than one migrant/generation into a population) or equivalently a value of genetic differentiation (Gst) > 0.25 is generally regarded as the threshold quantity beyond which significant population differentiation occurs (Slatin 1987). The high flow among the population detected in this study points towards the possibility of instances of single isolated populations possessing unique germplasms also found in other populations and which is in conformity with the studies of Naik et al. (2010).

Little studies have been carried out about the discriminatory power of RAPD primers in sesame (Salazar et al. 2006). But similar studies have been done in other crops such as *Glycin max* (Powell et al. 1996), *Hordeum vulgare* (Russell et al. 1997), *Jatropha curcus* (Grativol et al. 2011) and *Cicer arietinum* (Choudhary et al. 2013), *Phoenix dactylifera* (Kareem et al. 2018). In this study, a PIC of 0.40 was obtained, higher than the 0.37 value reported by Salazer et al. (2006). The UPGMA cluster analysis and PCoA showed a similar pattern in this study and similar relationship between both analyses have been reported by Ercan et al. (2004) and Salazer et al. (2006).

In conclusion, using as few as ten primers, RAPD marker analysis revealed a high level of genetic diversity among sesame germplasms collected from various geographical zones of West Bengal, India. Finally, it can be surmountable that high level of diversity was obtained by RAPD marker-based analysis and thus this technique can be used for the selection of parents in sesame breeding program.

Acknowledgements

This research is supported by a Grant from the University Grants Commission, New Delhi, Government of India. The first and second author contributed equally to this manuscript. Authors also gratefully acknowledge the DST-PURSE and Department of Botany, University of Kalyani for Central Instrumental Facilities.

References

Abdellatef E, Sirelkhatem R, Mohamed Ahmed MM, Radwan KH, Khalafalla MM (2008) Study of genetic diversity in Sudanese sesame (*Sesamum indicum* L.) germplasm using random amplified polymorphic DNA (RAPD) markers. Afr J Biotechnol 7:4423-4427.

Akbar F, Rabbani MA, Masood MS, Shinwari ZK (2011) Genetic diversity of sesame (*Sesamum indicum* L.) germplasm from Pakistan using RAPD markers. Pak J Bot 43:2153-2160.

Ali Al-Somain BH, Migdadi HM, Al-Faifi SA (2017) Assessment of genetic diversity of sesame accessions collected from different ecological regions using sequence-related amplified polymorphism markers. 3Biotech 7:82.

Ashri A (1989) Sesame. In Roebbelen G, Downey RK, Ashri A, Eds., Oil Crop of the World. McGraw Hill, New York, 375-387.

Ashri A (1998) Sesame breeding. Plant Breed Rev 16:179-228.

Bedigian D (2010) Characterization of sesame (*Sesamum indicum* L.) germplasm: A critique. Genet Resour Crop Evol 57:641-647.

Bedigian D, Seigler DS, Harlan JR (1985) Sesamin, sesamolin and the origin of sesame. Biochem Syst Ecol 13:133-139.

Bhat KV, Babrekar PP, Lakhanpaul S (1999) Study of genetic diversity in Indian and exotic sesame (*Sesamum indicum* L.) germplasm using random amplified polymorphic DNA (RAPD) markers. Euphytica 110:21-33.

Brar GS, Ahuja KL (1979) Sesame: It's culture, genetics, breeding and biochemistry. In Malik CP, ed., Annu Rev Plant Sci, Kalyani Publishers, New Delhi, India, 245-31.

Cagrgan MI (2006) Selection and morphological characterization of induced determinate mutants in sesame. Field Crops Res 96:19-24.

Choudhary P, Khanna SM, Jain PK, Bharadwaj C, Kumar K, Lakhera PC, Srinivasan R (2013) Molecular characterization of primary gene pool of chickpea based on ISSR markers. Biochem Genet 51:306-322.

Dar AA, Mudigunda S, Mittal PK, Arumugam (2017) Comparative assessment of genetic diversity in *Sesamum indicum* L. using RAPD and SSR markers. 3Biotech 7:10.

Dixit A, Jin MH, Chung JW (2005) Development of polymorphic microsatellite markers in sesame (*Sesamum indicum* L.). Mol Ecol Notes 5:736-738.

Doldi ML, Volmann J, Lelley T (1997) Genetic diversity in soybean as determined by RAPD and microsatellite analysis. Plant Breed 116:331-335.

Economic Review-Finance Department, Government of West Bengal (2011-2012) http://www.wbfin.nic.in/writereaddata/EconomicReview11_Part2.pdf accessed on 20 May 2014.

Ercan AG, Taskin M, Turgut K (2004) Analysis of genetic diversity in Turkish sesame (*Sesamum indicum* L.) populations using RAPD markers. Genet Resour Crop Evol 51: 599-607.

Ercan AG, Taskin KM, Turgut K, Bilgen M (2002) Characterization of Turkish sesame (*Sesamum indicum* L.) landraces using agronomic and orphologic descriptors. Akdeniz Univ Ziraat Fak Derg 15:45-52.

FAO (2016) FAOSTAT Database. http://faostat.fao.org/site/567/DesktopDefault.aspx?PageID=567#ancor. Accessed on 21 July 2018. http://www.fao.org/faostat/en/#data/QC.

Fitzgerald MA, McCouch SR, Hall RD (2009) Not just a grain of rice: the quest for quality. Trends Plant Sci 14:133-139.

Furat S, Uzun B (2010) The use of agro-morphological characters for the assessment of genetic diversity in sesame (*Sesamum indicum* L.). Plant Omics 3:85-91.

Grativol C, da Fonseca Lira-Medeiros C, Hemerly AS, Ferreira PCG (2011) High efficiency and reliability of inter-simple sequence repeats (ISSR) markers for evaluation of genetic diversity in Brazilian cultivated *Jatropha curcas* L. accessions. Mol Biol Rep 38:4245-4256.

Hamid KA, Ibrahim AS, Taha MB, Ahmed ME (2003) Performance, interrelationship and path analysis of some yield component in sesame. Univ Khartoum J Agric Sci 11:305-320.

Isshiki S, Umezaki T (1997) Genetic variations of isozymes in cultivated sesame (*Sesamum indicum* L.). Euphytica 93:375-377.

Jaccard P (1908) Nouvelles researches sur la distribution florale. Bull Soc vaud sci natur 44:223-270.

Joshi AB (1961) Monograph of Sesame. First Ed. Published by Indian Central Oilseeds Committee, Hyderabad. Junagadh, *Sesamum,* 366-434.

Kareem MAH, Al-Saadi AH, Naji HF (2018) Genetic diversity of Iraqi date palm (*Phoenix dactylifera* L.) by using RAPD technique. JUBPAS 26:114-131.

Kim DH, Zur G, Danin-Poleg Y, Lee SW, Shim KB, Kang CW, Kashi Y (2002) Genetic relationship of sesame germplasm collection as revealed by inter-simple sequence repeats. Plant Breed 121:259-262.

Ko MK, Yang J, Jin YH, Lee CH, Oh BJ (1998) Genetic relationships of *Viola* species evaluated by random amplified polymorphic DNA analysis. J Hortic Sci Biotech 73:601-605.

Kumar H, Kaura G, Bangaa S (2012) Molecular characterization and assessment of genetic diversity in sesame (*Sesamum indicum* L.) germplasm collection using ISSR markers. J Crop Improv 26:540-557.

Kumari A, Paul S, Sharma V (2017) Genetic diversity analysis using RAPD and ISSR markers revealed discrete genetic makeup in relation to fibre and oil content in *Linum usitatissimum* L. genotypes. Nucleus 61:45-53.

Li M, Midmore DJ (1999) Estimating the genetic relationships of Chinese water chestnut (*Eleocharis dulcis* (Burm. f.) Hensch.) cultivated in Australia, using random amplified polymorphic DNAs (RAPDs). J Hortic Sci Biotechnol 74:224-231.

Laurentin HE, Karlovsky P (2006) Genetic relationship and diversity in a sesame (*Sesamum indicum* L.) germplasm collection using amplified fragment length polymorphism (AFLP). BMC Genetics 7:1-10.

Lowe A, Harris S, Ashton P (2004) Ecological Genetics: Design Analysis and Application. Blackwell, Oxford.

Malviya N, Sarangi BK, Yadav MK, Yadav D (2012) Analysis of genetic diversity in cowpea (*Vigna unguiculata* L.Walp) cultivars with random amplified polymorphic DNA markers. Plant Syst Evol 298:523-526.

Mazanni B (1983) Ajonjoli. In Cultivo y Majoramiento de Plant as Oleaginosas. FONAIP. Caracas, Venezuela.

162-224.
Millan T, Osuna F, Cobos S, Torres AM, Cubero JI (1996) Using RAPDs to study phylogenetic relationships in Rosa. Theor Appl Genet 92:273-277.
Murray HG, Thompson WF (1980) Rapid isolation of high molecular weight DNA. Nucleic Acids Res 8:4321-4325.
Naik PK, Alam MF, Singh H, Goyal V, Parida S, Kalia S, Mohapatra T (2010) Assessment of genetic diversity through RAPD, ISSR and AFLP markers in *Podophyllum hexandrum*: A medicinal herb from the Northwestern Himalayan region. Physiol Mol Biol Plants 16:135-148.
Nei M (1973) Analysis of gene diversity in subdivided populations. Proc Natl Acad Sci USA 70:3321-3323.
Orhan E, Ercisli S, Yildirim N, Agar G (2007) Genetic variation among mulberry genotypes (*Morus alba*) as revealed by Randomly Amplified Polymorphic DNA (RAPD) markers. Plant Syst Evol 265:251-258.
Pandey SK, Das A, Rai P, Dasgupta T (2015) Morphological and genetic diversity assessment of sesame (*Sesamum indicum* L.) accessions differing in origin. Physiol Mol Biol Plants 21:519-529.
Pham TD, Bui TM, Werlemark G, Bui TC, Merker A, Carlsson AS (2009) A study of genetic diversity of sesame (*Sesamum indicum* L.) in Vietnam and Cambodia estimated by RAPD markers. Genet Resour Crop Evol 56:679-690.
Pham TD, Nguyen TDT, Carlsson AS, Bui TM (2010) Morphological evaluation of sesame (*Sesamum indicum* L.) varieties from different origins. Austral J Crop Sci 4:498-504.
Powell W, Morgante M, Andre C, Hanafey M, Vogel J, Tingey S, Rafalski A (1996) The comparison of RFLP, RAPD, AFLP and ISSR and SSR (microsatellite) markers for germplasm analysis. Mol Breed 2:225-238.
Prevost A, Wilkinson MJ (1999) A new system of comparing PCR primers applied to ISSR fingerprinting of potato cultivars. Theor Appl Genet 98:107-112.
Quenum F, Yan Q (2017) Assessing genetic variation and relationships among a mini core germplasm of sesame (*Sesamum indicum* L.) using biochemical and RAPD markers. Am J Plant Sci 8:311-327.
Russell JR, Fuller JD, Macaulay M, Hatz BG, Jahoor A, Powell W, Waugh R (1997) Direct comparison of levels of genetic variation among barley accessions detected by RFLPs, AFLPs, SSRs a RAPDs. Theor Appl Genet 95:714-722.
Rohlf FJ (1993) NTSYS-pc. Numerical Taxonomy and Multivariate Analysis System. version 2.11. Applied Biostatistics. Exeter Software, Setauket, New York.
Roldán-Ruiz I, Dendauw J, Van Bockstaele E, Depicker A, De Loose M (2000) AFLP markers reveal high polymorphic rates in ryegrasses (*Lolium* spp.). Mol Breed 6:125-134.
Salazar B, Laurentin H, Davila M, Castillo MA (2006) Reliability of the RAPD technique for germplasm analysis of sesame (*Sesamum indicum* L.) from Venezuela. Interciencia J 31:456-460.
Sangwan NS, Jadav U, Sangwan RS (2001) Molecular analysis of genetic diversity in elite Indian cultivars of essential oil trade types of aromatic grasses (*Cymbopogon* species). Plant Cell Rep 20:437-444.
Schontz D, Rether B (1999) Genetic variability in foxtail millet, *Setaria italic* (L.) P. Beauv.: Identification and classification of limes with RAPD markers. Plant Breed 118:190-192.
Shannon C, Weaver W (1949) The Mathematical Theory of Communication. University of Illinois Press, Urbana, USA.
Sharma SN, Kumar V, Mathur S (2009) Comparative analysis of RAPD and ISSR markers for characterization of sesame (*Sesamum indicum* L.) genotypes. J Plant Biochem Biotechnol 18:37-43.
Singh P, Singh SP, Tiwari AK, Sharma BL (2017) Genetic diversity of sugarcane hybrid cultivars by RAPD markers. 3Biotech 7:222.
Slatin M (1987) Gene flow and geographic structure of natural populations. Science 236:787-792.
Stankiewicz M, Gadamski G, Gawronski SW (2001) Genetic variation and phylogenetic relationships of triazine-resistant and triazine-susceptible biotypes of *Solanum nigrum* - analysis using RAPD markers. Weed Res 41:287-300.
Woldesenbet DT, Tesfaye K, Bekele E (2015) Genetic diversity of sesame germplasm collection (*Sesamum indicum* L.): implication for conservation, improvement and use. Int J Biotechnol Mol Biol Res 6:7-18.
Uzun B, Lee D, Donini P (2003) Identification of a molecular marker linked to the closed capsule mutant trait in sesame using AFLP. Plant Breed 122:95-97.
Varshney RK, Chabane K, Hendre PS, Aggarwal RK, Graner A (2007) Comparative assessment of EST-SSR, EST-SNP and AFLP markers for evaluation of genetic diversity and conservation of genetic resources using wild, cultivated and elite barleys. Plant Sci 173:638-649.
Vieira RF, Goldsbrough PB, Simon JE (2003) Genetic diversity of basil based on RAPD markers. J Am Soc Hortic Sci 128:94-99.
Williams JG, Kubelik AR, Livak KJ, Rafalski JA, Tingey SV (1990) DNA polymorphisms amplified by arbitrary primers are useful as genetic markers. Nucleic Acids Res 18:6531-6535.
Yeh FC, Yang R, Boyle T (1999) PopGene: Microsoft Windows-based freeware for population genetical analysis, version 3.2. University of Alberta, Edmonton.
Yermanos DM (1980) Sesame. In Fehr WR and Hadley HH, eds., Hybridization of Crop Plants. Am Soc Agron, CSSA, Madison, Wisconsin, USA. 549-563.
Zhang H, Wei L, Miao H, Zhang T, Wang C (2012) Development and validation of genetic-SSR markers in sesame by RNA-seq. BMC Genomics 13:316

Acta Biologica Szegediensis

Volume 63(1):25-30, 2019
Acta Biologica Szegediensis
http://abs.bibl.u-szeged.hu/index.php/abs
DOI:10.14232/abs.2019.1.25-30

ARTICLE

Genetic diversity within local and introduced cultivars of wheat (*Triticum aestivum* L.) grown under Mediterranean environment as revealed by AFLP markers

Arabi M.I.E., Shoaib A., Al-Shehadah E., Jawhar M.*

Department of Molecular Biology and Biotechnology, Atomic Energy Commission of Syria, Damascus, Syria

ABSTRACT Information on genetic diversity among cultivars is critical in wheat improvement. In this work, heterogeneity within local and introduced cultivars of bread wheat grown in Syria was investigated using amplified fragment length polymorphism (AFLP) markers. The eight primer pairs were used to detect 177 polymorphic bands among the 21 cultivars resulting in an average of 22.13 (57.3%) polymorphic loci per primer pair. Major allelic frequency ranged from 0.50 to 0.75 with a mean 0.64, and estimated gene diversity was 0.45. Values of average polymorphic information content (PIC) for these markers were estimated to be 0.34. This low value might be attributed to the rigorous selection pressure aimed at cultivar purity and associated breeding practices. Dissimilarity values ranged from 0.32 to 0.66 with an average of 0.54, indicating that such techniques sample distinct genome regions. Three major subgroups of wheat cultivars were identified using the unweighted pair-group method with arithmetic means analysis (UPGMA), with all local cultivars falling into one cluster, which was confirmed by a principal component analysis (PCA). The narrow genetic diversity observed among Syrian wheat cultivars suggests the need of broadening the genetic base of wheat breeding materials, including local landraces.

KEY WORDS
AFLP markers
bread wheat
genetic diversity
germplasm
PIC

ARTICLE INFORMATION
Submitted
16 May 2019.
Accepted
10 July 2019.
***Corresponding author**
E-mail: ascientific2@aec.org.sy

Introduction

Bread wheat (*Triticum aestivum* L.) is one of the most important cereal crops in the world. Simultaneously, the demand for food is increasing due to the growing world population and the dietary changes in countries with rapidly growing economies (Enghiad et al. 2017). In Syria, the production of bread wheat differs from year to year depending on climatic conditions and cultivated genotype (Wahid et al. 2007). Thus, development of high yielding wheat cultivars with better quality has always been a major objective of wheat breeding programs (Birhanu et al. 2016). However, success in wheat improvement in the long term generally depends on the magnitude of genetic variation and the extent to which the desirable characters are heritable (Naghavi and Marouf 2017).

Breeders usually cross elite wheat lines within a defined germplasm pool expecting to assemble better allele combinations in the progeny (Li et al. 2018). Intercrosses of existing elite wheat germplasm in each breeding cycle and selection has further narrowed the genetic diversity by the depletion of few alleles from a more diverse gene pool (Cox 1997). Importantly, monitoring genetic diversity levels within a breeding material is crucial for avoiding genetic erosion and for ensuring long-term selection potential (Fu 2015). Moreover, assessing and understanding the genetic structure of a crop population is an important first step towards linking genetics to phenotypic variation. The genetic structure of the *T. aestivum* cultivars grown in the Mediterranean basin including Syria varies largely and its is characterized by a high diversity, to modern varieties characterized by high yield potential, wide adaptation and technological quality (Mirali 2000; Shoiab and Arabi 2004). These differences could be caused by different breeding practices and requirements, one being that intensive selection pressure in wheat breeding began earlier in Northern and Western Europe (Orabi et al. 2014). Additionally, chromosomal differences can be caused by the introduction of certain germplasm in specific geographical regions (Purnhauser et al. 2010). However, genetic diversity in a modern agricultural setting can be estimated as a function of the range of wheat cultivars grown by farmers under geographical area at a given time (Matsuoka 2011).

The use of molecular markers for wheat genetic studies has recently received a great deal of attention from wheat breeders. However, the efficiency of polymorphism

detection by amplified fragment length polymorphism (AFLP) in wheat is high compared with other available marker systems (Martos et al. 2005; Ejaz et al. 2015) since the AFLP technique combines the RFLP reliability with the power of PCR to amplify simultaneously many restriction fragments (Vos et al. 1995).

The aim of this work was to study the AFLP-genetic diversity within local and introduced cultivars of bread wheat grown in Syria which is typical of Mediterranean environments.

Materials and Methods

Plant material

Seeds from twenty-one wheat (*Triticum aestivum* L.) cultivars were selected to represent the germplasm grown in Syria. Seeds were provided by Syrian General Commission for Scientific Agricultural Research (SGCASR) at Douma, Syria and used in this study. They included five old local cultivars (Cham 2, Cham 6, Cham 8, Bouhouth 4 and Bouhouth 6) and 16 introduced cultivars (Table 1). Cham 2, 6 and 8 were developed in CIMMYT/ICARDA and released in 1984, 1991 and 1998, respectively. Bouhouth 4 and 6 were developed by SGCASR in 1987 and 1991, respectively. Twenty seeds from each cultivar were randomly selected and sown in a growth chamber at 22 °C for 3 weeks and 1-2 g of fresh leaf material was harvested for DNA extraction.

DNA extraction

Genomic DNA was isolated from 15 individual plants of each cultivar according to the method of Doyle and Doyle (1990), with some modifications. DNA was quantified by spectrophotometer, by absorbance at 260/280 nm. The DNA quality was then checked on 2% agarose gel.

AFLP assays

The AFLP procedure (Vos et al. 1995) as modified by Pillay and Myers (1999) was used to assess the genetic diversity. DNA was double digested with *Eco*RI and *Mse*RI at 37 °C for 3 hrs. A small aliquot of the digested DNA was run on a 1.5% (w/v) agarose gel to check if the DNA digestion was complete. The digested samples were incubated at 70 °C for 15 min to inactivate the restriction endonucleases. *Eco*RI and *Mse*RI adapters were ligated to the digested DNA samples to generate template DNA for amplification. Pre-amplification was carried out with +1-primers each

Table 1. Names and origins of 21 bread wheat cultivars used in this study.

Species	Name	Code	Origin
Local cultivars	Cham2	Ch2	Syria (CIMMYT/ICARDA)*
	Cham6	Ch6	"
	Cham8	Ch8	"
Introduced cultivars	Bouhouth4	Bou4	Syria (Developed by SGCASR)**
	Bouhouth6	Bou6	"
	ACSAD 885	Ac885	Syria (Developed by ACSAD)***
	ACSAD 59	Ac59	"
	ACSAD 367	Ac367	"
	ACSAD 305	Ac305	"
	ACSAD 67	Ac67	"
	ACSAD 529	Ac529	"
	ACSAD 883	Ac883	"
	ACSAD 851	Ac851	"
	ACSAD 853	Ac853	"
	ACSAD 857	Ac857	"
	ACSAD 805	Ac805	"
	ACSAD 653	Ac653	"
	ICARDA MR17-41	Ic41	Syria (Developed by ICARDA)****
	ICARDA MR16-40	Ic40	"
	ICARDA MR19-43	Ic43	"
	ICARDA MR20-44	IC44	"

*The International Maize and Wheat Improvement Center, **Syrian General Commission of the Agricultural Scientific Research, ***The Arab Center for the Studies of Arid Zones and Dry Lands, Syria, ****The International Center for Agriculture Research in the Dry Areas

Table 2. AFLP band numbers and polymorphic bands revealed by eight primer pairs in 21 wheat cultivars.

Primer pair	Total	Polymorphic bands	% of polymorphic bands
E-ACG X M-CAG	40	25	62.5
E-ACT X M-CAG	30	21	70.0
E-ACG X CAT	42	33	78.6
E-AAG X M-CTA	45	27	60.0
E-ACG X M-CAC	43	25	58.1
E-AGC X M-CTA	41	17	41.5
E-ACG X M-CTA	33	15	45.5
E-AGG X M-CAG	33	14	42.4
Mean	38.38	22.13	57.3

carrying one selective nucleotide (*Eco*RI + A, *Mse*RI + C) in a Gene Amp 9700 Thermocycler (Applied Biosystems, USA) for 20 cycles set at 94 °C denaturation (30 sec), 56 °C annealing (40 sec), and 72 °C extension (50 sec). The initial denaturation was done at 94 °C for 30 sec and the final extension at 72 °C for 8 min. The amplification products were diluted 10-fold in H_2O and stored at -20 °C. Selective AFLP amplification was carried out with *Eco*RI + 3 and *Mse*RI +3 primers and 5 µL of the diluted PCR products from the pre-amplification.

Eight *Eco*RI, *Mse*I primer pairs were screened on 21 wheat cultivars to assess the ability of these primer pairs to detect molecular variation (Table 2). The PCR amplifications were carried out as follows: one cycle at 94 °C for 30 sec, 68 °C for 30 sec, and 72 °C for 60 sec; followed by 12 cycles of touchdown PCR in which the annealing temperature was decreased by 0.7 °C every cycle until a touchdown annealing temperature of 59 °C was reached. Once reached, another 20 cycles were conducted as described above for pre-amplification. The reaction product (8 µl) was mixed with 4 µl of formamide loading buffer (98% [v/v] formamide, 10 mM EDTA, 0.005% [v/v] of each of xylene cyanol and bromophenol blue) denatured by incubating at 90 °C for 3 min and quickly cooled on ice. The products were analyzed on a 6% (w/v) denaturing polyacrylamide gels. The gel was run at constant power (60 W) until the xylene cyanol was about two-thirds down the length of the gel. The experiments were repeated twice for each cultivar to confirm the repeatability and the monomorphic bands were removed from the analysis.

Marker polymorphism

Each silver stained AFLP gel was manually scored (1 for present, 0 for absent) and entered into a data matrix. The number of polymorphic and monomorphic bands was recorded for each primer combination; however, monomorphic bands were excluded from data analyses. Percentage of polymorphism was calculated as the proportion of polymorphic bands over the total number of bands. Allelic polymorphic information content (PIC) was calculated using the following formula:

$$PIC = 1-\Sigma(P_i)^2$$

Where Pi is the proportion of the population carrying the i^{th} allele, calculated for each AFLP locus (Anderson et al. 1993).

Genetic diversity estimation and cluster analysis

The genetic dissimilarity (*D*) matrix among cultivars was estimated according to Nei and Li (1979) coefficient. Principal coordinate analysis (PCA) based on genetic distance matrix was performed using the DCENTER and EIGEN algorithms of the NTSYS-pc software package (Rohlf 1992). Unweighted Pair-Group Method with Arithmetic Average (UPGMA), *i.e.* cluster analysis was used to assess pattern of diversity among wheat cultivars.

Results and Discussion

AFLP analysis generated a large number, of reproducible and unambiguous markers for fingerprinting T. *aestivum* cultivars used in the study. Initially DNA fingerprints were created using eight different AFLP primer combinations, from which three were selected for analysis. The primer pairs were sufficient to detect 177 polymorphic bands among the 21 cultivars resulting in an average of 22.13 (57.3%) polymorphic loci per primer pair. Details of the bands scored with the different primer combinations are illustrated in Table 2. The PIC values in the present study ranged from 0.30 to 0.37, with an average of 0.34. Major allelic frequency ranged from 0.50 (Ic43) to 0.75 (Ch2 and Ch6) with a mean of 0.64, and an estimated gene diversity of 0.45 (Table 3).

The pair-wise dissimilarity (*D*) matrix is presented in Table 4. Mean value of *D* was 0.54, ranging from 0.32 to 0.66. The highest *D* (0.64) was obtained between cultivars Ic41 and Ac805, and between Ic66 and Ch6. The lowest *D* was at AC885 and Bou6 with *D* of 0.32. This might be due to their common ecological and evolutionary story. Cluster analysis using the Nei's genetic distance algorithm separated the local from the introduced wheat cultivars into three clusters, with all local cultivars falling into one cluster, which can be further divided into three subgroups. Interestingly, all the local cultivars fall together under this cluster (Fig. 1). The PCA analysis with the entire AFLP data separated the local from the introduced wheat cultivars and formed distinct groups (Fig. 2). Knowledge about the genetic variation among bread wheat cultivars

Table 3. Polymorphic information content (PIC), amplified alleles and gene diversity as revealed by AFLP.

Cultivar	Major Allele Frequency	Gene Diversity	PIC
Ch2	0.7526	0.3724	0.3030
Ch6	0.7526	0.3724	0.3030
Ch8	0.6947	0.4242	0.3342
Bou4	0.6474	0.4566	0.3523
Bou6	0.6842	0.4321	0.3388
Ac885	0.7105	0.4114	0.3267
Ac59	0.5737	0.4891	0.3695
Ac367	0.5579	0.4933	0.3716
Ac305	0.6158	0.4732	0.3612
Ac67	0.6579	0.4501	0.3488
Ac529	0.7368	0.3878	0.3126
Ac883	0.7105	0.4114	0.3267
Ac851	0.6842	0.4321	0.3388
Ac853	0.6421	0.4596	0.3540
Ac857	0.6000	0.4800	0.3648
Ac805	0.6789	0.4360	0.3409
Ac653	0.5632	0.4920	0.3710
Ic41	0.5474	0.4955	0.3727
Ic40	0.5737	0.4891	0.3695
Ic43	0.5579	0.4933	0.3716
Ic44	0.5000	0.5000	0.3750
Mean	0.6401	0.4501	0.3480

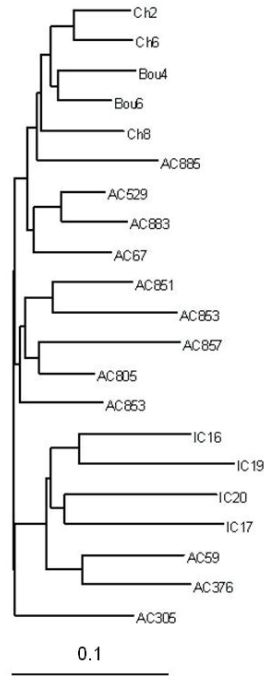

Figure 1. UPGMA dendrogram based on genetic similarities discriminated all the bread wheat cultivars used in this study.

is essential for the effective use of genetic resources in breeding programs (Li et al. 2018). The primary aim of this study was to examine the genetic diversity within Syrian local and introduced bread wheat cultivars using AFLP markers to obtain useful molecular data regarding the local gene pool. Results showed a decrease in the genetic diversity over time in Syrian bread wheat cultivars, which might be due to the intensive use of a limited number of cultivars as progenitors in different Syrian breeding programs.

The low PIC and dissimilarity values found among the local and introduced cultivars in this study, might be attributed to the rigorous selection pressure aimed at cultivar purity and associated breeding practices. Such practices, which are aimed at genetic homogenization and purity of varieties, may result in an improvement in yield and other agronomically important traits at the expense of reduction in the genetic base of crops. A low values of PIC were also obtained in other earlier studies on wheat (Plaschke et al. 1995; El-Esawi et al. 2018). Our results can be supported also by Huang et al. (2002) who suggested also that genetic diversity in wheat is narrow due to a modern breeding.

In this work, AFLP fingerprinting for estimating the levels of genetic diversity in local and introduced bread wheat cultivars revealed an apparent narrow genetic variability (Tables 2, 3). The estimated gene diversity was 0.45, which was lower than the estimates of 0.66 in 43 bread wheat cultivars from 7 USA market classes (Chao et al. 2007) and 0.77 in 998 accessions from 68 countries (Huang et al. 2002). Earlier works reported that the higher gene diversity among bread wheat cultivars attributed to the use of genetic materials from well defined market classes or landraces, or genotypes from gene banks, or cultivars from various geographic locations (Plaschke et al. 1995; Roussel et al. 2004). However, it is widely believed that modern breeding practices have led to a noticeable decrease of genetic diversity in modern cultivars (Vellve 1993). This erosion in genetic variation might result in reduction of the plasticity of crops to respond to changes in weather, agricultural practices, disease populations, or modern requirements (Manifesto et al. 2001). The AFLP marker dendrogram showing genetic relationships from UPGMA cluster analysis revealed three major groups and subgroups and separated the local from the introduced wheat cultivars. Reasons for the presence of subgroups within larger can be attributed to differences in genetic pool, geographical origin, human or environmentally driven selection or genetic drift (Buckler and Thornsberry 2002). However, the Syrian local cultivars were mainly grown in a very local and restricted geographical area, making transport to distant zones from their local origin

Table 4. Matrix of pair-wise genetic dissimilarity among Syrian bread wheat cultivars based on Nei and Li coefficients.

	Ch 8	Ch 2	Ch 6	Bo 4	Bo 6	AC 885	AC 59	AC 367	AC 305	AC 67	AC 529	AC 883	AC 851	AC 853	AC 857	AC 805	AC 963	IC 44	IC 41	IC 40
Ch 8	0.00																			
Ch 2	0.44	0.00																		
Ch 6	0.44	0.37	0.00																	
Bo 4	0.44	0.45	0.40	0.00																
Bo 6	0.44	0.43	0.40	0.38	0.00															
AC 885	0.40	0.44	0.46	0.41	0.32	0.00														
AC 59	0.55	0.55	0.59	0.57	0.50	0.47	0.00													
AC 367	0.56	0.57	0.62	0.59	0.53	0.52	0.42	0.00												
AC 305	0.53	0.51	0.55	0.53	0.50	0.51	0.55	0.52	0.00											
AC 67	0.47	0.48	0.49	0.44	0.43	0.42	0.51	0.53	0.48	0.00										
AC 529	0.46	0.45	0.44	0.48	0.41	0.40	0.53	0.54	0.46	0.40	0.00									
AC 883	0.44	0.51	0.45	0.48	0.46	0.42	0.58	0.60	0.50	0.45	0.35	0.00								
AC 851	0.48	0.50	0.49	0.53	0.48	0.49	0.52	0.55	0.49	0.52	0.48	0.52	0.00							
AC 853	0.45	0.45	0.49	0.46	0.46	0.44	0.52	0.52	0.49	0.44	0.45	0.48	0.46	0.00						
AC 857	0.53	0.54	0.56	0.55	0.53	0.53	0.58	0.58	0.54	0.51	0.54	0.57	0.52	0.47	0.00					
AC 805	0.47	0.48	0.49	0.49	0.45	0.42	0.53	0.55	0.51	0.46	0.43	0.46	0.44	0.39	0.43	0.00				
AC 653	0.58	0.59	0.62	0.61	0.57	0.54	0.55	0.58	0.53	0.56	0.55	0.55	0.45	0.54	0.55	0.46	0.00			
IC 44	0.60	0.62	0.63	0.64	0.60	0.60	0.55	0.58	0.64	0.61	0.62	0.62	0.57	0.57	0.61	0.55	0.55	0.00		
IC 41	0.58	0.60	0.58	0.59	0.58	0.57	0.59	0.58	0.65	0.61	0.61	0.62	0.61	0.58	0.64	0.60	0.67	0.58	0.00	
IC 40	0.57	0.59	0.59	0.58	0.55	0.56	0.58	0.57	0.58	0.55	0.55	0.59	0.58	0.54	0.59	0.56	0.61	0.60	0.56	0.00
IC 43	0.63	0.63	0.66	0.63	0.59	0.59	0.54	0.58	0.60	0.59	0.59	0.62	0.62	0.59	0.65	0.61	0.61	0.59	0.64	0.54

difficult with the exception of population movements. Moreover, cultivars derived from CIMMYT germplasm have been continuously introduced into Syria from the 1970s, and CIMMYT/ICARDA have enormously promoted shuttle breeding and the intensive interchange of germplasm around the world. This could be the reason why introduced bread wheat cultivars presently has a common genetic background. On the other hand, this work revealed that AFLP is a very sensitive method for detecting markers in genetic studies of wheat crops. The banding patterns attained using AFLP were found to be highly reproducible when the same DNA sample was used in independent experiments (Pillay and Myers 1999). Silver staining was used in this study because silver-stained AFLP gels are thought to produce a larger number of better-defined bands than phosphorous-32-labeled gels (Chalhoulb et al. 1997).The AFLP analysis used in the present work demonstrate low PIC and dissimilarity values found among local and introduced bread wheat cultivars grown in Syria, which can be attributed to the rigorous selection pressure aimed at variety purity and associated breeding practices. This suggests the need of broadening the genetic base of Syrian wheat breeding materials, including local landraces.

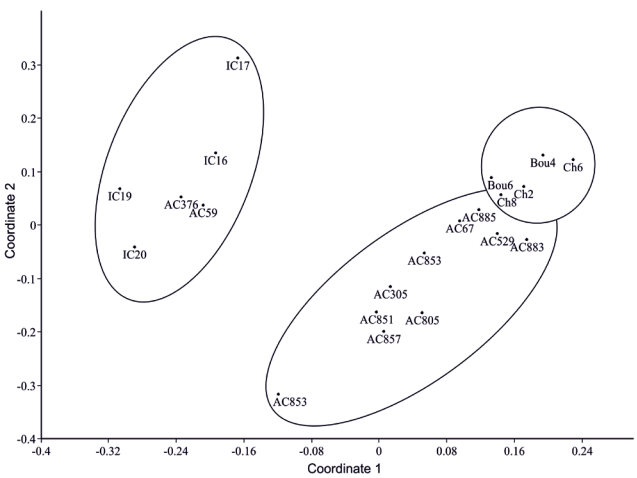

Figure 2. Principal coordinate map of the 21 bread wheat cultivars.

Acknowledgements

The authors thank the Director General of AECS and the Head of the Biotechnology Department for their support this work, and thanks also extended to Dr. Orabi (Copenhagen University) for his critical readings of the manuscript.

References

Anderson JA, Churchill JE, Autrique SD, Tanksley S, Sorrells ME (1993) Optimizing parental selection for genetic linkage maps. Genome 36:181-188.

Birhanu M, Sentayehu A, Alemayehu A, Ermias A, Dargicho D (2016) Genetic variability, heritability and genetic advance for yield and yield related traits in bread wheat (*Triticum aestivum* L.) genotypes. Glob J Sci Front Res 16:12-15.

Buckler ES, Thornsberry JM (2002) Plant molecular diversity and application to genomics. Curr Opin Plant Biol 5:107-111.

Chalhoulb BA, Thibault S, laucou V, Rameau C, Hofte H, Cousin R (1997) Silver staining and recovery of AFLP™ amplification products on large denaturing polyacrylamide gels. Biotech 22:216-220.

Chao S, Zhang W, Dubcovsky J, Sorrells M (2007) Evaluation of genetic diversity and genome-wide linkage disequilibrium among U.S. wheat (*Triticum aestivum* L.) germplasm representing different market classes. Crop Sci 47:1018-1030.

Cox T (1997) Deepening the wheat gene pool. J Crop Prod 1:145-168.

Doyle JJ, Doyle JL (1990) Isolation of plant DNA from fresh tissue. Focus 12:3-15.

El-Esawi M, Witczak J, Abomohra AE, Ali HM, Elshikh MS, Margaret AM (2018) Analysis of the genetic diversity and population structure of Austrian and Belgian wheat germplasm within a regional context based on DArT markers. Genes 9:47.

Ejaz M, Qidi Z, Gaisheng Z, Na N, Huiyan Z, Qunzhu W (2015) Analysis of genetic diversity identified by amplified fragment length polymorphism marker in hybrid wheat. Genet Mol Res 14:8935-8946.

Enghiad A, Danielle Ufer D, Countryman AM, Thilmany DD (2017) An overview of global wheat market fundamentals in an era of climate concerns. Int J Agron 17:1-15.

Fu YB (2015) Understanding crop genetic diversity under modern plant breeding. Theor Appl Genet 128:2131-2142.

Hung XQ, Borner A, Roder MS, Ganal MW (2002) Assessing genetic diversity of wheat (*Triticum aestivum* L.) germplasm using microsatellite markers. Theor Appl Genet 105:699-707.

Li A, Liu D, Yang W, Kishii M, Mao L (2018) Synthetic hexaploid wheat: yesterday, today, and tomorrow. Engineering 4:552-558.

Manifesto MM, Schlatter AS, Hopp HE, Suarez EY, Dubcovky J (2001) Quantitative evaluation of genetic diversity germplasm using molecular markers. Crop Sci 41:682-690.

Matsuoka Y (2011) Evolution of polyploid *Triticum* wheats under cultivation: the role of domestication, natural hybridization and allopolyploid speciation in their diversification. Plant Cell Physiol 52:750-764.

Martos V, Royo C, Rharrabti Y, Garcia del Morala LF (2005) Using AFLPs to determine phylogenetic relationships and genetic erosion in durum wheat cultivars released in Italy and Spain throughout the 20th century. Field Crop Res 91:107-116.

Mirali N (2000) Heterogeneity within old and modern durum and bread wheat grown in Syria using the A-PAGE and SDS-PAGE electrophoretic techniques. Plant Var Seeds 13:149-157.

Naghavi MR, Marouf K (2017) Evaluation of genetic diversity and traits relations in wheat cultivars under drought stress using advanced statistical methods. Acta Agric Slov 109:403.

Nei M, Li WH (1979) Mathematical model for studying genetic variation in terms of restricting endonucleases. Proc Natl Acad Sci USA 76:5269-5273.

Orabi J, Jahoor A, Backes G (2014) Changes in allelic frequency over time in European bread wheat (*Triticum aestivum* L.) varieties revealed using DArT and SSR markers. Euphytica 197:447-462.

Plaschke J, Ganal MW, Roder MS (1995) Detection of genetic diversity in closely related bread wheat using microsatellite markers. Theor Appl Genet 91:1001-1007.

Pillay M, Myers GO (1999) Genetic diversity in cotton assessed by variation in ribosomal RNA genes and AFLP markers. Crop Sci 39:1881-1886.

Purnhauser L, Bóna L, Láng L (2010) Occurrence of 1BL.1RS wheat-rye chromosome translocation and of Sr36/Pm6 resistance gene cluster in wheat cultivars registered in Hungary. Euphytica 179:287-295.

Rohlf FJ (1992) NTSY-pc. Numerical taxonomy and multivariate analysis system. Exeter Software, Setauket, New York, USA.

Roussel V, Koenig J, Beckert M, Balfourier F (2004) Molecular diversity in French bread wheat accessions related to temporal trends and breeding programs. Theor Appl Genet 108:920-930.

Shoaib A, Arabi MIE (2004) Genetic diversity among Syrian cultivated and landraces wheat revealed by AFLP markers. Genet Res Crop Evol 53:901-906.

Vellve R (1993) The decline of diversity in European agriculture. Ecologist 23:64-69.

Vos P, Hogers R, Bleeker M, Reijans M, Lee T, Hornes M, Frijters A, Pot J, Peleman J, Kuiper M, Zabeau M (1995) AFLP: a new technique for DNA fingerprinting. Nucl Acids Res 23:4407-4414.

Wahid A, Gelani S, Ashraf M, Foolad MR (2007) Heat tolerance in plants: an overview. Environ Exp Bot 61:199-223.

Acta Biologica Szegediensis

Volume 63(1):31-36, 2019
Acta Biologica Szegediensis
http://abs.bibl.u-szeged.hu/index.php/abs

DOI:10.14232/abs.2019.1.31-36

ARTICLE

Cooperative functioning of salicylic acid and phenylalanine ammonia lyase in barley plant challenged with spot blotch and powdery mildew diseases

Al-Daoude A.*, Al-Shehadah E., Shoiab A., Jawhar M., Arabi M. I. E.

Department of Molecular Biology and Biotechnology, AECS, P.O. Box 6091, Damascus, Syria

ABSTRACT Salicylic acid (SA) and phenylalanine ammonia-lyase (*PAL*) have been suggested as important signals during plant resistance towards several fungal pathogens. In this work, to better understand the defense responses initiated by resistant and susceptible barley genotypes challenged with a necrotrophic (*Cochliobolus sativus*; *Cs*) and a biotrophic (*Blumeria graminis*; *Bg*) pathogens, the relative contributions of SA and *PAL* were investigated at early time points of infection. SA signaling was activated in both genotypes 24 hours post infection (hpi) as compared with the non-inoculated plants. However, with or without pathogen pretreatment, SA significantly increased (P = 0.001) in the resistant genotype that contained three-folds of total SA in comparison with the susceptible one for *Bg*. Reverse transcription-polymerase chain reaction (RT-PCR) analysis revealed that *PAL* expression increases in the resistant and susceptible genotypes over the inoculation time points, with the maximum expression observed 48 hpi. *PAL* expression was paralleled by an increase in SA content in leaves as shown by the test coincidence ($F_{3, 32}$ = 1.09, P = 0.49 for *Cs* and $F_{3, 32}$ = 1.03, P = 0.48 for *Bg*). Results showed that the cooperatively function of SA and *PAL* in barley responses to both *Cs* and *Bg* appeared to be dependent on the plant genotype, and that SA signaling and *PAL* play a role in barley interactions with these both pathogens. This study might increase our understanding for a deeper molecular research on barley defense responses against pathogens with different lifestyles.

KEY WORDS

Hordeum vulgare
Blumeria graminis
Cochliobolus sativus
salicylic acid
RT-PCR
PAL expression

ARTICLE INFORMATION

Submitted
17 February 2019.
Accepted
16 April 2019.
***Corresponding author**
E-mail: ascientific@aec.org.sy

Introduction

Powdery mildew caused by the obligate biotrophic pathogen, *Blumeria graminis* f. sp. *hordei* (*Bg*), and spot blotch caused by the necrotrophic [*Cochliobolus sativus* (*Cs*) Drechs. ex Dastur] are two globally distributed fungal pathogens of barley causing substantial yield losses (Kumar et al. 2002; Rsaliyev et al. 2017). Barley plants respond to both pathogens by activating different mechanisms that are regulated through different plant signaling pathways, including plant hormones such as SA and pathogenesis-related (PR) proteins (Bindschedler et al. 1998; Jawhar et al. 2017).

Salicylic acid (SA) has been found to regulate the expression of many defense genes (Zwart et al. 2017), which results in altered accumulation of some secondary metabolites. Among them, phenylalanine lyase (*PAL*) which plays an important role in plant defence and is involved in SA biosynthesis, an essential signal involved in plant systemic resistance (Nugroho et al. 2002; Chaman et al. 2003). Therefore, discovery of SA targets and the understanding of their molecular modes of action in physiological processes could help dissect the SA signaling network, confirming its important role in plant responses to fungal diseases (Vásquez et al. 2015). However, the association between SA and the secondary metabolites synthesized via *PAL* under fungal pathogen with different lifestyles is unclear. SA effects associated with fungal pathogen infection. However, the role of SA accumulation has not been revealed in full details from the aspect of pathogen lifestyles. Previous works have suggested that plants synthesize SA from phenylalanine (Chen et al. 2009), however, SA could still be produced when this pathway was inhibited. Some bacteria and higher plants are able to synthesize SA using isochorismate synthase (ICS) and pyruvate lyase. In *Arabidopsis* SA is synthesized from chorismate by means of ICS, and SA made by this pathway is required for local and systemic acquired resistance (Wildermuth et al. 2001).

Reverse transcription-polymerase chain reaction (RT-PCR) is the most reliable technique for measuring the relative expression level of a particular transcript and determining its expression after exposure to a specific

alteration, such as infection by a fungal pathogen (Bates et al. 2001). In the current work, we studied the defense responses of two barley genotypes Banteng and WI 2291, which are integrated in international breeding programs aimed at developing *Cs* and *Bg* resistant barley genotypes. Banteng was described as a highly resistant to the both pathogens (Arabi and Jawhar 2004, 2012), i.e. exhibited a lower level (compared with WI2291) of *Cs* and *Bg* symptom development. We thus hypothesized that SA-triggered defenses could drive contrasted levels of resistance in Banteng and WI2291, inoculated by the same isolate of each pathogen. Thus, the current work aimed at evaluating the changes in SA content and induction of *PAL* gene expression in two barley cultivars with different levels of resistance towards *Cs* and *Bg* pathogens.

Materials and Methods

Plant material and experimental design

The most resistant cv. Banteng and the universal susceptible control cv. WI2291 to all *Cs* and *Bg* isolates available for more than 15 years (Arabi and Jawhar 2004, 2012) were used in this study. Seeds of each genotype were planted in plastic boxes (60 × 40 × 8 cm) filled with sterilized peat-moss with three replicates for each pathogen, and each experimental unit consisted of 10 seedlings. They were placed in a growth chamber in a randomized complete block design at temperatures 22 °C/18 °C (day/night) with 12-h photoperiod (light intensity was maintained > 200 w/m^2) and 90% relative humidity.

Infection with Cs

The most virulent pathotype (*Pt4*) of *C. sativus* (Arabi and Jawhar 2004) was used in the experiments. The fungus was incubated in Petri dishes containing potato dextrose agar (PDA, DIFCO, Detroit, MI, USA) for 10 days under 20-21 °C in the dark. Conidia were collected with sterile distilled water and the suspension was adjusted to 2 x 10^4 conidia/mL. A surfactant (polyoxyethylene-20-sorbitan monolaurate) was added (100 µL/L) to the conidial suspension to facilitate dispersion of the inoculum over the leaf surfaces. The primary leaves of 12-day-old seedlings were inoculated by uniformly spraying each plant with the conidial suspension using a hand-held spray bottle. *C. sativus* inoculum preparation, inoculation, post-inoculation and disease records were similar to those described by Fetch and Steffenson (1999) using the percentage of leaf area exhibiting disease symptoms for each genotype were determined using a numerical scale of 1 to 9 with 1 being the most resistant and 9 very susceptible (Fetch and Steffenson 1999). Infection responses 1-3 were deemed resistant, 4-5 moderate, and 6 to 9 deemed susceptible.

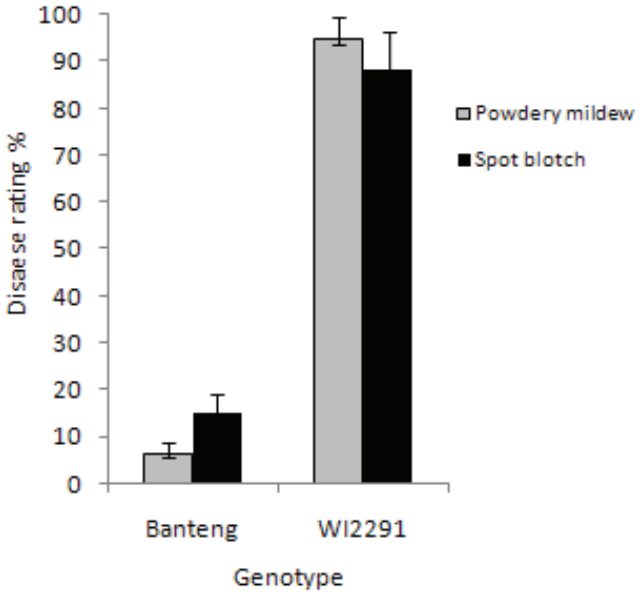

Figure 1. Frequency of disease reactions incited on barley highly resistant genotype Banteng and highly susceptible genotype WI2291 by *Cs* and *Bg*. Spot blotch and powdery mildew infections were scored according to Fetch and Steffenson (1999) and Moseman et al. (1981), respectively.

Infection with Bg

Infection was performed at 12-day-old seedlings following the protocol described by Chaure et al. (2000). Conidiospores of a virulent *Bg* isolate were used by employing a soft hair brush to give about 10-20 conidia per one microscope field at ×150 magnification. Inoculated plants were placed under growth chamber conditions, while uninoculated control plants were transferred to a separate "clean" growth chamber and kept under plastic boxes to avoid infection with *Bg*. Infections were recorded according to the scale 0-100 described by Moseman et al. (1981) where: 0 = no visible symptoms; 100 = heavy sporulation and all the leaf area covered by a layer of *powdery mildew* mycelium.

SA quantification

Pooled samples were prepared from barley leaves taken 24, 48, 72 and 96 hours post inoculation (hpi). For each time point studied, six pooled sample replicates were used for quantification. Free SA was extracted from approximately 200 mg of freshly ground leaves in 1.5 ml tubes following the method described by Trapp et al. (2014), with minor modifications. Briefly, 100 mg of plant material were dried overnight in a freeze drier at −42 °C. The extraction was achieved by adding 1.0 mL of ethyl acetate, dichloromethane, isopropanol, MeOH:H_2O into each tube containing dry plant material. Samples were shaken for 30 min and centrifuged at 16 000 g and

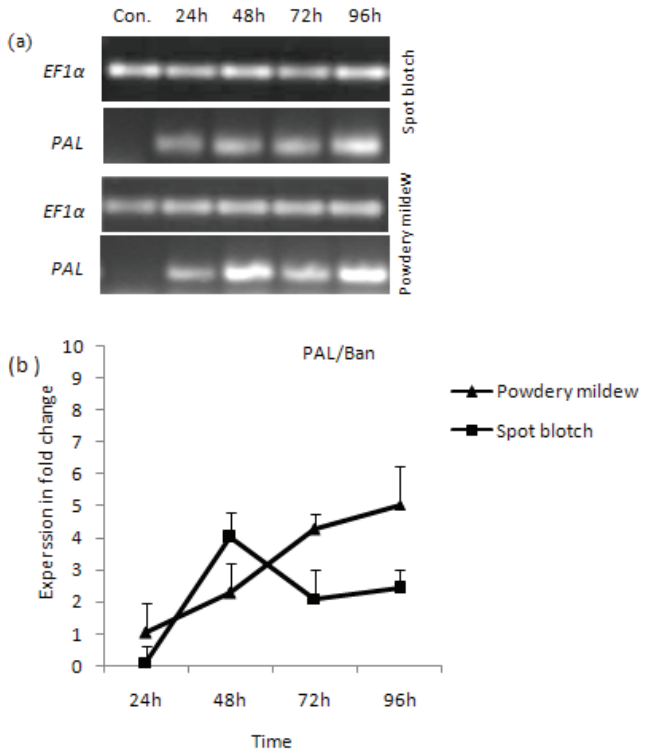

Figure 2. Relative expression profiles of *PAL* gene in the resistant cv. Banteng, 24, 48, 72 and 96 hours post inoculation with spot blotch and powdery mildew diseases on 1% agarose gel (a) and its quantification (b).

4 °C for 5 min. The supernatant was transferred into a new 1.5 microcentrifuge tube and dried in a speed vac. After drying, 100 µL of MeOH was added to each sample, homogenized under vortex and centrifuged at 16 000 g and 4 °C for 10 min. SA measurement was performed by a high-performance liquid chromatography (HPLC) system (Agilent Technologies, Germany) connected to a fluorescent detector using an excitation wavelength (λ_{EX}) of 300 nm and an emission wavelength (λ_{EX}) of 410 nm as described by Verberne et al. (2002). UV detection was performed at 300 nm. Changes in SA content were compared to the control for each time point. Six independent repetitions were performed for each time point. Data were analyzed using the standard deviation and t-test methods.

RNA isolation and cDNA synthesis

RNA extraction was carried out as described by Cao et al. (1997). Primary leaves of three individual biological replicates collected at 24, 48, 72 and 96 hpi and homogenized with a tube pestle in liquid nitrogen. mRNA was extracted with the Nucleotrap mRNA mini kit (Macherey-Nagel, Germany) following the manufacturer's instructions. RNA was used for cDNA synthesis with the QuantiTect Reverse Transcription Kit (Qiagen) following the manufacturer's instructions. At the same time points, samples from mock inoculated plants were collected as controls. The resulting cDNA products were diluted 20-fold with autoclaved distilled water, and 2.5 µL of the diluted solution was used for quantitative PCR (per). PAL expression was assayed in Step One Plus, 96 well using SYBR Green Master kit (Roche, USA). All cDNA samples, standards and controls (which were tested not to contain genomic DNA) were assayed in triplicate. PCR primers for *PAL* were designed based on the cDNA sequences of barley available at NCBI (http://www.ncbi.nlm.nih.gov) database (Id: M23548.1) using Primer 3 software. The sequence information for all RT-PCR primers is given in Table 1. The threshold cycle (Ct) value was automatically determined for each reaction by the real time PCR system with default parameters. Seedlings inoculated with distilled water served as a control.

Data analysis

The fluorescence readings of three replicated samples were averaged, and the blank value (from no-DNA control) was subtracted. Relative expression levels were determined using the average cycle threshold (Ct). Average Ct values were calculated from the triplicate experiment conducted for each gene, with the ΔCT value determined by subtracting the average Ct value of genes from the Ct value of the *EF1α* gene. Finally, the equation $2^{-\Delta\Delta CT}$ was used to estimate relative expression levels (Livak and Schmittgen 2001). Standard deviation was calculated from the replicated experimental data. The statistical analysis was conducted through the Tukey's test at the 0.05 level. The assumption of coincidence was tested using the ANOVA procedure implemented in the software package Statistica 6.1.

Table 1. List of the oligonucleotides used in this study.

Gene	Gene description	Accession number	Sequence	Amplified fragment (bp)
EF1α	Elongation factor-1 alpha	CV066174	GGCTGATTGTGCTGTGCTTA (R)	153
			TGGTGGCATCCATCTTGTTA (F)	
PAL	Phenylalanine amino lyase	AT2G14610	CCATTGATGAAGCCAAAGCAAG (R)	123
			ATGAGTGGGTTATCGTTGACGG (F)	

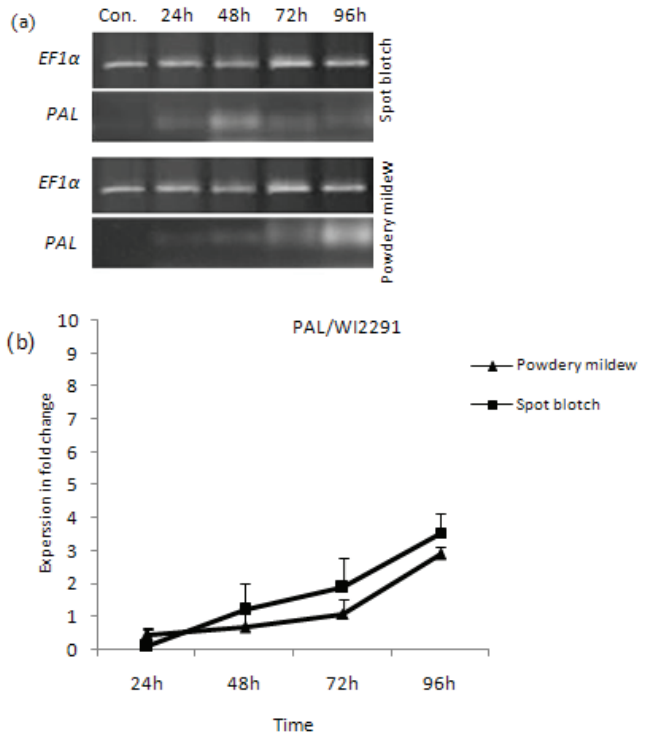

Figure 3. Relative expression of *PAL* in the susceptible cv. WI2291, 24, 48, 72 and 96 hours post infection by spot blotch and powdery mildew diseases on 1% agarose gel (a) and its quantification (b).

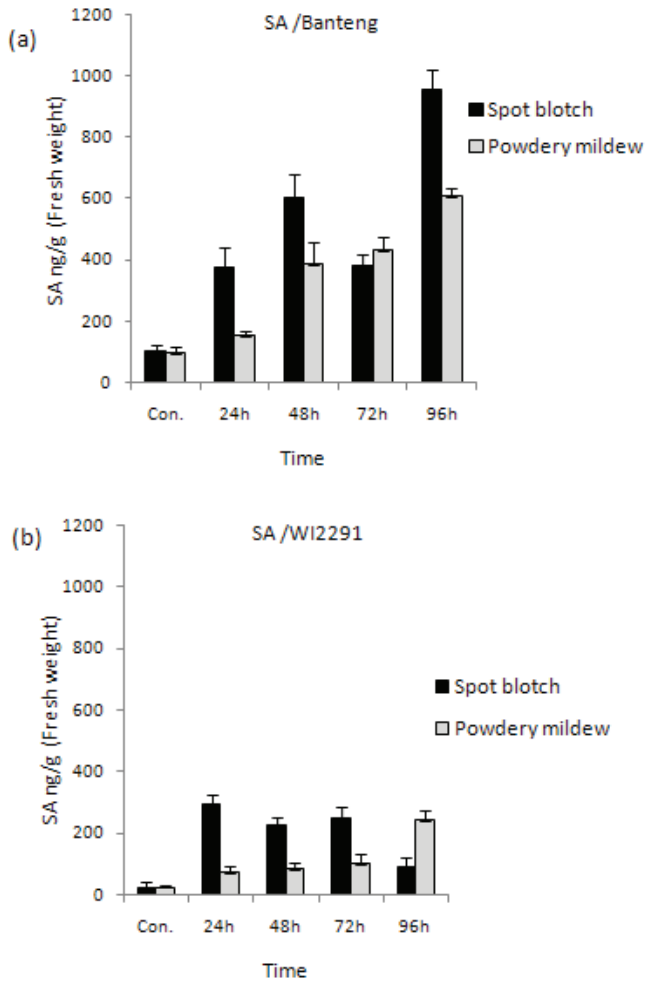

Figure 4. Free salycilic acid quatification in barley leaves post inoculation with spot blotch and powdery mildew in the resistant cv. Banteng (a) and the susceptible cv. WI2291 (b). Error bars represent the stantard error of the means (n = 3).

Results and Discussion

In this study, we used two barley genotypes with different resistant levels to *Cs* and *Bg* infections. As shown in Figure 1, both pathogens caused more severe infection on the susceptible genotype WI2291 as compared with the resistant one Banteng. These results are in agreement with our previous observations under natural field conditions (Arabi and Jawhar 2004, 2012).

Our analysis showed that *PAL* gene in the resistant barley genotype exhibited a differential expression by $P = 0.05$, and were inversely regulated during different time points post inoculation. However at 48 hpi, *PAL* expression was significantly expressed with 2.4- and 5.1-fold increases, respectively, for barley infected with *Bg* as compared with *Cs*. In contrast, *PAL* was up-regulated 24 hpi and down-regulated 72 hpi in *Cs* inoculated barley plants as compared to its expression in *Bg* infected plants, suggesting its role at early stages of defense against a biotrophic attack (Fig. 2 and 3). In addition, SA content increased at early time points after pathogen challenge, mainly at 24 hpi in comparison with non-inoculated plants (Fig. 4). It was found that Banteng contained significantly ($P = 0.001$) higher levels of total SA than WI2291 at each time point investigated for both pathogens, which might reflect the expected role of SA in signaling events during both *Cs* and *Bg* infection. However, *PAL* expression was paralleled by an increase in leaf SA content as shown by the coincidence test ($F_{3, 32} = 1.09$, $P = 0.49$ for *Cs* and $F_{3, 32} = 1.03$, $P = 0.48$ for *Bg*). This is supported by previous works indicating that *PAL* plays an important role in plant defence; it is involved in the biosynthesis of SA, which is an essential signal involved in plant systemic resistance (Nugroho et al. 2002; Chaman et al. 2003).

RT-PCR expression analysis revealed that the *PAL* expression increased in the resistant and susceptible genotypes over the inoculation time points for both pathogens, with the highest expression at 96 dpi. It has been found that *PAL* catalyses the non-oxidative deamination of phenylalanine to *trans*-cinnamate. This is the first step in the phenylpropanoid pathway, and is an important regulation point between primary and sec-

ondary metabolism (Huang *et al.* 2010; Vogt 2010). This phenomenon may be the cause of barley cell wall leakage during *Cs and Bg* infestations.

The resistant genotype Banteng used for this study was proved to be the most resistant genotype to all isolates of each pathogen available so far (Arabi and Jawhar 2004 2012). The higher activities of *PAL* and higher level of SA in infected Banteng leaf tissues compared with the susceptible genotype WI 2291 may explain its high level of resistance. Our finding might support the results of Häffner et al. (2014), who reported that the endogenous SA level in a plant is the main factor of the susceptibility in barley, since pathogen infection may induce plant responses regulated by SA. In addition, SA accumulation was closely associated with redox homeostasis, hypersensitive response, and systemic acquired resistance (Alvarez 2000; Dong 2004).

Moreover, the observed correlation between SA and *PAL* expression results strengthened when the seedlings were subjected to both *Cs* and *Bg* infections, which is expected given that most secondary metabolites function in improving barley resistance towards both pathogens. One possibility is that SA accumulating in pathogen-infected plants is specifically derived from the PAL isoforms whose expression is induced in the pathogen-infected plants (Chen et al. 2009). However, in contrast to necrotrophs, the biotroph pathogens secrete limited amounts of lytic enzymes, generally lack toxin production and evade detection or suppress immune responses through manipulation of host defenses (Oliver and Ipcho 2004). It has been found that biotrophic *Uromyces vignae* and the hemibiotrophs *Ustilago maydis* have suppressed the host defenses during the biotrophic phase (Doehlemann et al. 2008). These findings might support our results when *PAL* was activated at 24 hpi for *Bg* infection.

This work sheds some light on the relative contributions of SA and *PAL* during the necrotrophic (*Cs*) and biotrophic (*Bg*) barley interactions. Results showed that their contribution to the resistance response appears to depend on the plant genotype. It is noteworthy that both SA and *PAL* have a higher constitutive expression and faster induction in the resistant genotype as compared with the susceptible one. The data demonstrated that the *PAL* pathway is involved in SA synthesis in barley and more strongly correlated under both pathogens. The obtained results improve our understanding of the manner in which SA regulates secondary metabolites in barley-biotrophic and necrotrophic interactions.

Acknowledgements

The authors thank the Director General of AECS and the Head of Molecular Biology and Biotechnology Department for their much appreciated help throughout the period of this research.

References

Alvarez ME (2000) Salicylic acid in the machinery of hypersensitive cell death and disease resistance. Plant Mol Biol 44:429-442.

Arabi MIE, Jawhar M (2004) Identification of *Cochliobolus sativus* (spot blotch) isolates expressing differential virulence on barley genotypes in Syria. J Phytopathol 152:461-464.

Arabi MI E, Jawhar M (2012) Expression of resistance to *Blumeria graminis* in barley genotypes (*Hordeum vulgare* L.) under field and controlled conditions. J Plant Biol Res 2:107-112.

Bates J, Taylor E, Kenyon D, Thomas J (2001) The application of real-time PCR to the identification, detection and quantification of *Pyrenophora* species in barley seed. Mol Plant Pathol 2:49-57.

Bindschedler VL, Métraux JP, Schweizer P (1998) Salicylic acid accumulation in barley is pathogen specific but not required for defense-gene activation. Mol Plant-Microbe Inter 11:702-705.

Cao H, Glazebrook J, Clark JD, Volko S, Dong X (1997) The *Arabidopsis* NPR1 gene that controls systemic acquired resistance encodes a novel protein containing ankyrin repeats. Cell 88:57-64.

Chaman ME, Copaja SV, Argandoña VH (2003) Relationships between salicylic acid content, phenylalanine ammonia-lyase (*PAL*) activity, and resistance of barley to aphid infestation. J Agric Food Chem 51:2227-2231.

Chaure P, Gurr SJ, Spanu P (2000) Stable transformation of *Erysiphe graminis*, an obligate biotrophic pathogen of barley. Nat Biotechnol 18:205-207.

Chen Z, Zheng Z, Huang J, Lai Z, Fan B (2009) Biosynthesis of salicylic acid in plants. Plant Sign Behav 4:493-496.

Doehlemann G, Wahl R, Vranes M, De Vries RP, Kämper J, Kahmann R (2008) Establishment of compatibility in the *Ustilago maydis*/maize pathosystem. J Plant Physiol 165:29-40.

Dong XN (2004) NPR1 all things considered. Curr Opin Plant Biol 7:547-552.

Fetch TG, Steffenson BJ (1999) Rating scales for assessing infection responses of barley infected with *Cochliobolus sativus*. Plant Dis 83:213-217.

Häffner E, Karlovsky P, Splivallo R, Traczewska A, Diederichsen E (2014) ERECTA, salicylic acid, abscisic acid, and jasmonic acid modulate quantitative disease resistance of *Arabidopsis thaliana* to *Verticillium longisporum*. BMC Plant Biol 14:71-85.

Huang J, Gu M, Lai Z, Fan B, Shi K, Zhou YH, Yu JQ, Chen Z (2010) Functional analysis of the *Arabidopsis PAL* gene family in plant growth, development, and response to environmental stress. Plant Physiol 153:1526-1538.

Jawhar M, Shoiab A, Arabi MIE, Al-Daoude A (2017) Changes in transcript and protein expression levels in the barley - *Cochliobolus sativus* interaction. Cereal Res Comm 45:104-113.

Kumar J, Schafer P, Huckelhoven R, Langen G, Baltruschat H, Stein E, Nagarajan S, Kogel HK (2002) *Bipolaris sorokiniana*, a cereal pathogen of global concern: cytological and molecular approaches towards better control. Mol Plant Pathol 3:185-195.

Livak K J, Schmittgen TD (2001) Analysis of relative gene expression data using real-time quantitative PCR and the 2 (-Delta Delta C (T)) method. Methods 25:402-408.

Moseman JG, Baenziger PS, Kilpatrick RA (1981) Genes conditioning resistance of *Hordeum spontaneum* to *Erysiphe graminins* f. sp. *hordei*. Crop Sci 21(2):229-232.

Nugroho LH, Verberne MC, Verpoorte R (2002) Activities of enzymes involved in the phenylpropanoid pathway in constitutively salicylic acid-producing tobacco plants. Plant Physiol Bioch 40:775-760.

Oliver RP, Ipcho SVSM (2004) Arabidopsis pathology breathes new life into the necrotrophs-vs.-biotrophs classification of fungal pathogens. Mol Plant Pathol 58:347-352.

Rsaliyev A, Pahratdinova Z, Rsaliyev S (2017) Characterizing the pathotype structure of barley powdery mildew and effectiveness of resistance genes to this pathogen in Kazakhstan. BMC Plant Biol 17:178.

Trapp MA, De Souza GD, Filho ER, Boland W, Mithöfer A (2014) Validated method for phytohormone quantification in plants. Front Plant Sci 5:417.

Vásquez AH, Salinas P, Holuigue L (2015) Salicylic acid and reactive oxygen species interplay in the transcriptional control of defense genes expression. Front Plant Sci 6:171.

Verberne MC, Brouwer N, Delbianco F, Linthorst HJM, Bol JF, Verpoorte R (2002) Method for the extraction of the volatile compound salicylic acid from tobacco leaf material. Phytochem Anal 13:45-50.

Vogt T (2010) Phenylpropanoid biosynthesis. Mol Plant 3:2-20.

Wildermuth MC, Dewdney J, Wu G, Ausubel FM (2001) Isochorismate synthase is required to synthesize salicylic acid for plant defence. Nature 29:562-565.

Zwart L, Berger DK, Moleleki LN, van der Merwe NA, Myburg AA, Naidoo S (2017) Evidence for salicylic acid signalling and histological changes in the defence response of *Eucalyptus grandis* to *Chrysoporthe austroafricana*. Sci Rep 7:45402.

Acta Biologica Szegediensis

Volume 63(1):37-43, 2019
Acta Biologica Szegediensis
http://abs.bibl.u-szeged.hu/index.php/abs

DOI:10.14232/abs.2019.1.37-43

ARTICLE

Biological control of rice sheath blight disease with formulation of indigenous *Trichoderma* strains under paddy field conditions

Shahram Naeimi[1], Vahid Khosravi[2], Mohammad-Zaman Nouri[2], Hassan Hoda[1], Csaba Vágvölgyi[3], László Kredics[3]*

[1]Department of Biological Control Research, Iranian Research Institute of Plant Protection, Agricultural Research Education and Extension Organization, Tehran 19395, Iran
[2]Rice Research Institute of Iran, Mazandaran Branch, Agricultural Research Education and Extension Organization, Amol 46191-91951, Iran
[3]Department of Microbiology, Faculty of Science and Informatics, University of Szeged, Szeged, Hungary

ABSTRACT The effectiveness of indigenous *Trichoderma* strains in preventing sheath blight disease was evaluated during two growing seasons under paddy field conditions. Broom sorghum seeds were used for mass production of *Trichoderma* strains. Colonized seeds were ground to powder and mixed with talc and carboxymethyl cellulose. Suspensions were made from the bioformulations and sprayed onto rice plants. Effects of *Trichoderma* strains on disease incidence and severity as well as yield and other growth parameters were determined and compared with a chemical fungicide and a commercial biofungicide. A combined analysis of variance across two years was performed and a statistically significant effect of year, treatment and their interaction was reported. Results indicate that environmental factors and different biological fungicides had a strong effect on disease development under natural conditions. According to the results, propiconazole and *T. harzianum* AS12-2 resulted in the least disease severity and incidence. Overall, the efficacy of *T. harzianum* AS12-2 in reducing sheath blight development was significantly better than other *Trichoderma* treatments and was comparable to the conventional fungicide. **Acta Biol Szeged 63(3):37-43 (2019)**

KEY WORDS
biocontrol agents
biocontrol efficacy
formulation
Rhizoctonia solani AG1-IA
Oryza sativa

ARTICLE INFORMATION
Submitted
30 April 2019.
Accepted
06 May 2019.
***Correspondent author**
E-mail: kredics@bio.u-szeged.hu

Introduction

Rice (*Oryza sativa* L.) is the staple food crop of over half of the world's population living mainly in Asia (Qin and Zhang 2005). Sheath blight of rice caused by *Rhizoctonia solani* Kühn AG1-IA is a very destructive disease of high-yielding varieties under favorable conditions for the pathogen. This disease is widely spread in most of the rice growing areas of the world and causes considerable yield losses (Ou 1985). Chemical fungicides are primarily used for sheath blight control (Rabindran and Vidhyasekaran 1996), but management of the disease is difficult because *R. solani* survives in soil as sclerotia and in rice plant tissues as mycelia (Jayaprakashvel et al. 2010). However, the application of chemical fungicides has several disadvantages, such as the development of resistance in the pathogen, phytotoxicity, toxic effects on human health, pollution of the environment, high costs and loss of biodiversity (Groth et al. 1990; Sehajpal et al. 2009). Therefore, considering the negative impacts due to indiscriminate use of synthetic pesticides, it has become necessary to adopt ecofriendly approaches to avoid environmental pollution and ensure better crop management. Biological control using microbial biopesticides provides an attractive and environmentally safe alternative to chemical fungicides in the management of rice sheath blight (Mew and Rosales 1986; Vasantha Devi et al. 1989). The application of beneficial microorganisms in agriculture has recently become more important and several commercial biopesticides and biofertilizers are already on the market (Kumar et al. 2014).

Fungi belonging to the genus *Trichoderma* are ubiquitous over wide geographic areas of the world with the broadest impact on mankind (Kredics et al. 2014). Among the fungal biocontrol agents, *Trichoderma* spp. are the most promising in controlling foliar and root diseases of several crops (Elad 2000; Mathivanan et al. 2004). At present, several commercial formulations of *Trichoderma* are available worldwide as biopesticides, biofertilizers, growth enhancers and stimulants of natural resistance. Due to changing of the public viewpoint on consumption

of chemical-free food and protecting the environment, use of *Trichoderma*-based products can be expected to increase in the future (Woo et al. 2014).

Several *Trichoderma* isolates showed good potential in inhibiting *R. solani* AG-IA *in vitro* and in suppressing the sheath blight under greenhouse conditions (Roy 1977; Gokulapalan and Nair 1984; Cumagun and Lapis 1993; Khan and Sinha 2007; Naeimi et al. 2010, 2011; Chen et al. 2015), but their application for the control of the disease under natural conditions is limited (Nagaraju et al. 2002; Mathivanan et al. 2005; De França et al. 2015).

Many biocontrol agents (BCAs) have been found effective in inhibiting the growth of different plant pathogens under *in vitro* and greenhouse conditions, but they often fail to control the disease in fields and orchards (Alabouvette et al. 2006; Gerbore et al. 2014). Ecological factors, plant growth stages, the time and rate of application, the inoculum levels of the pathogen and the applied BCA, the diversity of the natural population of the pathogen, the method of delivery and other factors may affect the biological control efficacy in natural environments.

Before developing a biofungicide, production, formulation and application strategies need to be carefully studied (Burges 1998). In addition, the adaptation of a promising BCA to the agroecosystem and specific habitat in which it will be applied should primarily be evaluated (Ojiambo and Scherm 2006). In the case of rice sheath blight, the soil borne *R. solani* causes foliar damage, therefore the ideal BCA should survive in the phyllosphere (Chen et al. 2015) and the biocontrol success depends on the application and survival of antagonist populations at the target site (Savazzini et al. 2009).

In our previous study, several native *Trichoderma* isolates obtained from the paddy fields of northern Iran were screened against *R. solani in vitro* and their efficiencies in controlling rice sheath blight were evaluated under greenhouse conditions, where significant disease reduction was achieved (Naeimi et al. 2010). The present study was conducted to investigate the biocontrol efficacy of the four most effective strains as a talc-based powder formulation in preventing sheath blight disease development in field plots artificially infested with the pathogen over two successive years.

Materials and Methods

Field design

All trials were conducted in a paddy field located at the experimental farm of the Rice Research Institute of Iran, Amol, Mazandaran (36° 28' 691" N | 52° 27' 744" E, 30 m altitude), over two growing seasons (April-September 2012 and 2013). The field was divided into 24 plots; each with a size of 1 × 2 m, resulting in a total of 4 × 8 = 32 rice hills. Rice seedlings (Shiroodi, a susceptible, high-yielding cultivar) were raised in the seedling bed for 25 days and transplanted in the main field with a spacing of 25 cm between and within rows. Agronomic practices followed state recommendations for rice production and the recommended dose of fertilizers (100:30:80 kg of NPK/ha) was applied to the field. No chemical pesticides were applied to the experimental plots unless otherwise mentioned. The crop was harvested at maturity and threshed to calculate crop yield. The study was continued in the same field with the same layout during the next growing season.

Pathogen and biocontrol agents

The fungal strains applied in this study are listed in Table 1. A virulent strain of the sheath blight pathogen *Rhizoctonia solani* AG1-IA (RBL1) isolated from a naturally infected rice plant was used in all experiments. The *Trichoderma* strains used in this study (*T. harzianum* AS3-5, *T. harzianum* AS12-2, *T. virens* AD1-3 and *T. virens* AS16-22) had shown biocontrol activity against *R. solani in vitro* and suppressed the sheath blight incidence under glasshouse conditions in a previous study (Naeimi et al. 2010).

Table 1. Fungal strains applied during this study

Fungal strain	Habitat	Location	GenBank accession numbers	
			ITS	*tef1α*
T. harzianum AS12-2	Paddy soil	Chaloos	EU821789	FJ618586
T. harzianum AS3-5	Paddy soil	Amol	EU821780	FJ618586
T. virens AD1-3	Rice debris	Freydoonkenar	EU821794	FJ618575
T. virens AS16-22	Paddy soil	Sari	EU821795	FJ618575
R. solani RBL1	Infected sheath	Amol	HM211085	n/a

Inoculum preparation of R. solani

Five mycelial discs (5 mm in diameter) cut from the margin of 3-day-old culture of the pathogen (*R. solani* strain RBL1) on potato dextrose agar medium (Merck, Germany) were inoculated into 2 L Erlenmeyer flasks containing 1 kg autoclaved rice husk and rice bran (1:1) and incubated at 28 ± 1 ℃ for 30 days.

Preparation of talc-based formulation of Trichoderma strains

For mass production of *Trichoderma* strains, broom sor-

ghum (*Sorghum vulgare* var. *technicum*) grains were soaked in water overnight. Then, 300 g of grains were filled in 1 L Erlenmeyer flasks and sterilized in an autoclave for 30 min in three successive days. After cooling the grains to room temperature, three mycelial discs (5 mm) cut from the edge of growing colonies of *Trichoderma* strains were aseptically transferred to the flasks, which were subsequently kept at ambient laboratory temperature (26-32 ℃) for 30 days and periodically shaken in order to have uniform growth of BCAs. After this period, *Trichoderma* inocula were taken out from the flasks, air dried, ground to a powder with Mortar Grinder Pulverisette 2 (Fritsch, Germany) and mixed well with extra fine pure talc powder (Merck, Germany) and carboxymethyl cellulose (CMC; BDH, England) as sticker at a 1:2:0.005 ratio under aseptic conditions. The mixture of talc and CMC was autoclaved for 30 min for two consecutive days before adding the BCAs. All formulations were packed in plastic containers, sealed and stored at room temperature until use. In the first year of the experiment, the populations of *T. harzianum* AS3-5, *T. harzianum* AS12-2, *T. virens* AD1-3 and *T. virens* AS16-22 in the formulation were 6×10^9, 2.5×10^{10}, 2.0×10^{10} and 8.0×10^9 cfu/g of formulation, respectively at the time of application. Similarly, in the secon year the populations of these four strains were 6.1×10^9, 2.5×10^{10}, 1.8×10^{10} and 7.9×10^9 cfu/g of formulation, respectively.

Pathogen inoculation and application of biocontrol agents

To ensure uniform disease incidence and severity during both growing seasons, 40 days after transplanting at the maximum tillering stage of rice (one week after the first application of biocontrol formulation), 5 g of the prepared *R. solani* inoculum was placed among tillers in the centre of twelve rice hills per replication near the waterline (Tang et al. 2007).

Formulations of each native *Trichoderma* strain were dissolved in water, thoroughly mixed, filtered through two layers of cheesecloth (after 30 min) and sprayed four times on rice foliage at 750 L/ha as I) 7 days prior to pathogen inoculation; II) on the following day after inoculation of *R. solani*; III) 7 days and IV) 14 days after the second application. Tween 20 (Merck, Germany) at 0.05% was added to the suspensions as a surfactant before spraying. Trianum P (Koppert, the Netherlands), a commercial biofungicide which contains *Trichoderma harzianum* KRL-AG2 (T-22) (1×10^9 cfu/g) was also applied as above on rice foliage as a comparative treatment according to the manufacturer's instruction. All BCAs were sprayed on the phyllosphere of rice with a 2 L hand sprayer (EVA, Dimartino, Italy) after sunset. Propiconazole (TILT®, 250 EC, Syngenta, Switzerland) was used as the chemical fungicide control and applied as a foliar spray (1 L/ha) 2 days after inoculation. Plants inoculated only with *R. solani* were considered as inoculated control. Furthermore, for non-inoculated control, plants were sprayed with distilled water and no input (BCA and/or fungicide) was applied.

Disease assessment

Two weeks after artificial inoculation of the pathogen (AIP), 6 hills from each treatment per replication were randomly selected and tagged to observe the sheath blight incidence [in terms of the percentage of infected tillers (PIT)]. For assessing sheath blight severity, the relative lesion height (RLH) of 5 tillers from each 6 randomly selected hills was first calculated and then the disease severity was recorded according to the 0-9 scale of Standard Evaluation System developed by the International Rice Research Institute (IRRI 2002). The incidence and severity of sheath blight was also determined 35 days after AIP to see whether the formulations still had an effect on the prevention of disease development. Agronomic traits of rice including plant height (PH), number of tillers/hill, crop yield and 1000-grains weight (GW) were measured.

Meteorological data

All climate data including air temperature, relative humidity (RH), precipitation and sunlight hours were taken from Amol Weather Station located about 300 m from the experimental area.

Statistical analysis

All field experiments were established as a randomized complete block design with three replicates. A combined analysis of variance (ANOVA) was performed to determine the effect of year and treatments on disease development and agronomic traits, using the SAS software ver. 9.1.3 (SAS Institute, Cary, NC). All means of the treatments were compared by Duncan's multiple range tests at $P \leq 0.01$.

Results

Rice sheath blight severity and incidence were notably decreased in some BCA-treated plots under field conditions. The effect of year on RLH_{14}, PIT_{14}, 1000 GW, plant height ($P \leq 0.01$) and No. of tillers ($P \leq 0.05$) proved to be significant according to the results of the combined analysis of variance for both years (Table 2). Disease severity (in terms of RLH) and incidence (in terms of PIT) after 14 days as well as growth parameters were lower for the second year. The effect of treatment on all characteristics except for plant height and No. of tillers was significant at $P \leq 0.01$ (Table 2). In the case of traits with significant treatment × year interactions, including RLH_{14}, PIT_{14} and RLH_{35}, ANOVA was performed for each

Table 2. F-values for the effects of year, treatment and their interaction according to combined ANOVA over two years (2012-2013)

Source of variation	Degree of freedom	F-value							
		RLH_{14}	RLH_{35}	PIT_{14}	PIT_{35}	Yield	1000 GW	PH	No. of tillers
Year	1	40.21**	1.14	28.6**	0.61	5.31	308.9**	99.74**	16*
Treatment	7	21.03**	17.19**	19.56**	17.31**	6.13**	4.63**	0.93	2.2
Treatment × Year	7	5.05**	2.57*	6.46**	2.16	1.49	0.96	0.5	1.69

RLH= relative lesion height, PIT= percentage of infected tillers, GW=grain weight, PH=plant height. * , **: Significant at 5 and 1%, respectively.

growing season and means were compared using Duncan's multiple range test (Table 3). The minimum sheath blight incidence was recorded for propiconazole (PIT_{35} = 57.01%) and *T. harzianum* AS12-2 (PIT_{35} = 60.67%) 35 days after AIP ($P \leq 0.01$) (Fig. 1). Non-treated plots showed the highest yield (6433 kg/ha) and 1000-GW (27.79 g). It is important to note that agronomical characteristics were not significantly different among *Trichoderma*-treated and fungicide-treated plots (data not shown).

According to the first year data, 14 days after AIP, *T. harzianum* AS12-2 and propiconazole provided the lowest disease scores (2.55 and 2.78, respectively) (data not shown). The minimum RLH_{14} of 22.18 and 24.19 were recorded for *T. harzianum* AS12-2 and propiconazole, respectively, when compared to the inoculated control (Table 3). In addition, among the treatments, *T. harzianum* AS12-2 was found to be most effective in reducing disease incidence (PIT_{14} = 36.35%), which was less than in the case of chemical fungicide-treated plots (PIT_{14} = 72.27%). Other treatments were not significantly different in terms of disease incidence 14 days after AIP. Trianum P led to the lowest reduction of disease severity (RLH_{14} = 36.36%) and incidence (PIT_{14} = 98.21%) compared to the native biocontrol agents. Thirty five days after AIP, the lowest disease scale (3.44) and RLH_{35} (27.87%) were observed in propiconazole-treated plots. Formulation of native *Trichoderma* spp. together with Trianum P - although not significantly different from the chemical fungicide - resulted in relatively higher disease severity ranging from 44.22% to 51.73% (Table 3).

In the second year of the experiment, *T. harzianum* AS3-5, propiconazole and *T. harzianum* AS12-2 showed the lowest disease scores 14 days after AIP, as compared to the control (0.37, 0.48 and 0.55, respectively). The RLH_{14} values of the aforementioned treatments were 4.03%, 4.85% and 6.4%, respectively, which were not significantly different (Table 3). These treatments also showed the minimum disease incidences (PIT_{14} of 7.4%, 9.56% and 12.94%, respectively) and were not significantly different from each other and from the non-inoculated control (PIT_{14} = 5.87%). Similar to the results of the first year, Trianum P was the least effective in suppressing sheath blight (RLH_{14} = 25.49%, PIT_{14} = 93.83%). The lowest disease scales and RLH values were recorded for propiconazole (0.97 and 8.93%, respectively), *T. harzianum* AS12-2 (3.54 and 13.5%, respectively) and *T. harzianum* AS3-5 (3.84 and 30.27%, respectively) 35 days after AIP.

Table 3. Effect of bioformulation of native *Trichodema* strains on sheath blight incidence (as percentage of infected tillers = PIT) and severity (as relative lesion height = RLH) 14 and 35 days after artificial inoculation with *Rhizoctonia solani* in two successive years

Treatment	RLH_{14}		RLH_{35}		PIT_{14}	
	2012	2013	2012	2013	2012	2013
T. harzianum AS12-2	22.18 ± 5.5 b	6.4 ± 2.2 bcd	50.18 ± 14.3 ab	29.73 ± 7.5 ab	36.35 ± 16.7 b	12.94 ± 6.8 bc
T. harzianum AS3-5	31.28 ± 2.2 ab	4.03 ± 2.0 cd	51.73 ± 10.2 ab	30.27 ± 3.8 ab	94.79 ± 6.5 a	7.4 ± 4.6 bc
T. virens AD1-3	30.10 ± 7.1 ab	10.19 ± 4.3 abcd	46.67 ± 2.0 ab	58.1 ± 5.3 a	91.67 ± 7.2 a	25.73 ± 14.3 bc
T. virens AS16-22	31.10 ± 1.6 ab	22.57 ± 7.7 abc	44.22 ± 17.1 ab	61.63 ± 0.8 a	79.36 ± 18 a	58.85 ± 20.9 ab
Trianum P	36.36 ± 4.4 a	25.49 ± 0.45 ab	51.24 ± 4.1 ab	44.94 ± 3.3 a	98.21 ± 1.5 a	93.83 ± 5.4 a
Propiconazole	24.19 ± 4.9 b	4.85 ± 2.4 cd	27.87 ± 16.6 b	8.93 ± 4.2 b	72.27 ± 14.4 a	9.56 ± 6.5 bc
Inoculated control	35.97 ± 2.5 a	30.06 ± 1.5 a	55.50 ± 3.3 a	48.07 ± 4.8 a	98.1 ± 2.5 a	99.57 ± 0.7 a
Non-inoculated control	0.20 ± 0.07 c	2.86 ± 1.4 d	0.72 ± 0.34 c	13.5 ± 7.4 b	1.52 ± 1.1 c	5.87 ± 3.4 c

Values (means ± SE) within a column followed by the same letter(s) are not significantly different according to the Duncan's multiple range test (P = 0.01)

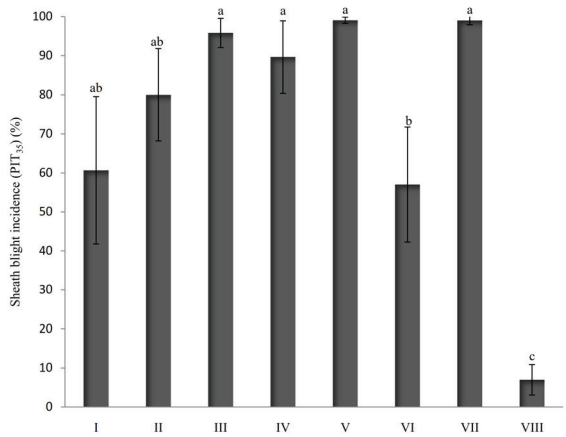

Figure 1. Effect of different treatments on sheath blight incidence (as percentage of infected tillers = PIT), 35 days after artificial inoculation with *Rhizoctonia solani* in two successive years.

I: *Trichoderma harzianum* AS12-2; **II**: *T. harzianum* AS3-5; **III**: *T. virens* AD1-3; **IV**: *T. virens* AS16-22; **V**: Biofungicide (Trianum P); **VI**: Chemical fungicide (propiconazole); **VII**: Inoculated control; **VIII**: Non-inoculated control. Values represented by the same letter(s) above the bars are not significantly different according to Duncan's multiple range test (P = 0.01). Each value represents the mean of three replicates.

Discussion

In order to commercialize a promising BCA as a microbial biopesticide, it has to be evaluated under the natural environmental conditions with a suitable formulation (Fravel and Larkin 1996; Alabouvette et al. 2006). In this study, four native *Trichoderma* strains were examined for prevention of the rice sheath blight disease and promotion of plant growth and grain yields under paddy field conditions. Application of talc-based formulations of some autochthonous *Trichoderma* strains significantly reduced the sheath blight severity and incidence caused by *R. solani*, which was comparable with the chemical fungicide propiconazole.

Although Shiroodi is a rice cultivar susceptible to sheath blight, the natural infection by the pathogen was very low in both years. On the other hand, the disease score recorded for inoculated control was not very high. This suggests that mild severity of sheath blight is probably related to environmental conditions. Optimum conditions for sheath blight infection and development are high temperature (30-32 ℃), high RH (>95%) and shading (Ou 1985). Meteorological data indicate that temperature, RH and sunlight hours during AIP to the second disease evaluation were below the optimum conditions of infection and development of pathogen in the field.

Initially, some biocontrol agents demonstrated effective biocontrol properties, but for a longer period of time they were not able to satisfactorily suppress the disease. For instance, although *T. harzianum* AS12-2 promisingly controlled sheath blight, even better than the chemical fungicide at first, disease severity increased at the harvesting stage in the plots treated with this strain. This is consistent with findings of Perelló et al. (2009), who reported that although *Trichoderma* spp. effectively reduced the severity of *Septoria* blotch at the tillering stage of wheat, they failed to control the disease at the heading stage. It is speculated that despite four times of application of *Trichoderma* strains in the field, probably due to inappropriate environmental conditions, high microbial competitions and presumably other factors, they could not maintain or increase their populations and adopt to the rice phylloplane, therefore they failed to inhibit the disease development until the end of the season. Effective antagonists must become established in crop ecosystems and remain active against the target pathogens during the periods favorable for infection (Lo et al. 1998). *Trichoderma* strains are not common phyllosphere inhabitants (Elad and Kirshner 1993; Latorre et al. 1997), and if they are applied to above-ground plant parts, their populations may decrease by a factor of 10-100 within a period of 2 weeks (Freeman et al. 2004). According to the climate data for the time span between the first application of BCAs and the second disease assessment (40 days), the average air temperature was 28 ℃ in both years which favored the fungal BCAs. However, the limiting factor was very likely the RH and wetness time of the rice phyllosphere. The average RH values during the mentioned time in 2012 and 2013 were 55% and 61%, respectively. Moreover, the average precipitation was less than 1 mm and 1.6 mm, respectively. Many fungi, including *Trichoderma* strains need moisture for germination, growth and colonization, therefore the low moisture and dryness of the rice phylloplane may ultimately have negative effects on the antagonistic potential of the applied BCAs in the field. The average sunlight hours in the first and second year were 7 h and 8 h, respectively. Direct exposure to solar radiation reduces conidial production, survival, germination, and can kill the conidia of most fungal species, which limits the size of the fungal population and reduces the efficacy of fungal BCAs (Braga et al. 2015). The deleterious effects of ultraviolet (UV) radiation on conidia have been demonstrated in several fungi including *Trichoderma* spp. (Moody et al. 1999; Stevenson and Weimer 2002). Solar UV may therefore have negatively affected the survival and biocontrol potential of native BCAs in the current study after field application. Under the aforementioned conditions, *R. solani* developed to panicles as well as neighboring tillers during the time between the two disease evaluations. This suggests that although native *Trichoderma* strains effectively suppressed the pathogen

during the initial stage of disease development, but for an extended period of time, when environmental conditions are conducive to *R. solani* or the BCAs can not adapt to the rice phylloplane, sheath blight may eventually develop, although still at a slower and less severe rate. The high inoculum load of *R. solani* applied in this study might also have contributed to the failure of the BCAs to provide striking disease control.

The BCAs applied during this study did not promote plant growth and grain yield. This is in disagreement with other works which were stating that talc formulations of *Trichoderma* not only significantly control the sheath blight disease, but also increase the growth and grain yields in the paddy field (Mathivanan et al. 2005; Khan and Sinha, 2007; Soe and De Costa, 2012). Lorito and Woo (2015) stated that although *Trichoderma* spp. are regarded as plant growth promoting microbes, this property is not present in every strain. It is important to note that in this study, the talc powder inside the formulation formed a white layer on rice leaves, which did not disappear for a long time due to low precipitation. This may negatively affect photosynthesis, respiration and ultimately the plant growth and yield. Consequently, changing the carrier/bulking agent or reducing the amount of talc powder in the current formulation may result in growth promotion along with an acceptable level of disease control.

In conclusion, findings of the present field study indicate the feasibility of *Trichoderma* strains for the biocontrol of rice sheath blight disease in the field as an alternative disease control strategy and formulations of *T. harzianum* AS12-2 can be recommended as one of the crop protection strategies for the management of sheath blight. Future research should be directed toward the optimization of the existing formulation, in order that the applied strain can be more capable of becoming established and surviving in the rice phylloplane. This will facilitate the commercialization of the biocontrol *Trichoderma* strain and the introduction of the resulting biofungicide to the market. Moreover, further experiments are needed to find out the appropriate amount, time and frequency of application.

Acknowledgements

LK is grantee of the János Bolyai (Hungarian Academy of Sciences) and Bolyai Plus (ÚNKP) Research Scholarships.

References

Alabouvette C, Olivain C, Steinberg C (2006) Biological control of plant diseases: the European situation. Eur J Plant Pathol 114:329-341.

Braga GU, Rangel DE, Fernandes ÉK, Flint SD, Roberts DW (2015) Molecular and physiological effects of environmental UV radiation on fungal conidia. Curr Genet 61:405-425.

Burges HD (1998) Formulation of Microbial Biopesticides: Beneficial Microorganisms, Nematodes and Seed Treatments. Kluwer Academic Publishers. The Netherlands.

Chen LH, Zhang J, Shao XH, Wang SS, Miao QS, Mao XY, Zhai YM, She DL (2015) Development and evaluation of *Trichoderma asperellum* preparation for control of sheath blight of rice (*Oryza sativa* L.). Biocontrol Sci Technol 25:316-328.

Cumagun CJR, Lapis DB (1993) Practical approach in mass production of *Trichoderma* spp. as a means of biological control against sheath blight of rice. Philippine Agriculturist 76:251-257.

de França SKS, Cardoso AF, Lustosa DC, Ramos EMLS, de Filippi MCC, da Silva GB (2015) Biocontrol of sheath blight by *Trichoderma asperellum* in tropical lowland rice. Agron Sustain Dev 35:317-324.

Elad Y, Kirshner B (1993) Survival in the phylloplane of an introduced biocontrol agent (*Trichoderma harzianum*) and populations of the plant pathogen *Botrytis cinerea* as modified by abiotic conditions. Phytoparasitica 21:303- 313.

Elad Y (2000) Biological control of foliar pathogens by means of *Trichoderma harzianum* and potential modes of action. Crop Protect 19:709-714.

Fravel DR, Larkin RP (1996) Availability and application of biocontrol products. In Canaday CH, ed., Biological and Cultural Tests for Control of Plant Diseases. Vol. 11. APS Press, St. Paul, USA. pp. 1-7.

Freeman S, Minz D, Kolesnik I, Barbul O, Zveibil A, Maymon M, Nitzani Y, Kirshner B, Rav-David D, Bilu A, Dag A, Shafir S, Elad Y (2004) *Trichoderma* biocontrol of *Colletotrichum acutatum* and *Botrytis cinerea* and survival in strawberry. Eur J Plant Pathol 110:361-370.

Gerbore J, Benhamou N, Vallance J, Le Floch G, Grizard D, Regnault-Roger C, Rey P (2014) Biological control of plant pathogens: advantages and limitations seen through the case study of *Pythium oligandrum*. Environ Sci Pollut Res 21:4847-4860.

Gokulapalan C, Nair MC (1984) Antagonism of a few fungi and bacteria against *Rhizoctonia solani*. Indian J Microbiol 24:57-58.

Groth DE, Rush MC, Lindberg GD (1990) Foliar fungicides for control of rice diseases in the United States. In Grayson BT, Green MB, Copping LG. Pest Management in Rice. Elsevier, London. pp. 31-52.

IRRI (2002) Standard Evaluation System for Rice. International Rice Research Institute, Los Banos, Philippines.

Jayaprakashvel M, Selvakumar M, Srinivasan K, Ramesh S, Mathivanan N (2010) Control of sheath blight disease in

rice by thermostable secondary metabolites of *Trichothecium roseum* MML003. Eur J Plant Pathol 126:229-239.

Khan AA, Sinha AP (2007) Biocontrol potential of *Trichoderma* species against sheath blight of rice. Indian Phytopathol 60:208-213.

Kredics L, Hatvani L, Naeimi S, Körmöczi P, Manczinger L, Vágvölgyi C (2014) Biodiversity of the genus *Hypocrea/Trichoderma* in different habitats. In Gupta VK, Schmoll M, Herrera-Estrella A, Upadhyay RS, Druzhinina I, Tuohy M, Eds., Biotechnology and Biology of *Trichoderma*. Elsevier Science BV, Amsterdam, The Netherlands. pp. 3-24.

Kumar S, Thakur M, Rani A (2014) *Trichoderma*: Mass production, formulation, quality control, delivery and its scope in commercialization in India for the management of plant diseases. Afr J Agr Res 9:3838-3852.

Latorre BA, Agosin E, San Martín R, Vasquez GS (1997) Effectiveness of conidia of *Trichoderma harzianum* produced by liquid fermentation against *Botrytis* bunch rot of table grape in Chile. Crop Protect 16:209-214.

Lo CT, Nelson EB, Hayes CK, Harman GE (1998) Ecological studies of transformed *Trichoderma harzianum* strain 1295-22 in the rhizosphere and on the phylloplane of creeping bentgrass. Phytopathology 88:129-136.

Lorito M, Woo SL (2015) *Trichoderma*: A multi-purpose tool for integrated pest management, In: Lugtenberg B (ed), Principles of Plant-Microbe Interactions. Springer International Publishing, pp. 345-353.

Mathivanan N, Prabavathy VR, Murugesan K (2004) Biocontrol potential of microorganisms - an overview: focus on *Trichoderma* as biofungicide for the management of plant diseases. In Mayee CD, Manoharachary C, Tilak KVBR, Mukadam DS, Despande J, Eds., Biotechnological Approaches for the Integrated Management of Crop Diseases. Daya Publishing House, Delhi, India, pp. 90-108.

Mathivanan N, Prabavathy VR, Vijayanandraj VR (2005) Application of talc formulations of *Pseudomonas fluorescens* Migula and *Trichoderma viride* Pers. ex S.F. Gray decrease the sheath blight disease and enhance the plant growth and yield in rice. J Phytopathol 153:697-701.

Mew TW, Rosales AM (1986) Bacterization of rice plants for control of sheath blight caused by *Rhizoctonia solani*. Phytopathology 76:1260-1264.

Moody SA, Newsham KK, Ayres PG, Paul ND (1999) Variation in the responses of litter and phylloplane fungi to UV-B radiation (290-315 nm). Mycol Res 103:1469-1477.

Naeimi S, Kocsubé S, Antal Z, Okhovvat SM, Javan-Nikkhah M, Vágvölgyi C, Kredics L (2011) Strain-specific SCAR markers for the detection of *Trichoderma harzianum* AS12-2, a biological control agent against *Rhizoctonia solani*, the causal agent of rice sheath blight. Acta Biol Hung 62:73-84.

Naeimi S, Okhovvat SM, Javan-Nikkhah M, Kredics L, Khosravi V (2010) Biological control of *Rhizoctonia solani* AG1-1A, the causal agent of rice sheath blight with *Trichoderma* strains. Phytopathol Mediterr 49:287-300.

Nagaraju P, Naresh D, Biradar DP, Dronavalli N (2002) Biological control of sheath blight (*Rhizoctonia solani*) in transplanted rice. Indian J Agr Sci 72:306-307.

Ojiambo PS, Scherm H (2006) Biological and application-oriented factors influencing plant disease suppression by biological control: a meta-analytical review. Phytopathology 96:1168-1174.

Ou SH (1985) Rice Diseases, 2nd ed. Commonwealth Mycological Institute, Kew, England

Perelló AE, Moreno MV, Mónaco C, Simón MR, Cordo C (2009) Biological control of *Septoria tritici* blotch on wheat by *Trichoderma* spp. under field conditions in Argentina. BioControl 54:113-122.

Qin Z, Zhang M (2005) Detection of rice sheath blight for in-season disease management using multispectral remote sensing. Int J Appl Earth Obs Geoinf 7:115-128.

Rabindran R, Vidhyasekaran P (1996) Development of a formulation of *Pseudomonas fluorescens* PfALR2 for management of rice sheath blight. Crop Protect 15:715-721.

Roy AK (1977) Parasitic activity of *Trichoderma viride* on the sheath blight fungus of rice (*Corticium sasaki*). J Plant Dis Protect 84:675-683.

Savazzini F, Longa CMO, Pertot I (2009) Impact of the biocontrol agent *Trichoderma atroviride* SC1 on soil microbial communities of a vineyard in northern Italy. Soil Biol Biochem 41:1457-1465.

Sehajpal A, Arora S, Kaur P (2009) Evaluation of plant extracts against *Rhizoctonia solani* causing sheath blight of rice. J Plant Protect Sci 1:25-30.

Soe KT, De Costa DM (2012) Development of a spore-based formulation of microbial pesticides for control of rice sheath blight. Biocontrol Sci Technol 22:633-657.

Stevenson DM, Weimer PJ (2002) Isolation and characterization of a *Trichoderma* strain capable of fermenting cellulose to ethanol. Appl Microbiol Biotechnol 59:721-726.

Tang Q, Peng S, Buresh RJ, Zou Y, Castilla NP, Mew TW, Zhong X (2007) Rice varietal difference in sheath blight development and its association with yield loss at different levels of N fertilization. Field Crop Res 102:219-227.

Vasantha Devi TV, Malar Vizhi R, Sakthivel N, Gnanamanickam SS (1989) Biological control of sheath blight of rice in India with antagonistic bacteria. Plant Soil 119:325-330.

Woo SL, Ruocco M, Vinale F, Nigro M, Marra R, Lombardi N, Pascale A, Lanzuise S, Manganiello G, Lorito M (2014) *Trichoderma*-based products and their widespread use in agriculture. Open Mycol J 8:71-126.

Acta Biologica Szegediensis

Volume 63(1):45-50, 2019
Acta Biologica Szegediensis
http://abs.bibl.u-szeged.hu/index.php/abs
DOI:10.14232/abs.2019.1.45-50

ARTICLE

Trilepisium madagascariense fruit-wastes as cheap feedstock for bioethanol production

Ademakinwa Adedeji Nelson[1,3*], Agunbiade Mayowa Oladele[2], Agboola Femi Kayode[3]

[1]Department of Physical and Chemical Sciences, Elizade University, Ilara-Mokin, Nigeria
[2]Biocatalysis and Technical Biology Research Group, Institute of Biomedical and Microbial Biotechnology, Cape Peninsula University of Technology, South Africa
[3]Department of Biochemistry and Molecular Biology, Obafemi Awolowo University, Ile-Ife, Nigeria

ABSTRACT *Trilepisium madagascariense* fruits are carbohydrate-rich and this study directly fermented the fruit wastes into bioethanol without the need for nutrient supplementation. The total reducing sugar (TRS) present in the mesocarp and seed of *T. madagascariense* fruit wastes (*Tm*fw) was fermented to bioethanol using *Aureobasidium pullulans*. Bioethanol production by *A. pullulans* was also optimized using Box-Behnken response surface methodology (RSM). The TRS in the mesocarp and seed of *Tm*fw were 11.2 ± 0.8 and 17.1 ± 1.2 g/L, respectively and further hydrolysis with cellulase resulted in increased TRS indicating the presence of cellulose. Pre-optimization, the bioethanol yield (Y_{ps}) and volumetric productivity (Q_p) obtained from the fermentation of the seed by *A. pullulans* were 0.57 ± 0.03 g/g and 0.21 ± 0.02 g/L^{-1}h^{-1}, respectively. The optimum conditions for maximum bioethanol production were pH (5.95), time (24 h) and substrate concentration (5 g/L) resulting in Y_{ps}, Q_p of 0.66 ± 0.06 g/g and 0.27 + 0.01 g/L^{-1}h^{-1}, respectively after model validation. *Tm*fw served as a suitable, cheap, non-toxic and readily available substrate especially in Nigeria to produce bioethanol while *A. pullulans* is a fungus that might be utilized for large-scale industrial bioethanol production.
Acta Biol Szeged 63(1):45-50 (2019)

KEY WORDS
Aureobasidium pullulans
bioethanol
submerged fermentation
Trilepisium madagascariense

ARTICLE INFORMATION
Submitted
26 June 2019.
Accepted
15 July 2019.
***Corresponding author**
E-mail: adedeji.ademakinwa@elizadeuniversity.edu.ng

Introduction

Bioethanol is produced by microbial fermentation of plants containing sugar, starch and lignocellulosic materials (Joshi et al. 2012). In contrast to ethanol, bioethanol can be obtained from biomass-based waste materials or other renewable sources such as high sugar-containing plant materials (Dash 2017). It can be used as fuel, chemical feedstock and as a solvent in various industrial processes (Alma et al. 2015).

Bioethanol is referred to as a sustainable alternative energy source, which is both renewable and environmentally acceptable (Lebaka 2013). It is by far most widely used in transportation and it is oxygenated, thereby provides the potential to reduce particulate emissions in compression ignition engines (Razmovski et al. 2012). A variety of plant materials has been used for the first, second and third generation bioethanol production. The first-generation bioethanol production involves plant materials rich in sucrose (sugarcane, sugar beet, sweet sorghum, and fruits) and starch (corn, wheat, rice, potato, cassava, sweet potato and barley). The sugar-based ethanol is predominantly produced from sugarcanes while starch-based ethanol is mainly from corn but also from grains. The production of first-generation ethanol poses a low risk and does not require harsh pretreatment of the substrate. However, the utilization of edible agricultural crops solely for biofuel production conflicts with food and feed production (Sharma and Sharma 2018). The focus of this study is, therefore, to exploit the under-utilized *Trilepisium madagascariense* fruit wastes for the possible production of bioethanol since these seeds have been reported to be rich in carbohydrates (60%) (Adewuyi et al. 2010). Several reports exist that shows the plant has medicinal values as it is applied in the treatment of some ailments mostly because of its rich antioxidant/phytochemical properties (Nwamarah et al. 2015). These fruit wastes, therefore, could serve as a source of bioethanol production in certain countries (*e.g.*, Nigeria) because it is cheap, cost-effective and readily available. The cost-effectiveness of bioethanol production is highlighted in this study since the process of production of this biofuel is free of enzymatic hydrolysis which is hitherto expensive. The economics of bioethanol production is greatly influenced by the cost of the feedstock, which accounts for more than half of the production costs. Hence, utilizing the cheap waste of the ripened fruits of *T. madagascariense* which is rich in

reducing sugars is exploitable for large-scale production of bioethanol locally in countries like Nigeria.

In this study, there was a determined effort to investigate if *Aureobasidium pullulans* can hitherto ferment reducing sugars present in the *T. madagascariense* into ethanol anaerobically. *A. pullulans* have been reported to contain enzymes that can hydrolyze sucrose to produce glucose and sucrose *e.g.,* invertases and fructosyltransferases (Ademakinwa et al. 2017). This will offer a new fungus-based method for large scale production of bioethanol in countries where *T. madagascariense* available.

Materials and Methods

Reagents

Trichoderma reesi cellulase, dinitrosalicyclic acid, sodium-potassium-tartrate, sodium hydroxide, glucose, carboxymethyl cellulose, sodium acetate, ethanol, sodium dichromate dihydrate, sulphuric acid and glacial acetic acid were of analytical grade and purchased from Sigma-Aldrich (USA).

Microorganisms and culture conditions

The industrial strain of *S. cerevisiae* was obtained from the Department of Chemical Engineering, Obafemi Awolowo University, Ile-Ife, Nigeria. *A. pullulans* were previously isolated from soil containing decayed plant litters and its molecular identification was based on sequencing of the ITS1-ITS4 genomic region (Ademakinwa and Agboola 2016). Both fungi were maintained on malt extract agar (MEA) for 96 hours at 4 °C on agar slants. Preparation of the inoculum and growth medium were as described by Ademakinwa et al. (2017). All the yeast was incubated anaerobically in an anaerobic jar during ethanol production.

Preparation of T. madagascariense seeds and mesocarp

Ripened fruits wastes were collected from the base of the *T. madagascariense* trees located in the Botanical Garden, Obafemi Awolowo University, Ile-Ife. The fruit wastes were then washed in sterile distilled water. The mesocarps were carefully separated from the seeds using a sterile razor blade and homogenized separately in distilled water (1:2) w/v. The homogenate was then clarified by centrifugation at 4000 g for 20 min. The supernatant was stored at 4 °C prior to further use. The total reducing sugars present were quantified using the dinitrosalicyclic acid method described by Miller (1959) with glucose as standard.

Enzymatic treatment of the homogenate

The supernatant obtained after centrifugation was investigated for possible increased release of more reducing sugar by hydrolysis of the cellulose present in the mesocarp and seeds. Cellulase assay was carried out according to methods described by Quadri et al. (2017) using 3,5 dinitrosalicyclic acid (Miller 1959). Cellulase (0.1-10% w/v) was added to the clarified homogenate for the hydrolysis of cellulose present in the seeds and mesocarp. The reducing sugars released were quantified as described above.

Fermentation and conditions

The clarified supernatant served as the medium for fermentation and it was fermented by *A. pullulans* and *S. cerevisiae* in 100 ml Erlenmeyer flasks that contained 20 ml of the clarified supernatant in an anaerobic jar. The medium for fermentation was inoculated with 1% (v/v) fungal cultures as inoculum. The effects fermentation time on reducing sugar consumption and ethanol production were determined. After every 24 h, 2 ml was aseptically withdrawn, centrifuged at 4000 g for 10 min and the ethanol and reducing sugar present in the supernatant were quantified. The ethanol yield and productivity were calculated using the Equation 1.:

$$\text{Ethanol yield } Y_{(p,s)}, (g/g) = \frac{\text{Ethanol Produced (g/L)}}{\text{Sugar consumed (g/L)}}$$

$$\text{Volumetric productivity } Q_p(g/L\times h) = \frac{\text{Ethanol Produced (g/L)}}{\text{Fermentation time (h)}}$$

Analytical processes

Ethanol was quantified using the dichromate method described by Hormitz (1980) as modified by Betiku et al. (2015). The reducing sugar was quantified using the dinitrosalicyclic method described by Miller (1959).

Optimization of the bioethanol production processes

Response surface methodology (RSM) was used to optimize the bioethanol production process from the seed of *T. madagascariense* and to investigate the influence of different fermentation process variables on the bioethanol yield. The variables considered are pH, fermentation time (h) and substrate concentration (g/L). To evaluate the effect of initial pH, the medium for fermentation

Table 1. Process parameters for Box-Behnken response surface methodology.

Variable	Coded factor levels		
	-1	0	+1
pH	4.95	5.95	6.95
Substrate concentration (g/L)	5	7.5	10
Time (h)	24	36	48

Table 2. Experimental runs for the Box-Behnken design for ethanol optimization.

Runs	pH	Substrate (g/L)	Time (h)	Bioethanol yield (Yps) (g/g)	
				Experimental value	Predicted value
1	4.95 (-1)	2.5 (-1)	36 (0)	0.53	0.53
2	6.95 (+1)	2.5 (-1)	36 (0)	0.57	0.57
3	4.95 (-1)	7.5 (+1)	36 (0)	0.53	0.53
4	6.95 (+1)	7.5 (+1)	36 (0)	0.57	0.57
5	4.95 (-1)	5.0(0)	24 (-1)	0.56	0.56
6	6.95 (+1)	5.0 (0)	24 (-1)	0.54	0.54
7	4.95 (-1)	5.0 (0)	48 (+1)	0.48	0.48
8	6.95 (+1)	5.0 (0)	48 (+1)	0.59	0.59
9	5.95 (0)	2.5 (-1)	24 (-1)	0.53	0.53
10	5.95 (0)	7.5 (+1)	24 (-1)	0.53	0.53
11	5.95 (0)	2.5 (-1)	48 (+1)	0.52	0.52
12	5.95 (0)	7.5 (+1)	48 (+1)	0.51	0.51
13	5.95 (0)	5.0 (0)	36 (0)	0.63	0.63
14	5.95 (0)	5.0 (0)	36 (0)	0.64	0.63
15	5.95 (0)	5.0 (0)	36 (0)	0.63	0.63
16	5.95 (0)	5.0 (0)	36 (0)	0.64	0.63
17	5.95 (0)	5.0 (0)	36 (0)	0.63	0.63

was subjected to pH 4.95, 5.95, and 6.95 using 1N NaOH and HCl, respectively. The Box-Behnken method was selected for the optimization of ethanol concentration. All variables were set at a central coded value of zero. The minimum and maximum ranges used in this optimization were selected based on, the basis of previous one-factor at-a-time independent study. The variables, factors, and levels are referenced in Table 1. Seventeen individual runs were conducted for the three independent variables (Table 2) for the quantification of ethanol. Ethanol yield was analyzed by using a second-order polynomial equation and data-fitting by multiple regression techniques using Design-Expert (version 6.0, Stat-Ease, Minneapolis, USA). The model equation for analysis is given in Equation 2.:

$$\alpha = \mu o + \mu_1 Z_1 + \mu_2 Z_2 + \mu_3 Z_3 + \mu_{12} Z_1 Z_2 + \mu_{13} Z_1 Z_3 + \mu_{23} Z_2 Z_3 + \mu_{11} Z_{12} + \mu_{22} Z_{22} + \mu_{33} Z_{32}$$

Where the predicted response (Bioethanol yield g/g) is denoted by α, μo is the model constant, Z_1, Z_2 and Z_3 are independent variables, μ_1, μ_2 and μ_3 are linear coefficients, μ_{12}, μ_{13} and μ_{23} are cross product coefficients and μ_{11}, μ_{22} and μ_{33} are the quadratic coefficients representing the constant process effect in total. The linear (α_i), quadratic effect (α_j) and the interaction effect between α_i and α_j for the production. The experimental/predicted values and the response surface plots were compared to determine the optimum conditions for bioethanol production.

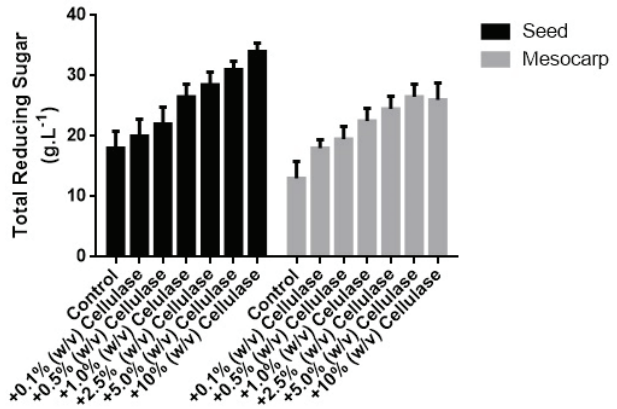

Figure 1. Total reducing sugars present in the seed and mesocarp of *T. madagascariense* fruit waste (*Tm*fw) with and without cellulase (0.1-10% w/v) pretreatment of the mesocarp and seed of (*Tm*fw).

Statistical analysis

The statistical software Design Expert 6.0.7. (Stat-Ease, Minneapolis, USA) was used for the design of experiments, regression, and graphical analysis of the data obtained and for statistical analysis of the model to evaluate the analysis of variance (ANOVA) and it was used also for the optimization of the bioethanol fermentation process.

Validation of the model under the optimized conditions

The optimum conditions obtained after the statistical optimization was used in bioethanol production to correlate the values obtained. The bioethanol yield and volumetric productivity were estimated as described in Equation 1.

Result and Discussion

Reducing sugars present in the T. madagascariense

T. madagascariense is known to be rich in carbohydrate (60%) Adewuyi et al. (2015). The mesocarp and seeds contained about 17.1 g/L and 11.2 g/L of the total reducing sugar without pretreatment. The addition of cellulase to the clarified homogenate increased the reducing sugar to 33.2 and 39 g/L in the mesocarp and seed, respectively (Fig. 1). This could be connected to the cellulose content of the seed and mesocarp that upon enzymatic digestion results in the release of soluble reducing sugars. There was not any significant ($p < 0.05$) increase in the total reducing sugar concentration in both seed and mesocarp of *T. madagascariense* as the enzyme concentration increased from 5.0 to 10% (w/v). This might be indicative of the complete digestion of the cellulose present in the mesocarp and seeds.

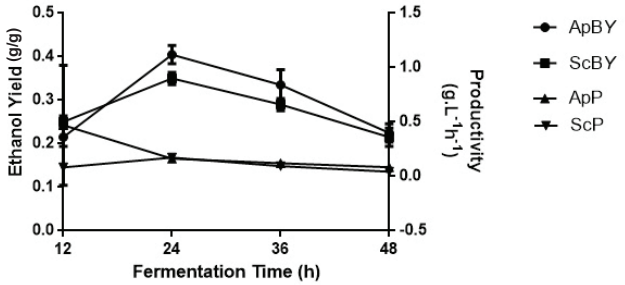

Figure 2. Bioethanol yield and volumetric productivity estimation by fermentation of the mesocarp of *T. madagascariense* fruit waste (*Tm*fw) using both *A. pullulans* and *S. cerevisiae*. ApBY and ScBY represent the bioethanol yield when *A. pullulans* and *S. cerevisiae* were used for the fermentation process while ApP and ScP represents the volumetric productivity when *A. pullulans* and *S. cerevisiae* were used for the fermentation of the mesocarp of (*Tm*fw).

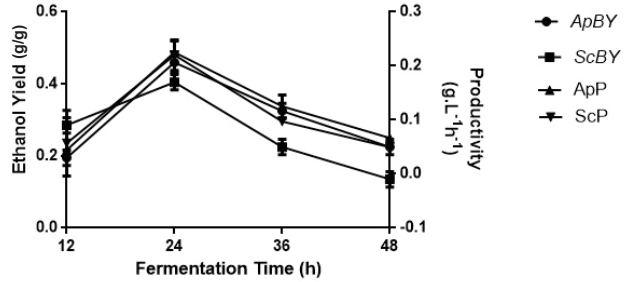

Figure 3. Bioethanol yield and volumetric productivity estimation by fermentation of the seeds of *T. madagascariense* fruit waste (Tmfw) using both *A. pullulans* and *S. cerevisiae* when *A. pullulans* and *S. cerevisiae* were used for the fermentation process while ApP and ScP represents the volumetric productivity when *A. pullulans* and *S. cerevisiae* were used for the fermentation of the seeds of (*Tm*fw).

Fermentation of the clarified homogenate to bioethanol

Depending on the yeast used for fermentation, the maximum ethanol yield (g/g) and % ethanol yield varied accordingly. *S. cerevisiae* and *A. pullulans* fermented the clarified supernatant of the seed and mesocarp to optimally produce ethanol after 24 h (Fig. 2). Comparatively, *A. pullulans* had higher bioethanol yield and productivity than *S. cerevisiae* and this suggests that *A. pullulans* might be exploited industrially for bioethanol production as a useful alternative to *S. cerevisiae*. The decline in bioethanol production observed after 24 h might be due to the decrease in the total reducing sugars present for the microorganisms to act upon. The findings in this present study were akin to that observed by Betiku and Taiwo (2015) where the authors reported that it took 24 h for *S. cerevisiae* to ferment bread fruit hydrolysate for production of bioethanol.

RSM optimization for bioethanol production and ANOVA analysis

In the present study, seventeen independent experiments to evaluate bioethanol yield using the mesocarp of *T. madagascariense* fruit waste by considering the interactive effects of pH, incubation time and substrate concentration. The observed and predicted bioethanol yield values are shown in Table 3. The optimum condition for bioethanol production was pH of 5.95, substrate

Table 3. ANOVA for response surface quadratic model.

Source	Sum of squares (x 10^{-3})	DF	F-value	Prob>F	
pH	0.32	1	335.18	< 0.0001	Significant
Substrate	0.03	1	230.49	< 0.0001	Significant
Time	0.39	1	2.33	0.1706	Not significant
pH x pH	0.39	1	28.41	0.0011	Significant
Substrate x substrate	0.011	1	280.06	< 0.0001	Significant
Time x time	0.015	1	822.73	< 0.0001	Significant
pH x substrate	0.001	1	1116.84	< 0.0001	Significant
pH x time	4.029	1	0.088	0.7755	Not significant
Substrate x time	0.11	1	291.26	< 0.0001	Significant
Model	0.0470	9	212.86	<0.0001	Significant
Residual	0.1220	7			
Lack of fit	2.48x10-5	3	1.92x10-4	1.0	Not significant
Pure error	0.172	4			
R2	0.9964				
Adj R2	0.9917				
Pred R2	0.9943				
Adeq precision	41.370				
C.V.	0.8700				

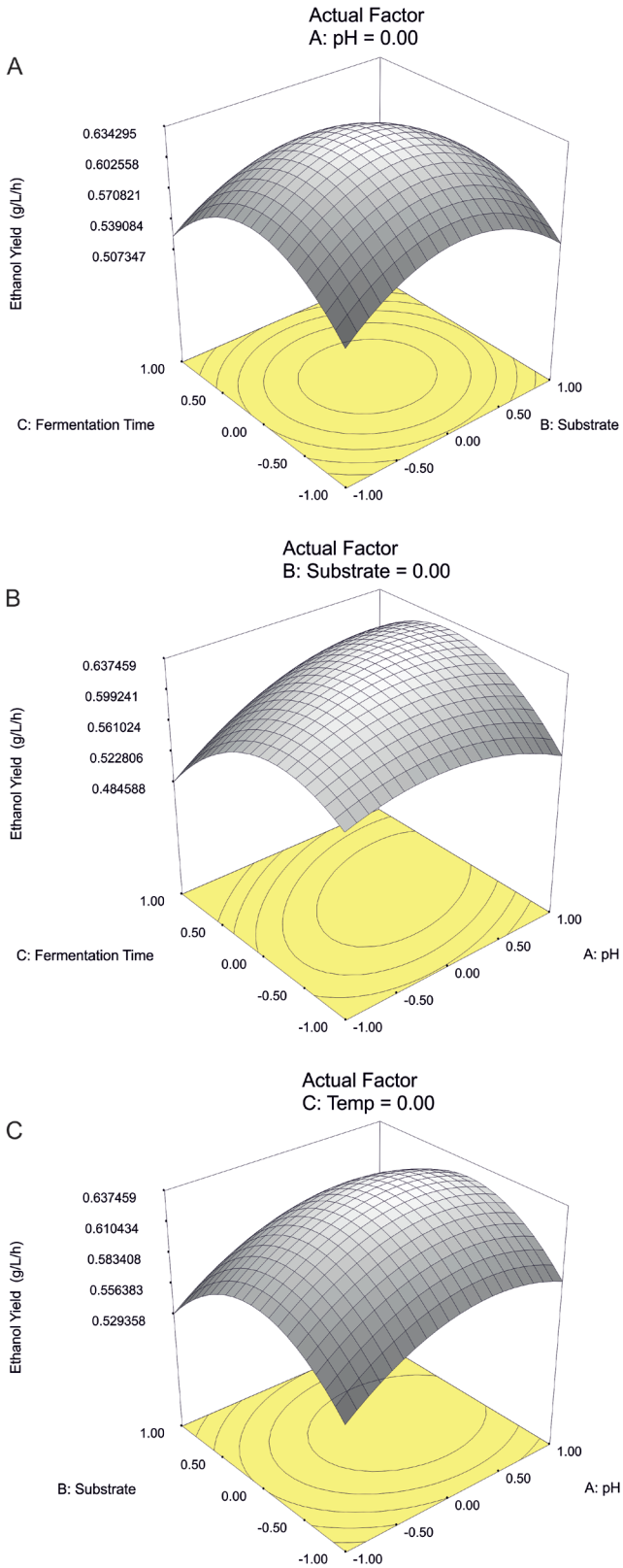

Figure 4. (A) Substrate vs pH with fermentation time held constant. (B) Fermentation time vs pH with substrate concentration held constant. (C) Fermentation time vs substrate with the pH held constant.

concentration of 5.0 g/L and incubation time of 24 h. It is reported that optimum ethanol production occurs at a pH range of 4-6 and ethanol production is influenced by pH of the broth as it affects bacterial contamination, yeast growth, fermentation rate, and byproduct formation. From the ANOVA of the quadratic model, it was noted that model terms such as pH, time, pH x pH, substrate concentration x substrate concentration, time x time and pH x time were significant ($p < 0.05$). The model F-value of 212.9 implied that the model was significant. The F-value is often used as a measure of how the factors aptly describe the variation in the data set. The F-values obtained for the data set in this study indicates that the model is significant when also considering the P-value (< 0.0001). The quadratic model was used in the theoretical prediction of the bioethanol yield reliably due to the R^2 value (Table 3). It is reported that the R^2 values must fall between 0.75 and 0.80 for a good model fit. The values obtained in this study allows for the predictability of the bioethanol yield from the quadratic equation in coded factors as shown below (Equation 3):

$$\text{Ethanol Yield} = +0.64 + 0.020 \times A - 2.008E\text{-}003 \times B - 7.009E\text{-}003 \times C - 0.034 \times A^2 - 0.056 \times B^2 - 0.064 \times C^2 + 5.512E\text{-}004 \times A \times B + 0.032 \times A \times C - 5.276E\text{-}003 \times B \times C$$

where A, B, and C represent pH, substrate concentration and time of fermentation, respectively.

The "Pred R^2" of 0.9943 is in reasonable agreement with the "Adj R^2 of 0.9917."Adeq Precision" measures the signal to noise ratio. A ratio greater than 4 is desirable. The ratio of 41.371 obtained in this process indicates an adequate signal. The summary of the ANOVA analysis is shown in Table 4.

Interaction between factors

From the response surface plots (Fig. 3-5), it was deduced that there were moderate interactions between the variables considered in this study. To obtain these response surface curves, the interactions between two variables were investigated by obtaining 3D response surface plots while the third variable was kept constant. The optimum pH obtained was mildly acidic and increasing the pH resulted in a decrease in the bioethanol yield. The pH plays a crucial role in fermentation as it is directly tied to most biological processes (Manohar and Divakar 2005). Also, decreasing or increasing the fermentation period above 24 h resulted in a decline the bioethanol production.

Conclusion

A readily available, cheap and non-toxic feedstock of *T. madagascariense* fruit wastes investigated in this study provides a novel source for bioethanol production. The reducing sugar present with and without enzymatic saccharification indicates that these agricultural wastes could be converted inexpensively to bioethanol. Validation of the model using the optimum conditions predicted after statistical optimization indicated that the volumetric productivity and bioethanol yield obtained was 0.24 g/L/h and 0.63 g/g, respectively.

Acknowledgment

The authors appreciate Mr. Tunde Oni, Department of Microbiology, Obafemi Awolowo University, Ile-Ife for providing useful technical assistance.

References

Ademakinwa AN, Agboola FK (2016) Biochemical characterization and kinetics of a purified yellow laccase from *Aureobasidium pullulans* (De Bary) isolated from soil containing decayed plant matter. J Genet Eng Biotechnol 14(1):143-151.

Ademakinwa AN, Ayinla ZA, Agboola FK (2017) Strain improvement and statistical optimization as a combined strategy for improving fructosyltransferase production by *Aureobasidium pullulans* NAC8. J Genet Eng Biotechnol 15(2):341-35.

Adewuyi A, Prasad BNR, Rao SK, Oderinde RA (2010) Oil composition, mineral nutrient and fatty acid distribution in the lipid classes of underutilized oils of *Trilepisium madagascariense* and *Antiaris africana* from Nigeria. Food Res Int 43:665-670.

Alma RD, Jorge AT, Ricardo AL (2015) Production of bioethanol from agro-industrial wastes. Fuel 149:85-89.

Betiku E, Taiwo AE (2015) Modelling and optimization of bioethanol production from breadfruit starch hydrolysate vis-à-vis response surface methodology and artificial neural network. Renew Energ 74:87-94.

Dash PK, Mohaptra S, Swain MR, Thatoi H (2017) Optimization of bioethanol production from saccharified sweet potato root flour by co-fermentation of *Saccharomyces cerevisiae* and *Pichia* sp. using OVAT and response surface methodologies. Acta Biol Szeged 61(1):13-23.

Joshi B, Bhatt MR, Sharma D, Joshi J, Malla R, Sreerama L (2011) Lignocellulosic ethanol production: Current practices and recent developments. Biotech Mol Biol Rev 6(8):172-182.

Lebaka (L)V (2013) Potential bioresources as future sources of biofuels production: An overview. In Gupta V, Tuohy M, eds, Biofuel Technologies. Springer, Berlin, Heidelberg.

Manohar B, Divakar S (2005) An artificial neural network analysis of porcine pancreas lipase catalysed esterification of anthranilic acid with methanol. Process Biochem 40(10):3372-3379.

Miller GL (1959) Use of dinitrosalicylic acid reagent for determination of reducing sugar. Anal Chem 31(3):426-428.

Nwamarah JU, Chikewendu JN, Otitoju GTO, Eme P (2015) Nutrients, anti-nutrients and phytochemical composition of *Bosquiea angolensis* fruits „Oze" consumed as snacks in Enugu State, Nigeria. Pak J Nutri 14(5):269-273.

Quadri HO, Ademakinwa NA, Adejumo AL, Agboola FK (2017) Partial purification and characterization of cellulolytic enzyme from *Bacillus pantothenicus* isolated from a dumpsite. Res Rev J Microbiol Biotechnol 6(2):4-11.

Razmovski R, Vucurovic V (2012) Bioethanol production from sugar beet molasses and thick juice using *Saccharomyces cerevisiae* immobilized on maize stem ground tissue. Fuel 92:1-8.

Sharma N, Sharma N (2018) Second generation bioethanol production from lignocellulosic wastes and its future perspective: A review. Int J Curr Microbiol Appl Sci 7(5):1285-1290.

Acta Biologica Szegediensis

Volume 63(1):51-58, 2019
Acta Biologica Szegediensis
http://abs.bibl.u-szeged.hu/index.php/abs
DOI:10.14232/abs.2019.1.51-58

ARTICLE

Optimization of the production of xylanases in corncob-based media by *Aspergillus niger* and *Trichoderma longibrachiatum* using Taguchi approach

Joseph Adetunji Elegbede, Agbaje Lateef*

Laboratory of Industrial Microbiology and Nanobiotechnology, Department of Pure and Applied Biology, Ladoke Akintola University of Technology, PMB 4000, Ogbomoso, Nigeria

ABSTRACT Xylanases are important in producing several commercially valued bioproducts. In this study, xylanases were produced by *Aspergillus niger* L3 and *Trichoderma longibrachiatum* L2 using corncob, an agricultural waste, as sole carbon source. The impact of important fermentation parameters at individual and interactive levels were studied using Taguchi L9 orthogonal array. Substantial variation in enzyme synthesis was observed among designated factor levels. The optimal conditions to produce xylanases were 20% inoculum size, 24 h fermentation time, substrate concentration of 15 g/l at pH 5.5 for *A. niger* L3; and inoculum size 12.5%, 72 h fermentation time, substrate concentration of 15 g/l at pH 5.5 for *T. longibrachiatum* L2. Validation of outcomes of the optimal combination of parameters resulted in a significant improvement of approximately 208.09 and 192.59% in the yield of xylanase by *A. niger* L3 (28.69 to 88.39 U/ml) and *T. longibrachiatum* L2 (22.13 to 64.75 U/ml), respectively. The study therefore established the optimal valorization of corncob to produce xylanase by the fungal isolates.
Acta Biol Szeged 63(1):51-58 (2019)

KEY WORDS
agrowastes
corncob valorization
optimization
Taguchi orthogonal array
xylanase

ARTICLE INFORMATION
Submitted
09 February 2019.
Accepted
04 May 2019.
***Corresponding author**
E-mail: agbaje72@yahoo.com
alateef@lautech.edu.ng

Introduction

Hemicellulose is part of the core constituents of lignocellulose and it is the next most abundant carbohydrate resource on Earth after cellulose (Radhika et al. 2011). Xylan represents the main component of hemicelluloses (Bajaj and Manhas 2012) and is the major backbone in the hemicellulosic portion of the plant cell wall, connecting compounds like arabinose, mannose, glucose and other sugars via an acetyl chain (Radhika et al. 2011). Xylan is a heterogeneous or diverse polysaccharide and contains a linear backbone of β-1,4-D-xylopyranoside residues and, also short side-chain branches. Xylan can only be completely hydrolyzed using several enzymes due to its composite structure (Bajaj and Manhas 2012). Thus, biodegradation of xylan, requires series of xylanolytic enzymes among which endo-β-1,4-xylanases (EC 3.2.1.8) hydrolyse the xylan backbones into short xylooligosaccharides (Pandey et al. 2014).

Extracellular xylanases synthesized by microorganisms have incredible industrial significance, with about 20% of global enzyme market being shared by cellulase, pectinase, and xylanase (Polizeli et al. 2005). The global market of industrial enzymes is said to have witnessed rapid growth in recent years. It was reported to be only 1 million US dollars in 1970 and has grown to 4.5 billion dollars in 2012, with projection to reach about 7.1 billion dollars in 2018 (Kalim et al. 2015).

Microbial enzymes, like xylanases are imperative in numerous fields from food processing to paper and pulp industries (Azin et al. 2007). It contributes a critical role in numerous biotechnological processes such as clarification of fruit juice, bleaching, beer and wine, improving poultry feed digestibility, pulp and paper, leather and baking industries (Uday et al. 2016a). They are utilized in extraction of extracellular polymeric substances (EPS) and plant oils and, also used to enhance the nutritional quality of silage, coffee, green feed and starch (Lakshmi et al. 2009). Moreover, an important usefulness of xylanase has been established to produce biofuel from lignocelluloses (Uday et al. 2016b). Its use most recently reported for the green synthesis of nanoparticles with profound biomedical applications (Elegbede et al. 2018a, 2018b, 2019) has further expanded the frontiers of enzyme technology in nanobiotechnology (Lateef and Adeeyo 2015; Lateef et al. 2015; Adelere and Lateef 2016). Broad types of fungi and bacteria are known to synthesize xylanases under various cultivation systems, but filamentous fungi are the most effective producers of xylanase, because they

secrete elevated levels of enzymes compared to yeasts and bacteria (Rani et al. 2014). On an industrial scale, xylanases are principally synthesized by *Aspergillus* and *Trichoderma* spp. (Shahi et al. 2011). Also, Aspergilli have capability to synthesize broad range of enzymes responsible for degrading plant cell wall. *Trichoderma* spp., which are foremost agents causing decay and decomposition of agricultural wastes possess an array of different enzymes, and hence they are known as excellent producers of lignocellulolytic enzymes (Azin et al. 2007).

Pure substrates are highly expensive and are not affordable for bulk production of enzymes at industrial level. Therefore, it is essential to survey cheap substrates for cost-effective production of enzymes. Agricultural residues, including animal wastes present a cheap source of raw materials for the industrial production of enzymes (Geetha and Gunasekaran 2010; Lateef et al. 2008, 2010, 2012; Lateef and Gueguim-Kana 2012; Ganaie et al. 2014; Lateef et al. 2015), and they are available in great quantity in countries with wide-ranging agricultural practices (Bajaj and Manhas 2012).

Optimization of production of xylanase is a prerequisite for its large-scale economical production (Azin et al. 2007), and this can be achieved by manipulating important parameters that affect the fermentation process (Rani et al. 2014). Production of xylanase differs in diverse strains and this can be regulated by the nutritional, physiological, and biochemical nature of microbes that are employed (Lakshmi et al. 2009). In this case, it becomes imperative to optimize all fermentation parameters since no definite medium has been authenticated for the maximum production of any metabolite, because the genetic diversity in various microbial sources causes each microorganism or strain to have its unique conditions for the best yield of production (Rao et al. 2008a). Notable fermentation and environmental factors that can manipulate metabolism-mediated yields include temperature, aeration, pH, agitation, carbon and nitrogen sources, incubation time, initial inoculum size, ion requirement amongst others (Prakasham et al. 2007a). Hence, for industrial and commercial production, optimization of growth medium is one of the critical steps to reduce the quantity of unutilized constituents for a cost-effective yield (Lakshmi et al. 2009).

The conventional optimization procedures, including one-factor-at-a-time design entail experimental work which is time consuming and does not provide necessary information about the common interactions of the parameters (Mandal et al. 2015). On the contrary, statistical optimization techniques help to investigate the influence of controlled factor in a multivariate system. Furthermore, bioprocesses have been optimized using response surface methodology (RSM), artificial neural networks (ANN), and genetic algorithm (Gueguim-Kana et al. 2007, 2012a,b; Adeoye et al. 2015; Adeeyo et al. 2016).

Taguchi orthogonal array (OA) design of experiment (DOE) encompasses the investigation of a system by a set of independent variables (factors or parameters) over specific levels of interest (Taguchi 1986). The technique also determines the relationship or correlation between variables and operational conditions (Mandal et al. 2015). Recent literature reviews reveal that Taguchi methodology has been used to optimize reaction variables in several biochemical processes by studying a given set of independent variables, which may be controllable or uncontrollable over a definite region of interest. It is also imperative that experiments conducted in small scale are valid over an entire experimental region (Uday et al. 2016a). The use of ANOVA (analysis of variance) is to investigate the accuracy of experimental data and gives the statistical relationship of the output (Mandal et al. 2015). Taguchi methodology has been efficiently applied in bioprocesses (Rao et al. 2008b), to optimize the synthesis of some industrial enzymes such as tannase (Mohapatra et al. 2009), alkaline protease (Laxman et al. 2005), α-amylase (Uysal et al. 2010) and L-asparaginase (Prakasham et al. 2007b). It is better and superior over other analogous statistical designs, including the RSM, because much less time is needed to execute the experiment. Also, Taguchi method is advantageous to achieve consistency and reliability at little cost with fewer experiments, when compared with RSM and ANN. Its application normally leads to improved quality or yield of products and process performance (Rao et al. 2008b). The improved performance is ensured by the orthogonal layout, whereby interactive effects of different factors are studied with fewer numbers of experimental runs (Rao et al. 2008b). However, Taguchi DOE does not take into accounts of the influence of all the controlling factors in a process, but chiefly concerned about the main effects of the important factors. Also, its application requires a critical brainstorming on the discovery of key parameters, and competence in statistical analysis. It is also expedient that for reliability, the noise factors in the experiment must be properly identified (Rao et al. 2008b).

Most recently, we reported xylanase activities of some fungal isolates, including *Aspergillus niger, A. flavus, Trichoderma longibrachiatum, A. fumigatus, Fusarium solani,* and *Botryodiplodia* sp. in our laboratory with potent dough rising and juice clarification activities (Elegbede and Lateef 2018). In the present study, Taguchi method was applied to optimize process parameters to synthesize xylanase by two of the isolates; namely *A. niger* L3 and *T. longibrachiatum* L2 in corncob-based media with the aim of improving the enzyme yield for biotechnological applications. The experiments were designed using 4 factors at 3 levels with OA layout of L9 (3^4).

Materials and Methods

Microorganisms and maintenance

Isolates of *A. niger* L3 and *T. longibrachiatum* L2 which were previously isolated in our laboratory (Elegbede and Lateef 2018) were used in this study. They were sub-cultured on fresh sterile potato dextrose agar (PDA) plates, incubated at room temperature (30 ± 2 °C) for 72 h and stored on PDA at 4 °C.

Substrate

Corncobs were locally sourced from Ajegunle market, Oyo, Oyo state, Nigeria, and processed through grinding (0.5 mm mesh) to obtain fine powder. The percentage moisture content of the corncob powder was estimated by drying the powder to a constant weight at 110 °C in a hot air oven (Lateef and Gueguim-Kana 2012).

Inoculum preparation

Inoculum was developed according to the methods of Lateef and Gueguim-Kana (2012) through the transfer of a loopful mycelium of the fungal strain from the plate into a sterilized 50 ml inoculum medium in a 250 ml capacity flask (containing 1% sucrose, 0.2% yeast extract, final pH 5.5). The flask was incubated at 30 ± 2 °C on a shaker at 100 rpm for 24 h.

Submerged fermentation

The basal medium composition for enzyme production was corncob (20.0 g/L), $MgSO_4$ (2.0 g/L), $NaNO_3$ (1.4 g/L), KH_2PO_4 (1.8 g/L), NH_4Cl (2.0 g/L), and $CaCO_3$ (1.2 g/L) at starting pH of 5.7 as previously reported (Elegbede and Lateef 2018). Then, 40 ml of basal medium was dispensed in 250 ml flask, sterilized at 121 °C for 15 min and inoculated with 10% (v/v) 24 h old inoculum (5×10^6 spores per ml). The culture was incubated at 30 ± 2 °C on a shaker at 100 rpm for up to 120 h. After specific period of fermentation, the contents were filtered with the aid of Whatman No.1 filter paper, followed by centrifugation at 4000 rpm at 10 °C for 25 min. The cell-free supernatant was used as crude enzyme and kept at 4 °C until further use.

Xylanase assay

Xylanase activity was determined following the methods of Bailey et al. (1992). Exactly 0.9 ml of 0.5% (w/v) of beechwood xylan (Megazyme, Ireland) prepared in 0.1 M sodium citrate buffer at pH 5.4 was reacted with 0.1 ml of the crude enzyme, and incubated in a water bath shaker at 50 °C for 30 min. The reaction was terminated by adding 1 ml of 3,5-dinitrosalicyclic acid reagent (DNS acid) to the reaction mixture followed by heating at 100 °C for 10 min. This was followed by cooling to room temperature and subsequent measurement of the absorbance at 540 nm using Spectrumlab S23A spectrophotometer (Yuchengtech, Beijing City, China). Earlier, xylose standard curve was prepared for the extrapolation of the amount of xylose released through the enzymatic hydrolysis of xylan. A unit (U) of xylanase was defined as the amount of enzyme that liberated 1.0 μmol of reducing sugar as xylose equivalent per minute in the reaction mixture as described in the above assay conditions. All enzyme determinations were investigated in duplicates.

Taguchi optimization

Taguchi method was employed in investigating the relationships that exist among the variables of medium components and to optimize for higher yields of enzyme production. Taguchi design methodology was performed using modified steps as stated in Figure 1, and it was used to set up the critical fermentation factors: inoculum size (%), fermentation time (h), initial pH, and substrate (corncob) concentration (g/L). The effective levels were set as low, intermediate and high (Table 1) based on earlier experimental values (Elegbede and Lateef 2018). Conditions such as temperature (30 ± 2 °C), agitation (100 rpm), and media: flask volume ratio (40 ml/250 ml flask) were not changed and fixed as standard conditions for the fermentation.

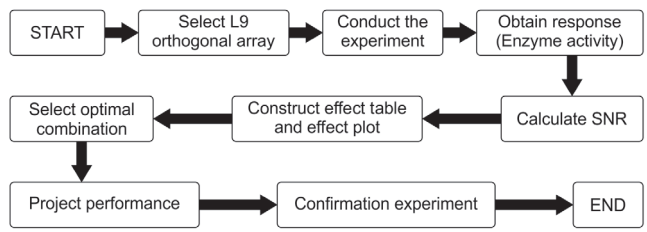

Figure 1. Flowchart for Taguchi optimization method used for xylanase synthesis

Table 1. Culture parameters and their respective levels of variation.

Culture parameters	Units	Levels of variation		
		1	2	3
Inoculum size	%	5	12.5	20
Fermentation time	h	24	72	120
Substrate (corncob)	g/l	5	15	25
Initial pH		4	5.5	7

The appropriate Taguchi design arrangement for data analysis was selected. The L9-orthogonal array method

Table 2. Experimental set-up (L9 orthogonal array) for xylanase production by *A. niger* L3 and *T. longibrachiatum* L2.

Exp. no	Inoculum size	Fermentation time	Substrate concentration	Initial pH	Xylanase activity (U/ml)	Signal-to-noise ratio	Xylanase activity (U/ml)	Signal-to-noise ratio
					A. niger		*T. longibrachiatum*	
1	1	1	1	1	18.44	25.31522	16.53	24.36546
2	1	2	2	2	53.28	34.53128	56.83	35.09155
3	1	3	3	3	12.57	21.98671	4.51	13.08353
4	2	1	2	3	39.07	31.83687	55.87	34.94357
5	2	2	3	1	1.50	3.521825	7.24	17.19477
6	2	3	1	2	41.53	32.36724	43.45	32.75980
7	3	1	3	2	62.43	35.90787	6.15	15.77750
8	3	2	1	3	31.69	30.01844	59.16	35.44056
9	3	3	2	1	43.58	32.78574	47.68	33.56672

based on modified methods described by Taguchi (1986), which overcomes many problems related with conventional methodology, was used for the aforementioned control parameters with three levels of factor variation. In Taguchi method, the summary statistic η is called signal-to-noise ratio (SNR). The value of η is an effective indicator for the assessment of the impact of process parameters on enzyme synthesis. The larger-the-better signal-to-noise was utilized to evaluate the summary statistic η in the present study, because an improved production of xylanase was targeted, and it was defined as follows:

$$SNR\ (\eta) = -10 \log (R^{-2}) \qquad \text{Eqn. 1. (Chou et al. 2003)}$$

Where, SNR represents the signal-to-noise ratio, while R represents the response or yield of correspondent trials. For each component, the optimal conditions give the largest SNR ratio.

The optimal combination of fermentation parameters was selected using the effect table, and the result was predicted using the formula (Eqn. 2). To validate or confirm the optimized methodology, fermentation experiments were run in duplicates and the samples collected were assayed for xylanase production. ANOVA was performed to evaluate the fermentation parameters that were statistically significant.

$$y_{pr} = y_{av} + \sum_{i=1}^{n=4} (y_{opt}(n) - y_{ave}) \qquad \text{Eqn. 2}$$

Results and Discussion

Unoptimized xylanase production

Xylanase was produced by *A. niger* L3 and *T. longibrachiatum* L2 strains on corncob supplemented minimal salt media since the use of pure xylan for industrial production of xylanases is uneconomical because of its high cost. Hence, use of cost-effective xylan-rich substrates is highly recommended (Lakshmi et al. 2009). The two fungi utilized corncob effectively as potential source of carbon to produce xylanase (Elegbede and Lateef 2018). Carbon source has been well-known as a noteworthy factor during the growth and metabolic process of any

Table 3. Effect table of xylanase production by *A. niger* L3 and *T. longibrachiatum* L2.

Levels of parameters	Parameters			
	Inoculum size	Fermentation time	Substrate concentration	Initial pH
A. niger L3				
1	27.27774	31.01998	29.23363	20.54093
2	22.57531	22.69052	33.05130	34.26880
3	32.90402	29.04656	20.47213	27.94734
T. longibrachiatum L2				
1	24.18018	25.02884	30.85527	25.04232
2	28.29938	29.24230	34.53395	27.87628
3	28.26160	26.47002	15.35193	27.82256

Table 4. Performance of selected optimal combination of parameters.

Parameters	Levels	
	A. niger L3	*T. longibrachiatum* L2
Inoculum size (%)	20	12.5
Fermentation time (h)	24	72
Substrate concentration (g/L)	15	15
Initial pH	5.5	5.5
Optimum profile	A3B1C2D2	A2B2C2D2
*Signal-to-noise ratio	38.92731	36.220975
*Xylanase activities (U/ml)	88.39	64.75

*Average of two readings. A: inoculum size, B: fermentation time, C: substrate concentration, D: initial pH

microorganism; therefore, the choice of a suitable carbon source has been identified as a key determinant in the production economics of xylanase (Pandya and Gupte 2012).

Xylanase production was performed in 250 ml Erlenmeyer fasks containing 40 ml of fermentation medium as earlier stated. The time course analysis of xylanase activities showed the commencement of production of xylanase at 24 h of fermentation for both isolates and reached maximum of 28.69 U/ml at 96 h for *A. niger* L3, and 22.13 U/ml at 72 h for *T. longibrachiatum* L2 as previously reported (Elegbede and Lateef 2018). These productivities were achieved at pH values of 6.7 and 6.6 for *A. niger* and *T. longibrachiatum* L2, respectively. Maximum yields of fungal xylanases have been achieved at pH of 4.0-6.5 in similar studies (Murthy and Naidu 2012; Yegin 2017).

Optimization of xylanase production through Taguchi method

Enhancement of production of metabolites by microbes is influenced by the nutritional, physiological, and biochemical nature of the microbe utilized, and these influential factors vary from microorganism to microorganism (Lakshmi et al. 2009). The Taguchi L9 orthogonal array revealed noteworthy variation in xylanase synthesis (Table 2). Initial maximum xylanase production values were observed to be 62.43 and 59.16 U/ml for *A. niger* L3 and *T. longibrachiatum* L2, respectively. These results are regarded as the local optimal for xylanase production by both fungal strains. The data presented a very significant improvement in xylanase yields compared to the conventional unoptimized production; 117.60 and 167.33% for *A. niger* L3 and *T. longibrachiatum* L2, respectively. Similar variation of enzyme activity was reported by Lakshmi et al (2009). This data further showed that xylanase production by fungal strains is determined by fermentation parameters and their levels.

The Taguchi DOE used for optimization in this study provided the predicted profile for maximum yield of xylanase from the effect tables. The S/N ratio was used to determine the influence of each variable on the output, and the effect table (Table 3) was employed for the analysis of the relative effect of different parameters. This is because the change in signal leads to a larger effect on the output variable being evaluated. The S/N ratio values help in the assessment of the combination of factors that have the maximum influence on the response characteristic of concern, such that higher values of S/N ratio indicate greater influence of the combined parameters (Rani et al. 2012). The profiles A3B1C2D2 (interpreted as inoculum; 20%, fermentation time; 24 h, substrate concentration; 15 g/L, and pH; 5.5) and A2B2C2D2 (interpreted as inoculum; 12.5%, fermentation time; 72 h, substrate concentration; 15 g/L, and pH; 5.5) were generated for *A. niger* L3 and *T. longibrachiatum* L2, respectively, being the optimum conditions for achieving higher xylanase yields (Table 4).

The optimal combination of parameters was evaluated and the verification experiments, in which optimized conditions were used yielded highest activities of 88.39 and 64.75 U/ml for *A. niger* L3 and *T. longibrachiatum* L2, respectively as the global maximum (Table 4). These global maxima obtained from the optimum combination profiles represented 41.58 and 9.45% increase on the local maxima obtained from the initial orthogonal array experiments. The results indicated a total significant increment of 208.09 and 192.59% when compared with the conventional unoptimized xylanase synthesis by both *A. niger* L3 and *T. longibrachiatum* L2, respectively. These results compared well with previous reports of xylanase production that were optimized using Taguchi method where 277%, 161.5%, 41.9 and 10.24% higher enzyme yields were obtained (Lakshmi et al. 2009; Rani et al. 2014; Mandal et al. 2015). The increase can be claimed to have resulted from the interactions and relations among the various factors (Mandal et al. 2015).

Analysis of Variance (ANOVA)

Understanding of the influence or effect of each individual factor is crucial for the implementation of a successful bioprocess operation (Rani et al. 2014). Therefore, ANOVA was employed in evaluating results of the orthogonal array experiment and to study the level of consequence of the fermentation parameters on the deviation of the responses (Lakshmi et al. 2009). ANOVA (Table 5) showed that the initial pH, substrate concentration, inoculum size and fermentation time contributed 35.10, 30.93, 19.88 and 14.09%, respectively, to the optimal yield of xylanase by *A. niger* L3, while substrate concentration, inoculum size, fermentation time and initial pH contributed 88.99, 4.81, 3.94 and 2.26%, respectively, to the optimal yield of

Table 5. Analysis of variance of main effects of fermentation factors on xylanase production by *A. niger* L3 and *T. longibrachiatum* L2.

	Inoculum size	Fermentation time	Substrate concentration	Initial pH	Error	Pooled error	Total
A. niger L3							
DF	2	2	2	2	0	0	8
SS	213.9334	151.5649	332.7652	377.6934			1075.957
Variance	106.9667	75.78247	166.3826	188.8467			
Percentage contribution	19.88308	14.08652	30.92737	35.10302			100
T. longibrachiatum L2							
DF	2	2	2	2	0	0	8
SS	44.83626	36.68758	829.1145	21.01863			931.657
Variance	22.41813	18.34379	414.5572	10.50932			
Percentage contribution	4.812529	3.937885	88.99354	2.256048			100

*DF: degree of freedom, SS: sum of squares

xylanase in the case of *T. longibrachiatum* L2. While initial pH has the highest effect on yield of xylanase by *A. niger* L3, it has the least effect and a very minute significance on *T. longibrachiatum* L2. This further shows that factors that influence the production of metabolites vary from microorganism to microorganism which can be adduced to genetic diversity, physiology and metabolic differences. The inference of this finding is that more interest should be focused on initial pH and substrate concentration for *A. niger* L3, and mainly substrate concentration for *T. longibrachiatum* L2, if the production of xylanases by either of these fungal isolates is to be modulated significantly. Such carbon source or substrate concentration dependent enzyme production has been reported in diverse xylanase synthesizing microbial strains (Oliveira et al. 2006; Kapoor et al. 2008). Also, Rani et al (2014) reported that carbon source (rice straw) produced the greatest effect in the production of xylanase.

Conclusion

Xylanase production by *A. niger* L3 and *T. longibrachiatum* L2 on corncob based media was successfully enhanced through optimization of the fermentation conditions with Taguchi method. Four factors (Inoculum concentration (%), substrate concentration (g/l), fermentation time and initial pH) at three levels of variation were used and the analysis confirmed the participation and, also the interactions of the factors. It was ascertained that the optimal conditions for production of xylanases by *A. niger* L3 and *T. longibrachiatum* L2 were inoculum; 20%, fermentation time; 24 h, substrate concentration; 15 g/l, and pH; 5.5 and inoculum; 12.5%, fermentation time; 72 h, substrate concentration; 15 g/l, and pH; 5.5, respectively. Using the optimum conditions, enzyme yield was significantly improved to about 208.09 and 192.59% for *A. niger* L3 and *T. longibrachiatum* L2, respectively. Also, it was established that more attention should be focused on initial pH and substrate concentration for *A. niger* L3, and mainly substrate concentration for *T. longibrachiatum* L2, if the production of xylanases by any of the fungal isolates is to be significantly adjusted or altered. It can therefore be concluded that corncob can be valorized to produce xylanase by the fungal isolates.

Acknowledgement

Authors thank Dr. T.B. Asafa of Department of Mechanical Engineering, LAUTECH, Ogbomoso, Nigeria for the assistance on Taguchi optimization technique.

References

Adeeyo AO, Lateef A, Gueguim-Kana EB (2016) Optimization of the production of extracellular polysaccharide from the Shiitake medicinal mushroom *Lentinus edodes* (Agaricomycetes) using mutation and a genetic algorithm-coupled artificial neural network (GA-ANN). Int J Med Mushrooms 18:571-581.

Adelere IA, Lateef A (2016) A novel approach to the green synthesis of metallic nanoparticles: the use of agro-wastes, enzymes and pigments. Nanotechnol Rev 5:567-587.

Adeoye AO, Lateef A, Gueguim-Kana EB (2015) Optimization of citric acid production using a mutant strain of *Aspergillus niger* on cassava peel substrate. Biocatal Agric Biotechnol 4:568-574.

Azin M, Moravej R, Zareh D (2007) Production of xylanase by *Trichoderma longibrachiatum* on a mixture of wheat bran and wheat straw: Optimization of culture condition by

Taguchi method. Enzyme Microb Technol 40:801-805.
Bailey MJ, Biely P, Poutanen K (1992) Interlaboratory testing for methods of assay of xylanase activity. J Biotechnol 23:257-270.
Bajaj BK, Manhas K (2012) Production and characterization of xylanase from *Bacillus licheniformis* P11(C) with potential for fruit juice and bakery industry. Biocatal Agric Biotechnol 1:330-337.
Chou WJ, Sun CH, Yu GP, Huang JH (2003) Optimization of the deposition process of ZrN and TiN thin films on Si(1 0 0) using design of experiment method. Mater Chem Phys 82:228-236.
Elegbede JA, Lateef A (2018) Valorization of corn-cob by fungal isolates for production of xylanase in submerged and solid-state fermentation media and potential biotechnological applications. Waste Biomass Valor 9:1273-1287.
Elegbede JA, Lateef A, Azeez MA, Asafa TB, Yekeen TA, Oladipo IC, Adebayo EA, Beukes LS, Gueguim-Kana EB (2018a) Fungal xylanases-mediated synthesis of silver nanoparticles for catalytic and biomedical applications. IET Nanobiotechnol 12:857-863.
Elegbede JA, Lateef A, Azeez MA, Asafa TB, Yekeen TA, Oladipo IC, Aina DA, Beukes LS, Gueguim-Kana EB (2018b) Biofabrication of gold nanoparticles using xylanases through valorization of corncob by *Aspergillus niger* and *Trichoderma longibrachiatum*: antimicrobial, antioxidant, anticoagulant and thrombolytic activities. Waste Biomass Valor. (https://doi.org/10.1007/s12649-018-0540-2).
Elegbede JA, Lateef A, Azeez MA, Asafa TB, Yekeen TA, Oladipo IC, Abbas SH, Beukes LS, Gueguim-Kana EB (2019) Silver-gold alloy nanoparticles biofabricated by fungal xylanases exhibited potent biomedical and catalytic activities. Biotechnol Prog. 2019 May 3:e2829. doi:10.1002/btpr.2829.
Ganaie MA, Lateef A, Gupta US (2014) Enzymatic trends of fructooligosaccharides production by microorganisms. Appl Biochem Biotechnol 172:2143-2159.
Geetha K, Gunasekaran P (2010) Optimisation of nutrient medium containing agricultural wastes for xylanase production by *Bacillus pumilus* B20. Biotechnol Bioprocess Eng 15:882-889.
Gueguim-Kana EB, Oloke JK, Lateef A, Adesiyan MO (2012a) Modeling and optimization of biogas production on saw dust and other co-substrates using Artificial Neural Network and Genetic Algorithm. Renew Energy 46:276-281.
Gueguim-Kana EB, Oloke JK, Lateef A, Oyebanji A (2012b) Comparative evaluation of artificial neural network coupled genetic algorithm and response surface methodology for modelling and optimization of citric acid production by *Aspergillus niger* MCBN 297. Chem Eng Trans 27:397-402.
Gueguim-Kana EB, Oloke JK, Lateef A, Zebaze Kana MG (2007) Novel optimal temperature profile for acidification process of *Lactobacillus bulgaricus* and *Streptococcus thermophilus* in yoghurt fermentation using artificial neural network and genetic algorithm. J Ind Microbiol Biotechnol 34:491-496.
Kalim B, Böhringer N, Ali N, Schäberle TF (2015) Xylanase from microbial origin to industrial application. Br Biotechnol J 7:1-20.
Kapoor M, Nair LM, Kuhad RC (2008) Cost-effective xylanase production from free and immobilized *Bacillus pumilus* strain MK001 and its application in saccharification of *Prosopis juliflora*. Biochem Eng J 38:88-97.
Lakshmi GS, Rao CS, Rao RS, Hobbs PJ, Prakasham RS (2009) Enhanced production of xylanase by a newly isolated *Aspergillus terreus* under solid state fermentation using palm industrial waste: A statistical optimization. Biochem Eng J 48:51-57.
Lateef A, Adeeyo AO (2015) Green synthesis and antibacterial activities of silver nanoparticles using extracellular laccase of *Lentinus edodes.* Not Sci Biol 7:405-411.
Lateef A, Adelere IA, Gueguim-Kana EB, Asafa TB, Beukes LS (2015) Green synthesis of silver nanoparticles using keratinase obtained from a strain of *Bacillus safensis* LAU 13. Int Nano Lett 5:29-35.
Lateef A, Gueguim-Kana EB (2012) Utilization of cassava wastes in the production of fructosyltransferase by *Rhizopus stolonifer* LAU 07. Rom Biotechnol Lett 17:7309-7316.
Lateef A, Oloke JK, Gueguim-Kana EB, Oyeniyi SO, Onifade OR, Oyeleye AO, Oladosu OC, Oyelami AO (2008) Improving the quality of agro-wastes by solid-state fermentation: enhanced antioxidant activities and nutritional qualities. World J Microbiol Biotechnol 24:2369-2374.
Lateef A, Oloke JK, Gueguim-Kana EB, Sobowale BO, Ajao SO, Bello BY (2010) Keratinolytic activities of a new feather-degrading isolate of *Bacillus cereus* LAU 08 isolated from Nigerian soil. Int Bioremed Biodegrad 64:162-165.
Lateef A, Oloke JK, Gueguim-Kana EB, Raimi OR (2012) Production of fructosyltransferase by a local isolate of *Aspergillus niger* in both submerged and solid substrate media. Acta Aliment 41:100-117.
Lateef A, Adelere IA, Gueguim-Kana EB (2015) *Bacillus safensis* LAU 13: a new source of keratinase and its multi-functional biocatalytic applications. Biotechnol Equip 29:54-63.
Laxman RS, Sonawane AP, More SV, Rao BS, Rele MV, Jogdand VV, Deshpande VV, Rao MB (2005) Optimization and scale up of production of alkaline protease from *Conidiobolus coronatus*. Process Biochem 40:3152-3158.
Mandal A, Kar S, Dutta T, Pati BR, Mondal KC, Mohapatra PKD (2015) Parametric optimization of submerged fermentation conditions for xylanase production by *Bacillus*

cereus BSA1 through Taguchi Methodology. Acta Biol Szeged 59:189-195.

Mohapatra PD, Maity C, Rao RS, Pati BR, Mondal KC (2009) Tannase production by *Bacillus licheniformis* KBR6: Optimization of submerged culture conditions by Taguchi DOE methodology. Food Res Int 42:430-435.

Murthy PS, Naidu MM (2012) Production and application of xylanase from *Penicillium* sp. utilizing coffee by-products. Food Bioprocess Technol 5:657-664.

Oliveira LA, Porto AL, Tambourgi EB (2006) Production of xylanase and protease by *Penicillium janthinellum* CRC 87M-115 from different agricultural wastes. Bioresour Technol 97:862867.

Pandey S, Shahid M, Srivastava M, Sharma A, Singh A, Kumar V, Yatindra S (2014) Isolation and optimized production of xylanase under solid state fermentation condition from *Trichoderma* sp. Int J Adv Res 2:263-273.

Pandya JJ, Gupte A (2012) Production of xylanase under solid-state fermentation by *Aspergillus tubingensis* JP-1 and its application. Bioprocess Biosystems Eng 35:769-779.

Polizeli MLTM, Rizzatti ACS, Monti R, Terenzi HF, Jorge JA, Amorim DS (2005) Xylanases from fungi: properties and industrial applications. Appl Microbiol Biotechnol 67:577-591.

Prakasham RS, Subba Rao C, Sreenivas Rao R, Sarma PN (2007a) Enhancement of acid amylase production by an isolated *Aspergillus awamori*. J Appl Microbiol 102:204-211.

Prakasham RS, Rao C, Rao RS, Lakshmi GS, Sarma PN (2007b) L-asparaginase production by isolated *Staphylococcus* sp. - 6A: design of experiment considering interaction effect for process parameter optimization. J Appl Microbiol 102:1382-1391.

Radhika K, Ravinder R, Ravindra P (2011) Bioconversion of pentose sugars into ethanol: a review and future directions. Biotechnol Mol Biol Rev 6:8-20.

Rani GB, Chiranjeevi T, Chandel AK, Satish T, Radhika K, Narasu ML, Uma A (2014) Optimization of selective production media for enhanced production of xylanases in submerged fermentation by *Thielaviopsis basicola* MTCC 1467 using L16 orthogonal array. J Food Sci Technol 51:2508-2516.

Rao CS, Sathish T, Mahalaxmi M, Laxmi GS, Rao RS, Prakasham RS (2008a) Modeling and optimization of fermentation factors for enhancement of alkaline protease production by isolated *Bacillus circulans* using feed-forward neural network and genetic algorithm. J Appl Microbiol 104:889-898.

Rao RS, Kumar CG, Prakasham RS, Hobbs PJ (2008b) The Taguchi methodology as a statistical tool for biotechnological applications: A critical appraisal. Biotechnol J 3:510-523.

Shahi SS, Alemzadeh I, Khanahmadi M, Roostaazad R (2011) Xylanase production under solid state fermentation by *Aspergillus niger.* Int J Trans B: Applications 24:197.

Taguchi G (1986) Introduction to Quality Engineering: Designing Quality into Products and Processes. Asian Productivity Organization (American Supplier Institute, Dearborn, MI, USA)

Uday USP, Bandyopadhyay TK, Bhunia B (2016a) Rapid development of xylanase assay conditions using Taguchi methodology. Bioengineered 7:424-431.

Uday USP, Choudhury P, Bandyopadhyay TK, Bhunia B (2016b) Classification, mode of action and production strategy of xylanase and its application for biofuel production from water hyacinth. Int J Biol Macromol 82:1041-1054.

Uysal E, Akcan N, Baysal Z, Uyar F (2010) Optimization of α-amylase production by *Bacillus subtilis* RSKK96: using the Taguchi experimental design approach. Prep Biochem Biotechnol 41:84-93.

Yegin S (2017) Xylanase production by *Aureobasidium pullulans* on globe artichoke stem: Bioprocess optimization, enzyme characterization and application in saccharification of lignocellulosic biomass. Prep Biochem Biotechnol 47:441-449.

Acta Biologica Szegediensis

Volume 63(1):59-62, 2019
Acta Biologica Szegediensis
http://abs.bibl.u-szeged.hu/index.php/abs
DOI:10.14232/abs.2019.1.59-62

ARTICLE

Isometric beak morphology in *Phoenicopterus ruber roseus*, Phoenicopteriformes

Pere M. Parés-Casanova*, Sandra Arcas

Department of Animal Science, University of Lleida, Lleida, Catalonia, Spain

ABSTRACT It is well documented that size of various body parts tends to correlate within the same individual. In the current study, we explore the relationship between body weight and some area and lineal beak measurements in a sample of 17 corpses of Greater flamingo *Phoenicopterus ruber roseus* (10 immatures and 7 adults), collected and after obtaining beak radiographic latero-lateral projections. On images, the following traits were obtained: area of rhinotheca –the sheath covering the maxilla- and gnathotheca –the sheath covering the mandibular-, rhamphotheca height, ocular area, ocular height, ocular width, height, width and area of nares. Our results suggest that some beak measurements are positively correlated with body weight, while nostril area is not. Specifically, rhinotheca and gnathotheca areas and rhamphotheca height were strongly coupled and largely correlated to body weight. The observed differences in beak dimensions are merely a consequence of body weight difference. It is suggested, that the cranial skeleton and musculature are closely linked at least developmentally, allowing for efficient functional integration, but genetic and functional tests must have been performed to reveal the exact nature of the flamingo beak change.
Acta Biol Szeged 63(1):59-62 (2019)

KEY WORDS
avian
ecomorphology
gnathotheca
rhamphotheca
rhinotheca

ARTICLE INFORMATION
Submitted
23 November 2018.
Accepted
29 March 2019.
***Corresponding author**
E-mail: peremiquelp@ca.udl.cat

Introduction

Bird beaks are relevant for foraging, parental care and singing (Shao et al. 2016) and being a highly malleable structure, it permits birds to adapt to different requirements (van Hemert et al. 2012) (Cheng et al. 2017).

The Greater flamingo (*Phoenicopterus ruber roseus*) is a species of the flamingo family. With its bent bill it filters out small shrimp, seeds, algae, plankton, tiny fish, fly larvae and mollusks (Zweers et al. 1995) (Deville et al. 2013). Its beak has a filter-like structure to remove food from the water before the liquid is expelled (Zweers et al. 1995), being the upper jaw movable and not rigidly fixed to its skull.

It is well documented that size of various body parts tends to correlate within the same individual. Although literature on beak morphology for Greater flamingo is abundant (Mascitti and Kravetz 2002) in the current study, we explore the relationship between body weight and some area and lineal beak measurements. We explore its beak structure employing an unusual tool, e.g., radiographic projection on which we obtained classical lineal measurements. The advantage of classical measurements is that they are obtained rapidly and that they can be taken on every parts of the body. This study offers a unique opportunity to understand how bill change arises in Greater flamingo. Here, we complement existing data on its external morphology and provide baseline data needed to understand the developmental mechanisms driving the observed changes.

Materials and methods

A sample of 17 corpses of *Phoenicopterus ruber roseus* (10 immatures and 7 adults), collected in one of the known breeding colonies of the species (Parc Natural del Delta de l'Ebre; Ebro Delta Natural Park, South Catalonia, Spain), were obtained from its wildlife recuperation center. After obtaining the body weight of each fresh corpse (BW), radiographic latero-lateral projections were obtained and the following traits were obtained with the Digimizer version 4.6.1 software (available at www.digimizer.com) on the rhamphotheca (beak): area of rhinotheca (the sheath covering the maxilla), area of gnathotheca (the sheath covering the mandibular), height of rhamphotheca, ocular area, ocular height, ocular width, height, width and area of nares (Fig. 1). A Multivariate Analysis of Variance (MANOVA) test was done to detect differences between immature and adult animals. A Principal Components Analysis (PCA) from var-covar matrix was done to gener-

Table 1. Main descriptive statistics. Body weight in kg. The rest of values in cm or cm^2.

	Body weight	Area of rhinotheca	Area of gnathohteca	Height of rhamphotheca	Ocular area	Ocular height	Ocular width	Area of nares	Height of nares	Width of nares
W	0.951	0.950	0.903	0.944	0.954	0.974	0.919	0.953	0.933	0.936
P	0.476	0.457	0.077	0.362	0.518	0.888	0.143	0.508	0.246	0.272
Min	0.83	12.85	18.45	2.91	1.90	1.48	1.39	1.19	0.61	2.51
Max	3.40	18.49	34.71	4.43	2.60	1.88	1.82	2.04	0.81	3.31
Mean	1.85	16.37	26.08	3.73	2.26	1.68	1.67	1.59	0.70	2.84
Stand. dev.	0.59	1.58	3.29	0.33	0.22	0.12	0.10	0.21	0.06	0.24
Std. error	0.14	0.38	0.80	0.08	0.05	0.03	0.02	0.05	0.02	0.06
CV (%)	31.98	9.68	12.60	8.84	9.87	7.16	6.08	13.03	8.91	8.49

W: Shapiro-Wilk's *W*, CV: Coefficient of Variation

ate a morphospace of beak shape variation.

Data analysis were performed with PAST version 2.17c software (Hammer et al. 2001). Classical morphological measurements were transformed into log-shape ratios in order to control for the size effect on the body parts measured (Cardini and Polly 2013). Following this method, the overall size of each individual was defined as the mean of the log transformed measurements. Each measurement was then standardized by subtracting the overall size of the individual to the log-transformed measured value, and Pearson's correlation was applied (Bookstein 1991). Allometry was studied regressing body weight against normalized data.

Results and discussion

As no statistical differences appeared between immatures and adults (Wilk's $\lambda = 0.191$, $p = 0.245$), values were mixes for ulterior analysis. Main descriptive statistics appear in Table 1 and correlation coefficients in Table 2.

Our results suggest that some beak measurements are positively correlated with body weight, while nostril area is not. Specifically, rhinotheca and gnathotheca areas and rhamphotheca height, were strongly coupled, and largely correlated to body weight. This relationship means that beak size is highly constrained to evolve in the particular way of body weight. Similar to the present findings, Palacios and Tubaro (2000) demonstrated a positive correlation between body mass and beak length in woodcreepers. Similarly, Clegg and Owens (2002) found that there was a significant general trend toward heavier BW with larger bill size in island-dwelling birds. By contrast, Laiolo and Rolando (2003) reported no significant correlations between BW and bill size in 28 species of crow. The different findings may relate to between-species differences in foraging and beak functionality. In fact, among wild birds, body weight and beak size may found related to competition, adaptation, or both (Fahey et al. 2007).

Furthermore, beak mandibular area evolves cohesively with ocular dimensions. Size is also an important consideration when assessing ocular area variation. Larger flamingos would have access to larger feed volumes due to their increased gape and greater absolute muscular power, and size is further related to morphology via allometry, e.g., the tendency of traits to vary with size throughout a morphological structure. In fact, allometry has been demonstrated as a key contributing factor to craniofacial form across a range of animal groups. Moreover, our results reconsider the view that the beak and braincase act as independent modules. When the configurations are divided in subsets that separately the beak and the ocular conformations, we find that orbitary socket morphology is more conservative (less variable) than the beak.

To assess the effect of allometric (size) signal in our dataset we conducted a PCA on the residuals of the regression

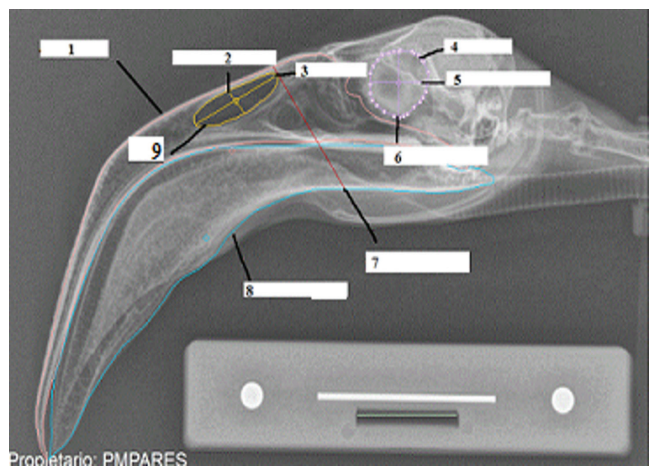

Figure 1. Measurements on the rhamphotheca (beak): area of rhinotheca (1), height (2) and width (3) of nares, ocular area (4), ocular width (5) and height (6), height of rhamphotheca (7), area of gnathotheca (8) and area of nares (9).

Table 2. Correlation values for analyzed traits. Pearson's coefficients appear under the diagonal, *p*-values above. Significative values appear in bold. Bonferroni corrected values.

	Body weight	Area of rhinotheca	Area of gnathotheca	Height of rhamphotheca	Ocular area	Ocular height	Ocular width	Area of nares	Height of nares	Width of nares
Body weight		0.000	0.004	0.000	0.069	0.496	0.460	0.005	0.062	0.072
Area of rhinotheca	0.972		0.001	0.000	0.078	0.585	0.556	0.006	0.069	0.047
Area of gnathotheca	0.666	0.711		0.116	0.187	0.237	0.278	0.083	0.384	0.933
Height of rhamphotheca	0.792	0.793	0.396		0.014	0.436	0.597	0.003	0.090	0.006
Ocular area	0.452	0.438	0.336	0.582		0.346	0.991	0.075	0.046	0.946
Ocular height	-0.177	-0.143	-0.303	-0.202	-0.244		0.016	0.143	0.072	0.104
Ocular width	0.192	0.154	-0.279	0.138	-0.003	0.574		0.854	0.004	0.061
Area of nares	-0.642	-0.639	-0.433	-0.673	-0.444	0.371	0.048		0.857	0.452
Height of nares	-0.462	-0.451	-0.225	-0.424	-0.490	-0.447	-0.662	-0.047		0.096
Width of nares	-0.447	-0.488	-0.022	-0.636	-0.018	-0.408	-0.464	0.196	0.416	

of biometrical data against body weight. PC1 represented 74.04% of the variation, while PC2 decreased to 12.22%. When the allometric effect was analyzed a significative signal was present ($r^2 = 0.699$, $F_{10,6} = 36.71$, $p = 0.00013$).

Birds adapt to different consumptions either by increasing bill dimensions independently of body size or by increasing all the body and bill characters isometrically until a desirable bill size (width and/or depth) (Clabaut et al. 2009). Greater flamingo is an example of this latter adaptation: beak traits are increased equally. This would indicate a close and continued relationship between skeletal bill morphology and jaw musculature (but no functionality, as indicated by negative correlations with nares area), due to increased demands for space and attachment sites for the musculature. Detected correlation that would support the hypothesis of integration between these tissues, many beak morphological descriptions being coupled with a corresponding change in jaw musculature, too (Foster et al. 2008; Riyahi et al. 2013). Therefore, we suggest that the cranial skeleton and musculature are closely linked at least developmentally, allowing for efficient functional integration. Further genetic and functional tests must have been performed to reveal the exact nature of the flamingo beak change.

Thus, in addition to be an interesting model system for the study of change in beak morphology, flamingos offer an exciting and unique opportunity to understand the mechanism of an adaptive musculo-skeletal integration in birds.

Acknowledgements

We are very grateful to the staff of Parc Natural del Delta de l'Ebre, especially to the responsible of the wildlife recuperation center in Canal Vell Station and the Director of that Park. We thank also anonymous referees for their very constructive comments.

References

Bookstein FL (1991) Morphometric Tools for Landmark Data. Geometry and Biology. Cambridge University Press. Cambridge.

Cardini A, Polly PD (2013) Larger mammals have longer faces because of size-related constraints on skull form. Nature Commun 4:2458.

Cheng Y, Gao B, Wang H, Han N, Shao S, Wu S, Song G, Zhang YE, Zhu X, Lu X, Qu Y, Lei F (2017) Evolution of beak morphology in the Ground Tit revealed by comparative transcriptomics. Front Zool 14:58.

Clabaut C, Herrel A, Sanger TJ, Smith TB, Abzhanov A (2009) Development of beak polymorphism in the African seedcracker, *Pyrenestes ostrinus*. Evol Dev 11(6):636-646.

Clegg SM, Owens IPF (2002) The "island rule" in birds: Medium body size and its ecological explanation. Proc R Soc Lond B Biol Sci 269:1359-1365.

Deville AS, Grémillet D, Gauthier-Clerc M, Guillemain M, Von Houwald F, Gardelli B, Béchet A (2013) Non-linear feeding functional responses in the Greater Flamingo (*Phoenicopterus roseus*) predict immediate negative impact of wetland degradation on this flagship species. Ecol Evol 3(5):1413-1425.

Fahey AG, Marchant-Forde RM, Cheng HW (2007) Relationship between body weight and beak characteristics in one-day-old white Leghorn chicks: Its implications for beak trimming. Poult Sci 86(7):1312-1315.

Foster DJ, Podos J, Hendry AP (2008) A geometric morphometric appraisal of beak shape in Darwin's finches. J Evol Biol 21(1):263-275.

Hammer Ø, Harper DAT, Ryan PD (2001) PAST v. 2.17c'.

Palaeontol Electron 4(1):1-229.
Laiolo P, Rolando A (2003) The evolution of vocalizations in the genus *Corvus*: Effects of phylogeny, morphology, and habitat. Evol Ecol 17:111-123.
Mascitti V, Kravetz FO (2002) Bill morphology of South American flamingos. The Condor 104(1):73-83.
Palacios MG, Tubaro PL (2000) Does beak size affect acoustic frequencies in woodcreeper. The Condor 102:553-560.
Riyahi S, Hammer Ø, Arbabi T, Sánchez A, Roselaar CS, Aliabadian M, Sætre G-P (2013) Beak and skull shapes of human commensal and non-commensal house sparrows *Passer domesticus*. BMC Evol Biol 13(1):200.
Shao S, Quan Q, Cai T, Song G, Qu Y, Lei F (2016) Evolution of body morphology and beak shape revealed by a morphometric analysis of 14 Paridae species. Front Zool 13:30.
van Hemert C, Blake JE, Swor RM, O'Hara TM (2012) Microanatomy of passerine hard-cornified tissues: Beak and claw structure of the black-capped chickadee (*Poecile atricapillus*). J Morphol 273(2):226-240.
Zweers G, De Jong F, Berkhoudt H (1995) Filter feeding in flamingos (*Phoenicopterus ruber*). The Condor 97(2):297-324.

Acta Biologica Szegediensis

Volume 63(1):63-68, 2019
Acta Biologica Szegediensis
http://abs.bibl.u-szeged.hu/index.php/abs
DOI:10.14232/abs.2019.1.63-68

ARTICLE

Insecticidal activity of isolated essential oils from three medicinal plants on the biological control agent, *Habrobracon hebetor* Say (Hymenoptera: Braconidae)

Mohammad Asadi, Hooshang Rafiee-Dastjerdi*, Gadir Nouri-Ganbalani, Bahram Naseri, Mahdi Hassanpour

Department of Plant Protection, Faculty of Agriculture and Natural Resources, University of Mohaghegh Ardabili, Ardabil, Iran

ABSTRACT The effects of *Allium sativum* L. (Alliaceae), *Piper nigrum* L. (Piperaceae) and *Glycyrrhiza glabra* L. (Fabaceae) essential oils were investigated on the biological control agent, *Habrobracon hebetor* Say. The female wasps of *H. hebetor* were treated by LC_{30} concentrations of the tested essential oils for 24 h and their demography was investigated. Results indicated that the adult longevity, survival, fecundity, fertility, hatch rate, offspring sex ratio and the other demographic parameters negatively were affected by these essential oils. At the same time, our findings indicated that *G. glabra* essential oil has the less severe effect on *H. hebetor*. Accordingly, *G. glabra* essential oil seems to be a compatible botanical compound with *H. hebetor* for applying in integrated pest management programs. **Acta Biol Szeged 63(1):63-68 (2019)**

KEY WORDS
integrated pest management
natural enemy
plant compounds
toxicity

ARTICLE INFORMATION
Submitted
4 May 2019.
Accepted
11 July 2019.
***Corresponding author**
E-mail: hooshangrafiee@gmail.com

Introduction

The synthetic pesticides concern environmental pollution, emergence of resistance in insect pests and negative effects on non-target organisms in agricultural ecosystems (Sagheer et al. 2014; Yazdgerdian et al. 2015; Asadi et al. 2018a). During the last decades, application of various natural compounds were seriously considered for the effective control of insect pests (Mwine et al. 2013; Rafiee-Dastjerdi et al. 2013; Kramer et al. 2016; Asadi et al. 2018a). According to this, the compounds of plant origin including essential oils and extracts have been recommended as natural and effective compounds in integrated pest management (IPM) programs (Koul et al. 2008; Manzoor et al. 2011; Asadi et al. 2018a; Razmjou et al. 2018). The essential oils are a chemically diverse group of volatile plant metabolites (Bakkali et al. 2008; Isman et al. 2008; Rafiee-Dastjerdi et al. 2013). Most of these odor compounds have fumigant, contact, repellent and antifeedant properties and, therefore, they are frequently recommended for control of insect pests due to their high insecticidal activity and low negative effects on non-target organisms (Isman 2000; Yildirim et al. 2011; Rafiee-Dastjerdi et al. 2013; Shiva Parsia and Valizadegan 2015; Asadi et al. 2018a).

Application of any compounds of synthetic or natural origin potentially can have harmful effects on demography of the natural enemies of pests including predators and parasitoids (Stark et al. 2004; Mahmoudvand et al. 2011). The acute toxicity of different compounds on insect populations previously have been investigated in detail, but the sublethal effects of them have not been considered completely (Motazedian et al. 2012; Mwine et al. 2013). The negative sublethal effects can change the demographic parameters and finally will reduce the efficiency of natural enemies for control of their hosts (Croft 1990; Stark and Wennergren 1995; Salerno et al. 2002; Stark and Banks 2003; Desneux et al. 2007; Hamedi et al. 2010 and 2011).

There are several reports describing the harmful effects of some plant essential oils and the other compounds of plant origin on non-target organisms especially on the natural enemies of pests (Abramson et al. 2006; Asadi et al. 2018a). If the application of plant essential oils will be widespread, they can disrupt the biological control agents in IPM programs (Desneux et al. 2007). Accordingly, co-application of biological control agents with plant-based compounds requires suitable knowledge about their obvious and hidden interactions (Dent 1995; Banks and Stark 1998; Desneux et al. 2007). These researches are defined as demographic toxicology that is a useful tool for understanding the effects of different compounds on populations of different insects and their natural enemies (Walthall and Stark 1996; Stapel et al. 2000; Stark and

Banks 2003; Desneux et al. 2007).

Habrobracon hebetor Say is one of the important natural enemies of different destructive lepidopteran larvae especially from families Pyralidae and Noctuidae in agricultural crops (Gerling 1971; Youm and Gilstrap 1993; Magro and Parra 2001; Navaei et al. 2002). The projects on the mass rearing of this ectoparasitoid wasp have been started in Iran in different commercial insectariums and it has been released for the control of some invasive lepidopteran pests (Navaei et al. 2002; Ahmadpour 2017). However, little information is available regarding the lethal and sublethal effects of plant essential oils and the other plant compounds on this important ectoparasitoid wasp (Seyyedi 2011; Hashemi et al. 2014; Ahmadpour 2017; Asadi et al. 2018a; Razmjou et al. 2018).

Three medicinal plants were selected for this study, including garlic (*A. sativum*), black pepper (*P. nigrum*) and liquorice (*G. glabra*). It is known from previous studies that they have sufficient amount of essential oil with high insecticidal activity (Koul et al. 2008; Ajayi and Olonisakin 2011; Rafiee-Dastjerdi et al. 2013). In this research we investigated the effects of isolated essential oils from above-mentioned medicinal plants on *H. hebetor* for evaluation the possibility of their integration with this important biocontrol agent in IPM programs.

Materials and Methods

Essential oils isolation and analysis

The mature plants of garlic (*Allium sativum* L., Alliaceae), black pepper (*Piper nigrum* L., Piperaceae) and liquorice (*Glycyrrhiza glabra* L., Fabaceae) were collected in different regions of Islam-Abad Gharb city (34.11° N and 46.52° E) (Kermanshah province, Iran) during May to June 2016. The collected plants were dried in shadow conditions under room temperature (approximately 25 °C). Parts of the collected plants (bulbs of *A. sativum*, seeds of *P. nigrum* and leaves of *G. glabra*) that contained the highest insecticidal activity were considered. Analyses of the isolated essential oils were carried out with a Gas Chromatography-Mass spectroscopy (GC-MS; Agilent, 7890 B) as described earlier (Asadi et al. 2018b). Investigation of fumigant toxicity on the young female wasps of *H. hebetor* (less than 24 h old) also was carried out as described earlier (Asadi et al. 2018b).

Rearing of biological control agent

The primitive adult wasps of *H. hebetor* were obtained from a private insectarium (registered name: Kesht-Gostar Pishgam) in Islam-Abad Gharb city (Kermanshah province, Iran), during 2017. The obtained parasitoids urgently were transferred to laboratory conditions at 25 ± 1 °C, 60 ± 5% relative humidity (RH) and photoperiod of 16:8 (L:D) h and were reared on the larvae of flour moth (*Ephestia kuehniella* Zeller) as its laboratory host. During the rearing processes, the honey solution (10%) was used for feeding of this biocontrol agent (Rafiee-Dastjerdi et al. 2008, 2009a, 2009b; Mahdavi 2013; Abedi et al. 2012, 2014; Asadi et al. 2018a).

Table 1. The biological parameters of *H. hebetor* females treated by the isolated essential oils.

Treatment	Female longevity (day)	Daily fecundity (egg)	Daily fertility (egg)
Control	25.60 ± 0.56 [a]	17.23 ± 0.57 [a]	11.54 ± 0.38 [a]
A. sativum	14.12 ± 0.65 [c]	12.58 ± 0.68 [b]	6.41 ± 0.35 [c]
P. nigrum	15.84 ± 0.69 [c]	11.88 ± 0.69 [b]	6.89 ± 0.40 [c]
G. glabra	21.88 ± 0.79 [b]	15.96 ± 0.73 [a]	10.22 ± 0.47 [b]

Values in each column that characterized by different letters showed significant difference (Tukey test; $P < 0.05$).

Demography of H. hebetor

For studying the demography of *H. hebetor* on its laboratory host, first one-hundred young female wasps (less than 24 h old) were exposed to sublethal concentration (LC_{30}) of each essential oil consist of *A. sativum* (2.22 µl/l air), *P. nigrum* (5.41 µl/l air) and *G. glabra* (8.72 µl/l air) on filter paper (2×2 cm) in glass Petri dish with approximately volume of 60 ml. The selection of LC_{30} values for these testes was based on the results of earlier studies of IPM programs with synthetic and plant-derived compounds (Borzoui et al. 2016). This concentration (LC_{30}) was calculated from the analyses of bioassay experiments by using SPSS version 20 software. In the control experiments, the wasps were treated by distilled water. After 24 h of exposure, twenty-five live females randomly were selected and released singly to Petri dishes (80 mm in diameter) and were paired with untreated males (less than 24 h old) (Ahmadpour 2017; Asadi et al. 2018a; Razmjou et al. 2018). The wasps were fed daily with honey solution (10%) and seven larvae of *E. kuehniella* as host for oviposition. The biological features of the treated wasps (total 25 paired wasps) including survival and fecundity were recorded daily to death time of all treated females. Then, among deposited eggs by them, one-hundred eggs were selected randomly and the number of emerged larvae, pupae and adult wasps (male and female) were recorded. The life table of Carey (1993) that is the base of one-six life table analysis was used for studying the demography of this parasitoid wasp.

Data analysis

For statistical analysis, jackknife and pseudovalues were

Table 2. The stable population parameters of *H. hebetor* females treated by the isolated essential oils.

Treatment	GRR (female offspring)	R_0 (female offspring)	λ (day^{-1})	T (day)	DT (day)
Control	275.24 ± 17.72 [a]	144.68 ± 4.83 [a]	1.32 ± 0.003 [a]	18.14 ± 0.16 [b]	2.53 ± 0.02 [c]
A. sativum	55.34 ± 3.33 [c]	19.32 ± 1.07 [d]	1.17 ± 0.003 [d]	19.19 ± 0.12 [a]	4.49 ± 0.08 [a]
P. nigrum	90.38 ± 6.01 [c]	40.96 ± 2.39 [c]	1.23 ± 0.004 [c]	17.93 ± 0.13 [b]	3.34 ± 0.05 [b]
G. glabra	182.48 ± 10.70 [b]	88.51 ± 4.05 [b]	1.30 ± 0.004 [b]	17.10 ± 0.12 [c]	2.64 ± 0.03 [c]

Values in each column that characterized by different letters showed significant difference (Tukey test; P < 0.05). GRR: Gross reproductive rate, R0: Net reproductive rate, λ: Finite rate of increase, T: Mean generation time, DT: Doubling time

calculated for the control and each essential oil treatment and then the obtained pseudovalues were tested for normal distribution. The square-root and logarithmic transformations were performed on those parameters that had not normal distribution. Finally the normal data were analyzed by one-way ANOVA and the means were compared by Tukey test at probability level ($p < 0.05$) by using SPSS version 20 software (Meyer et al. 1986; Maia et al. 2000).

Results

Biological parameters

The biological parameters from treated females of *H. hebetor* by three isolated essential oils are shown in Table 1. The shortest and longest females' longevity was obtained in *A. sativum* essential oil and the control, respectively ($F_{3,96} = 40.18$, $P < 0.05$). The daily fecundity also significantly was affected by the tested essential oils; but, there was no significant difference between the control and *G. glabra* essential oil and also between the essential oils of *A. sativum* and *P. nigrum* ($F_{3,96} = 14.92$, $P < 0.05$). Moreover, the lowest and highest daily fertility were observed in *A. sativum* essential oil (6.41 eggs) and the control (11.54 eggs), respectively ($F_{3,96} = 39.01$, $P < 0.05$).

Stable population parameters

The stable population parameters from treated females of *H. hebetor* by the isolated essential oils are given in Table 2. The gross reproductive rate (GRR) significantly was affected by the isolated essential oils, being the lowest in *A. sativum* essential oil and the highest in the control ($F_{3,96} = 82.01$, $P < 0.05$). The R_0 value in *A. sativum* essential oil (19.32 female offspring) was significantly lower than the control and the other essential oils ($F_{3,96} = 266.06$, $P < 0.05$). The finite rate of increase (λ) also varied under different essential oils treatments compared with the control. The lowest λ value being in *A. sativum* essential oil and the highest was in the control ($F_{3,96} = 376.05$, $P < 0.05$). Moreover, the shortest and longest values of mean generation time (T) were obtained in *G. glabra* and *A. sativum* essential oils, respectively ($F_{3,96} = 42.13$, $P < 0.05$). In addition; the shortest and longest values of doubling time (DT) were seen in the control and *A. sativum* essential oil, respectively ($F_{3,96} = 296.77$, $P < 0.05$).

Population growth parameters

The population growth parameters from treated females of *H. hebetor* by the isolated essential oils are shown in Table 3. About the intrinsic birth rate (b), there were no significant differences among the control, *P. nigrum* and *G. glabra* essential oils ($F_{3,96} = 234.28$, $P < 0.05$). The highest intrinsic death rate (d) also was observed in *P. nigrum* essential oil that showed significant differences with the other essential oils ($F_{3,96} = 772.20$, $P < 0.05$). The intrinsic rate of increase (r_m) was strongly affected in offsprings of the treated females. The lowest r_m value was determined in the treated wasps of *H. hebetor* by *A. sativum* essential oil and the highest was in the control ($F_{3,96} = 381.23$, $P < 0.05$). The gross hatch rate (h_x) in *A. sativum* essential oil (0.51) was lower than the control and the other isolated

Table 3. The population growth parameters of *H. hebetor* females treated by the isolated essential oils.

Treatment	Birth rate (day^{-1})	Death rate (day^{-1})	r_m (day^{-1})	Hatch rate (%)	Sex ratio (%)
Control	0.38 ± 0.003 [a]	0.11 ± 0.001 [c]	0.27 ± 0.002 [a]	0.67	0.63
A. sativum	0.26 ± 0.003 [b]	0.11 ± 0.001 [c]	0.15 ± 0.003 [d]	0.51	0.34
P. nigrum	0.39 ± 0.005 [a]	0.18 ± 0.002 [a]	0.21 ± 0.003 [c]	0.58	0.56
G. glabra	0.38 ± 0.003 [a]	0.12 ± 0.001 [b]	0.26 ± 0.003 [b]	0.64	0.57

Values in each column that characterized by different letters showed significant difference (Tukey test; P < 0.05). rm: Intrinsic rate of increase

Table 4. The reproductive parameters of *H. hebetor* females treated by the isolated essential oils.

Treatment	Gross fertility rate (egg)	Net fertility rate (egg)	Gross fecundity rate (egg)	Net fecundity rate (egg)
Control	292.72 ± 18.84 [a]	152.80 ± 5.07 [a]	436.90 ± 28.12 [a]	228.06 ± 7.56 [a]
A. sativum	83.01 ± 5.00 [c]	27.94 ± 1.52 [d]	162.77 ± 9.81 [c]	54.78 ± 2.98 [c]
P. nigrum	93.60 ± 6.23 [c]	41.60 ± 2.41 [c]	161.39 ± 10.74 [c]	71.72 ± 4.15 [c]
G. glabra	204.89 ± 12.01 [b]	97.95 ± 4.47 [b]	320.14 ± 18.77 [b]	153.05 ± 6.99 [b]

Values in each column that characterized by different letters showed significant difference (Tukey test; $P < 0.05$).

essential oils. Also, the offspring sex ratio (S_x) value based on the number of emerged females on total number of emerged male and female wasps was affected in offsprings of *H. hebetor*; indicating that *A. sativum* essential oil significantly have decreased the emergence of female offspring in *H. hebetor*.

Reproductive parameters

The reproductive parameters from treated wasps of *H. hebetor* by the isolated essential oils are given in Table 4. The lowest and highest gross fertility rate were determined in *A. sativum* essential oil and the control and the difference between *A. sativum* and *P. nigrum* essential oil wasn't significant ($F_{3,96} = 70.26$, $P < 0.05$). The net fertility rate also significantly was lower in *A. sativum* essential oil than the control and the other essential oils ($F_{3,96} = 243.17$, $P < 0.05$). Moreover, the results of gross fecundity rate indicated that there was no significant difference between *A. sativum* and *P. nigrum* essential oils ($F_{3,96} = 52.82$, $P < 0.05$). In addition, the net fecundity rate showed significant differences among the control and the essential oils treatments ($F_{3,96} = 193.41$, $P < 0.05$).

Discussion

The demographic parameters based on the demographic toxicology are very useful tools for studying the responses of different insects to any synthetic or natural compounds (Forbes and Calow 1999). The sublethal results showed that application of the isolated essential oils negatively have changed the biological parameters of *H. hebetor* including the adult longevity, daily fecundity and daily fertility. Similar observations were reported by Seyyedi (2011), Hashemi et al. (2014) Ahmadpour (2017), Asadi et al. (2018a) and Razmjou et al. (2018).

In our study, the sublethal concentration of *A. sativum* essential oil caused the most significant negative effects on the above-mentioned parameters; while, *G. glabra* essential oil induced the less negative effects. The obtained values from reproductive parameters in the treated females of *H. hebetor* including the net and gross fecundity and fertility rates were in agreement with the results reported earlier. According to the results of Ahmadpour (2017) and Razmjou et al. (2018), *F. vulgare* and *C. carvi* essential oils showed the most and *A. millefolium* and *H. persicum* essential oils caused the lowest adverse effects on these parameters, respectively. In another study, Asadi et al. (2018a) found that concerning these parameters *R. officinalis* and *S. officinalis* showed the highest and lowest negative effects, respectively.

In our study there were significant differences on the stable population parameters in the treated wasps of *H. hebetor*. The lowest female fecundity in *A. sativum* essential oil caused the lowest gross (GRR) and net reproductive (R_0) rates among three examined essential oils. The net reproductive rate in all treatments was significantly lower than the gross reproductive rate indicating that the survival rate (l_x) was negatively affected by the isolated essential oils. The longest mean generation time was observed after *A. sativum* essential oil treatment. Hashemi et al. (2014), Ahmadpour (2017); Asadi et al. (2018a) and Razmjou et al. (2018) concluded that *F. assafoetida*, *F. vulgare*, *R. officinalis* and *C. carvi* essential oils showed the substantially negative effects on the gross and net reproductive rates, finite rate of increase, mean generation and doubling time of *H. hebetor*. In our investigation *G. glabra* essential oil caused the lowest adverse effects on these parameters.

This research showed that the tested essential oils had negative sublethal effects on *H. hebetor*. Among the different demographic parameters, the intrinsic rate of increase (r_m) is the most important parameter for evaluating the total effect of different compounds on insect populations. Hashemi et al. (2014), Ahmadpour (2017); Asadi et al. (2018a) and Razmjou et al. (2018) stated that r_m value of *H. hebetor* under all examined essential oils decreased compared with the control. At the same time, our findings indicated that *G. glabra* essential oil has the less negative effects and is relatively safe on *H. hebetor*. It means that this essential oil can be recommended as a suitable plant-derived compound on *H. hebetor* containing IPM approaches.

Acknowledgement

This research was supported by University of Mohaghegh Ardabili (Ardabil, Iran), under grant number [95/15/18581].

References

Abedi Z, Saber M, Gharekhani G, Mehrvar A, Mahdavi V (2012) Effects of azadirachtin, cypermethrin, methoxyfenozide and pyridalil on functional response of *Habrobracon hebetor* Say (Hymenoptera: Braconidae). J Plant Prot Res 52(3):353-358.

Abedi Z, Saber M, Gharekhani G, Mehrvar A, Kamita SG (2014) Lethal and sublethal effects of azadirachtin and cypermethrin on *Habrobracon hebetor* Say (Hymenoptera: Braconidae). J Econ Entomol 107:638-645.

Abramson CI, Wanderley PA, Wanderley MJA, Mina AJS, De Souza OB (2006) Effect of essential oil from citronella and alfazema on fennel aphids *Hyadaphis foeniculi* Passerini (Hemiptera: Aphididae) and its predator *Cycloneda sanguinea* L. (Coleoptera: Coccinellidae). American J Environ Sci 3(1):9-10.

Ahmadpour R (2017) The effects of isolated essential oils from four medicinal plants on the ectoparasitoid wasp, *Habrobracon hebetor* Say. under laboratory conditions. M.Sc. Thesis. University of Mohaghegh Ardabili, Ardabil, Iran.

Ajayi FA, Olonisakin A (2011) Bioactivity of three essential oils extracted formidable seeds on the rust-red flour beetle *Tribolium castaneum* (Herbest) infesting stored pearl millet. Trakia J Sci 9(1):28-36.

Asadi M, Nouri-Ganbalani G, Rafiee-Dastjerdi H, Hassanpour M, Naseri B (2018a) The effects of *Rosmarinus officinalis* L. and *Salvia officinalis* L. (Lamiaceae) essential oils on demographic parameters of *Habrobracon hebetor* Say (Hym.: Braconidae) on *Ephestia kuehniella* Zeller (Lep.: Pyralidae) Larvae. J Essent Oil Bear Plants 21(3):713-731.

Asadi M, Rafiee-Dastjerdi H, Nouri-Ganbalani G, Naseri B, Hassanpour M (2018b) The effects of plant essential oils on the functional response of *Habrobracon hebetor* Say (Hymenoptera: Braconidae) to its host. ISJ 15:169-182.

Banks JE, Stark JD (1998) What is ecotoxicology? An ad-hoc grab bag or an interdisciplinary science? Integr Bio1 (5):195-204.

Bakkali F, Averbeck S, Averbeck D, Idomar M (2008) Biological effects of essential oils. Food Chem Toxic 46:446-475.

Borzoui E, Naseri B, Abedi Z, Karimi-Pormehr MS (2016) Lethal and sublethal effects of essential oils from *Artemisia khorassanica* and *Vitex pseudo-negundo* against *Plodia interpunctella* (Lepidoptera: Pyralidae). Environ Entomol 45(5):1220-1226.

Carey JR (1993) Applied Demography for Biologists with Special Emphasis on Insects. Oxford University Press, New York.

Croft BA (1990) Arthropod Biological Control Agents and Pesticides. John Wiley and Sons, New York.

Dent D (1995) Integrated Pest Management. Chapman and Hall, London.

Desneux N, Decourtye A, Delpuech JM (2007) The sublethal effects of pesticides on beneficial arthropods. Annu Rev Entomol 52:81-106.

Forbes VE, Calow P (1999) Is the per capita rate of increase a good measurement of population level-effect of in ecotoxicology? Environ Toxic Chem 18:1544-1556.

Gerling D (1971) Occurrence, abundance and efficiency of some local parasitoids attacking *Spodoptera littoralis* (Lepidoptera: Noctuidae) in selected cotton fields in Israel. Ann Entomol Soc Am 64:492-499.

Hamedi N, Fathipour Y, Saber M (2010) Sublethal effects of fenpyroximate on life table parameters of the predatory mite *Phytoseius plumifer*. BioControl 55:271-278.

Hamedi N, Fathipour Y, Saber M (2011) Sublethal effects of abamectin on the biological performance of the predatory mite, *Phytoseius plumifer* (Canestrini & Fanzago) (Acari: Phytoseiidae). Exper Appl Acar 53:29-40.

Hashemi Z, Goldansaz H, Hosseini-Naveh V (2014) Effects of essential oil of *Ferula assafoetida* L. on biological parameters of the parasitoid wasp, *Habrobracon hebetor* (Hym.: Braconidae) under laboratory conditions. Proceedings 21th Iranian Plant Protection Congress, 9-13 September, University of Urmia, Iran.

Isman MB (2000) Plant essential oils for pest and disease management. Crop Prot 19:603-608.

Isman MB, Wilson JA, Bradbury F (2008) Insecticidal activities of commercial rosemary oils (*Rosmarinus officinalis*) against larvae of *Pseudaletia unipunctata* and *Trichoplusia ni* in relation to their chemical compositions. Pharma Biol 46(1-2):82-87.

Kramer S, Gvozdic V (2016) Field studies of the efficacy of some commercially available essential oils against horse flies (Diptera: Tabanidae). Entomol General 36(2):97-105.

Koul O, Walia S, Dhaliwal GS (2008) Essential oils as green pesticides: potential and constraints. Biopest Inter 4(1):63-84.

Magro SR, Parra JRP (2001) Biologia do ectoparasitoide *Bracon hebetor* Say (Hymenoptera: Braconidae) em sete especies de lepidopteros. Sci Agr 58:693-698.

Mahdavi V (2013) Residual toxicity of some pesticides on the larval ectoparasitoid *Habrobracon hebetor* Say (Hymenoptera: Braconidae). J Plant Prot Res 53:27-32.

Mahmoudvand M, Abbasipour H, Basij M, Hosseinpour MH, Rastegar F, Nasiri MB (2011) Fumigant toxicity of some essential oils on adults of some stored-products pests. Chil J Agric Res 71(1):83-89.

Maia AHN, Alferdo JBL, Campanhola C (2000) Statistical inference on associated fecundity life table parameters using jackknife technique: computational aspects. J Econ Entomol 93:511-518.

Manzoor F, Nasim G, Saif S, Malik SA (2011) Effect of ethanolic plant extracts on three storage green pests of economic importance. Pakistan J Biotech 43(6):2941-2946.

Meyer JS, Ingersoll CG, Mac Donald LL, Boyce MS (1986) Estimating uncertainty in population growth: jackknifes vs. bootstrap techniques. Ecol 67:1156-1166.

Motazedian N, Ravan S, Bandani AR (2012) Toxicity and repellency effects of three essential oils against *Tetranychus urticae* Koch (Acari: Tetranychidae). J Agri Sci Tech 14:275-284.

Mwine J, Ssekyewa C, Kalanzi K, Van Damme P (2013) Evaluation of selected pesticidal plant extracts against major cabbage insect pests in the field. J Medic Plant Res 7(22):1580-1586.

Navaei AN, Taghizadeh M, Javanmoghaddam H, Oskoo T, Attaran MR (2002) Proceedings of 15th Iranian Plant Protection Congress 7-11 September, Razi University, Kermanshah, Iran.

Rafiee-Dastjerdi H, Hejazi MJ, Nouri-Ganbalani G, Saber M (2008) Toxicity of some biorational and conventional insecticides to cotton bollworm, *Helicoverpa armigera* (Lepidoptera: Noctuidae) and its ectoparasitoid, *Habrobracon hebetor* Say (Hymenoptera: Braconidae). J Entomol Soc Iran 28(1):27-37.

Rafiee-Dastjerdi H, Hejazi MJ, Nouri-Ganbalani G, Saber M (2009a) Sublethal effects of some biorational and conventional insecticides on ectoparasitoid, *Habrobracon hebetor* Say (Hymenoptera: Braconidae). J Entomol Soc Iran 6(2):82-89.

Rafiee-Dastjerdi H, Hejazi MJ, Nouri-Ganbalani G, Saber M (2009b) Effects of some insecticides on functional response of ectoparasitoid, *Habrobracon hebetor* Say (Hymenoptera: Braconidae). J Entomol Soc Iran 6(3):161-166.

Rafiee-Dastjerdi H, Khorrami F, Razmjou J, Esmaielpour B, Golizadeh A, Hassanpour M (2013) The efficacy of some medicinal plant extracts and essential oils against potato tuber moth, *Phthorimaea operculella* (Zeller) (Lepidoptera: Gelechiidae). J Crop Prot 2(1):93-99.

Razmjou J, Mahdavi V, Rafiee-Dastjerdi H, Farhoomand A, Molapour S (2018) Insecticidal activities of some essential oils against larval ectoparasitoid, *Habrobracon hebetor* Say (Hymenoptera: Braconidae). J Crop Prot 7(2):151-159.

Sagheer M, Hassan M, Najam-ul-Hassan M, Farhan M, Ahmad Khan FZ, Rahman A (2014) Repellent effects of selected medicinal plant extracts against rust-red flour beetle, *Tribolium castaneum* (Herbst) (Coleoptera: Tenebrionidae). J Entomol Zool Stud 2(3):107-110.

Salerno G, Colazza S, Conti E (2002) Sublethal effects of deltamethrin on walking behavior and response to host kairomone of egg parasitoid, *Trissolcus basalis*. Pest Manag Sci 58:663-668.

Seyyedi A (2011) Insecticidal effects of *Ferula gummosa* L. on *Ephestia kuehniella* Zeller and its parasitoid wasp, *Habrobracon hebetor* Say. M.Sc. thesis. University of Shahed, Tehran, Iran.

Shiva Parsia A, Valizadegan O (2015) Fumigant toxicity and repellent effect of three Iranian eucalyptus species against the lesser grain beetle, *Rhyzopertha dominica* (F.) (Col.: Bostrychidae). J Entomol Zool Stud 3(2):198-202.

Stark JD, Wennergren U (1995) Can population effects of pesticides be predicted from demographic toxicological studies? J Econ Entomol 88:1089-1096.

Stark JD, Banks E (2003) Population level effects of pesticides and other toxicants on arthropods. Annu Rev Entomol 48:505-519.

Stark JD, Banks E, Acheampong S (2004) Estimating susceptibility of biological control agents to pesticides: influence of life history strategies and population structure. Biol Cont 29:392-398.

Stapel JO, Cortesero AM, Lewis WJ (2000) Disruptive sublethal effects of insecticides on biological control: altered foraging ability and life span of a parasitoid after feeding on extrafloral nectar of cotton treated with systemic insecticides. BioControl 17:243-249.

Walthall WK, Stark JD (1996) A comparison of acute mortality and population growth rate as endpoints of toxicological effect. Ecotoxic Environ Safe 37:45-52.

Yazdgerdian AR, Akhtar Y, Isman MB (2015) Insecticidal effects of essential oils against woolly beech aphid, *Phyllaphis fagi* (Hemiptera: Aphididae) and rice weevil, *Sitophilus oryzae* (Coleoptera: Curculionidae). J Entomol Zool Stud 3(3):265-271.

Yildirim E, Kordali S, Yazici G (2011) Insecticidal effects of essential oils of eleven plant species from Lamiaceae on *Sitophilus granarius* (L.) (Coleoptera: Curculionidae). Romani Biotech Let 16(6):6702-6709.

Youm O, Gilstrap FE (1993) Life-fertility tables of *Bracon hebetor* Say (Hymenoptera: Braconidae) reared on *Heliocheilus albipunctella* de Joannis (Lepidoptera: Noctuidae). Int J Trop Insect Sci 14(4):455-459.

Acta Biologica Szegediensis

Volume 63(1):69-81, 2018
Acta Biologica Szegediensis
http://abs.bibl.u-szeged.hu/index.php/abs
DOI:10.14232/abs.2018.1.69-81

ABSTRACTS OF UNKP CONFERENCE (14 June 2019, Szeged)

Chitosan-induced changes of immune responses in tomato plants

Zalán Czékus

Department of Plant Biology, Faculty of Science and Informatics, University of Szeged, Szeged, Hungary

Fungal cell wall-derived elicitor chitosan (CHT) is one of the most commonly-used microbe-associated molecular patterns (MAMP) to examine plant defence reactions, hence its ability to activate pattern-triggered immunity by inducing stomatal closure as well as inhibiting the opening of stomata at dawn among the first defence reactions. Plant defence responses can be different in the light and dark, but the daytime- and light-dependent effects of CHT on the stomatal movements, generation of reactive oxygen species (ROS) and photosynthetic activity in guard cells compared to the mesophyll cells remained unexplored.

Plants were treated with CHT at different times of the day. To clarify the role of light in plant defence reactions, we kept some plants under light and simultaneously in the dark following the treatment in the morning. We found that CHT not only inhibited the light-triggered stomatal opening at dawn but also induced the closure of stomata in the morning, independently of the daytime of the treatments. Production of ROS was enhanced in the morning after CHT treatments, whereas significant nitric oxide accumulation was observed only in the late light phase in the guard cells. CHT decreased the actual quantum yield of the second photosystem (F_{PSII}) and the photochemical quenching coefficient (qP) at dawn both in mesophyll- and guard cells. Moreover, increased *PR1* (*Pathogenesis-related 1*) expression was found at dawn and in the morning after the application of the elicitor, which demonstrates the induction of plant defence responses, whose light-dependence was further confirmed by the artificial-darkening experiments. Based on our results, we can conclude that the presence or absence of light has an elemental role in the regulation of plant immune responses in case of elicitor treatments.

This work was supported by the UNKP-18-3-I-SZTE-17 New National Excellence Program of the Ministry of Human Capacities and by the grant from the National Research, Development and Innovation Office of Hungary – NKFIH (NKFIH FK 124871).

Supervisors: Péter Poór, Attila Ördög
E-mail: czekus.z@bio.u-szeged.hu

Tight junction structural studies using superresolution microscopy

Attila E. Farkas[1,2], János Haskó[2], István Krizbai[2]

[1]Department of Physiology, Anatomy and Neuroscience, Faculty of Science and Informatics, University of Szeged, Szeged, [2]Hungary Institute of Biophysics, Biological Research Centre of the Hungarian Academy of Sciences, Szeged, Hungary

The neurovascular unit is responsible for maintaining brain homeostasis and therefore neuronal function. This is provided by the concerted function of the endothelial and glia cells, pericytes and neurons constituting the NVU. One of the main tasks of the NVU is controlling the transport of solutes between the blood circulation and the brain parenchyma. This is achieved by the blood-brain barrier that on one hand blocks paracellular transport via the continuous tight junctions that very tightly connect adjacent brain endothelial cells and on the other hand by strictly regulating transcellular transport through numerous transporter proteins and by keeping pinocytosis and transcytosis at a low level. The main proteins of tight junctions are claudins that polymerize to form strands making an intricate net interconnecting the plasma membranes of adjacent cells.

The structure and composition of the tight junction exhibits changes in pathologies such as inflammation, brain injury and neurological disorders. Changes of tight junction structure and composition cause changes in barrier permeability often exacerbating diseases and causing oedema.

Based on freeze fracture electron microscopy, the grid size of the claudin net is too small to resolve by conventional microscopy but with superresolution microscopy it is achievable.

We studied the tight junction structure of brain endothelial cells - that is mainly constituted by claudin 5 - *in vitro* and e*x vivo* using superresolution STED microscopy. As tight junctions are universal in all endothelia and epithelia, we compared brain endothelial and intestinal tight junctions. We also developed methods to image the tight junction structure in the lateral

Volume 63(1):69-81, 2019
Acta Biologica Szegediensis
http://abs.bibl.u-szeged.hu/index.php/abs

DOI:10.14232/abs.2019.1.69-81

membrane of cells.

Supported by the New National Excellence Program of the Ministry of Human Capacities (UNKP-18-4-SZTE-90).

E-mail: farkas.attilae@brc.mta.hu

New therapeutic targets - Investigation of autophagy induction role of *Neosartorya fischeri* antifungal protein (NFAP) in the native producer

László Galgóczy

Institute of Plant Biology, Biological Research Centre of the Hungarian Academy of Sciences, Szeged, Hungary
Department of Microbiology, Faculty of Science and Informatics, University of Szeged, Szeged, Hungary

Neosartorya fischeri NRRL 181 is able to produce a small, cysteine-rich, cationic antifungal protein, the NFAP with anti-mould activity. NFAP did not show toxic effect on mammalian cell lines (keratinocytes, intestinal epithelial cells, and leukocytes) suggesting specific fungal target(s) in its mode of action. Based on this, NFAP is a promising candidate as new antifungal compound. One of the limiting factors of its applicability as medical drugs is the poor pharmacokinetic property. However, extra- or intracellular targets of NFAP in sensitive-fungal strains or the native producer could be considered as bases to develop new antifungal compounds. The present work was aimed to investigate the antifungal effect, uptake and localisation of NFAP in *N. fischeri* NRRL 181; furthermore, to isolate its potential intracellular targets from this fungus for deducing its potential biological role.

Depending on the applied concentration, NFAP showed growth inhibitory activity itself on the native producer *N. fischeri* NRRL 181 *in vitro*, and evoked morphological aberrations of germlings and hyphae. Localization studies using a green fluorophore-labelled NFAP demonstrated that it is able to bind to the outer layers of *N. fische*ri NRRL 181 conidia and ascomata to exert these effect; and when these asexual reproductive spores start to form germ tube, NFAP enters in the cell and causes cell death. Target-screening experiments in *N. fischeri* NRRL 181 using the Random Oligopeptide Phage Display System (New England Biolabs) signed that NFAP possibly interacts with a regulatory factor of the autophagy induction (ATG11) in connected with programmed cell death during nutrient depletion. Our results suggest that ATG11 is a potential NFAP-specific target, and NFAP can induce autophagy in the native producer by specific binding to it. Far-Western blot analysis is in progress to confirm this finding.

Research of LG has been supported by the János Bolyai Research Scholarship of the Hungarian Academy of Sciences. Present work of LG was supported by the UNKP-18-4-SZTE-25 New National Excellence Program of the Ministry of Human Capacities.

E-mail: galgoczi@bio.u-szeged.hu

Size-dependent activity of silver nanoparticles on the morphological switch of *Candida albicans*

Nóra Igaz

Department of Biochemistry and Molecular Biology, Faculty of Science and Informatics, University of Szeged, Szeged, Hungary

Candida albicans is one of the most common opportunistic pathogenic fungi causing invasive infections especially in immune compromised patients. Several factors influence the pathogenicity of the opportunistic pathogens, among them secreted enzymes, heat tolerance, toxin production as well as dimorphic growth. During the dimorphic switch the yeast forms convert into virulent hyphae, which promote the adhesion and invasion of the fungal cells and the development of biofilm. In the biofilms the cells are surrounded by extracellular matrix, which protects them from antifungal agents, thus the surviving biofilm-resident cells are intrinsic sources of recurrent infections.

Silver nanoparticles (AgNPs) are the most frequently used metal nanoparticles due to their antibacterial, antiviral and antifungal activity. The toxic effect of AgNPs are caused by the intracellular release of silver ions, which leads to the generation of reactive oxygen species resulting in mitochondrial disfunction and apoptosis. Nevertheless, the efficacy of the applied AgNPs might largely depend on their size, shape and surface charge. Although the antifungal activity of AgNPs has already been proven

DOI:10.14232/abs.2018.1.69-81

on numerous species, the impact of nanoparticle size on the morphological switch of dimorphic fungi has not been investigated yet. To examine the size-dependent activity of AgNPs on the morphological switch of *Candida albicans,* citrate-coated nanoparticles of 7, 21 and 50 nm average size were synthesized by chemical reduction method. The effect on the hyphae formation and the biofilm production of *C. albicans* was detected on fungal monocultures, and on co-cultures using human keratinocytes. The yeast-to-hyphae conversion was completely inhibited by 24-hour exposure to small sized nanoparticles (AgNP-I). When fungal cells were treated with medium sized AgNPs (AgNP-II) and with large particles (AgNP-III), both yeast and elongated cellforms of *C. albicans* were observed. Biofilm formation was not detected upon AgNP treatments after 72 hour incubation. Moreover, AgNP-I reduced the number of elongated *C. albicans* cells co-cultured with HaCaT cells to a greater extent than AgNP-II, while AgNP-III did not affect the hyphae formation of the *C. albicans* compared to the control.

In summary, the smallest AgNPs were the most effective in inhibiting biofilm production of *C. albicans* in monoculture and in co-culture with keratinocytes, respectively. The medium sized AgNPs were also efficient, but the biggest AgNPs did not influence the morphological switch of *C. albicans* co-cultured with keratinocytes. These results suggest a size-dependent impact of AgNPs on the morphological conversion of opportunistic pathogenic fungi.

Supported by the New National Excellence Program of the Ministry of Human Capacities (UNKP-18-3-I-SZTE-42) and by GINOP 2.3.2-15-2016-00035.

Supervisor: Dr. Csontné Dr. Kiricsi Mónika
E-mail: noraigaz@gmail.com

Minimising the risks related to resistance evolution to therapeutic antimicrobial peptides

Balint Kintses

Synthetic and Systems Biology Unit, Institute of Biochemistry, Biological Research Centre of the Hungarian Academy of Sciences, Szeged, Hungary
Department of Biochemistry and Molecular Biology, Faculty of Science and Informatics, University of Szeged, Szeged, Hungary

Antimicrobial peptides (AMPs) are key effectors of the innate immune system and promising therapeutic agents. Yet, knowledge on how to design resistance-proof AMPs with minimal cross-resistance to human host-defense peptides remains limited. Here, we systematically assessed resistance evolution of *Escherichia coli* against a large set of different AMPs by applying metagenomics, chemical-genetics, and adaptive laboratory evolution. Although generalizations about AMP resistance are common in the literature, in general, we found that *E. coli's* capacity to evolve resistance to AMPs with different physicochemical properties and cellular targets varies considerably. The modes of action of the AMPs also influence the cross-resistance to human host AMPs. A special group of AMPs emerged with lower potential to induce resistance by horizontal gene transfer or genomic mutations. Our work can inform future efforts on how to minimize cross-resistance between therapeutic and human host AMPs.

Supported by the New National Excellence Program of the Ministry of Human Capacities (UNKP-18-4-SZTE-83).

Supervisor: Csaba Pál
E-mail: kintses.balint@brc.mta.hu

Biocontrol agents from field-to-lab and lab-to-field: genus *Trichoderma* in the spotlight

László Kredics

Department of Microbiology, Faculty of Science and Informatics, University of Szeged, Szeged, Hungary

The filamentous fungal genus *Trichoderma* is a popular subject of basic and applied mycology research, which is due to the fact, that *Trichoderma* species play important roles in various agricultural environments. Several members of the genus have the potential to biologically control plant pathogenic fungi and nematodes by antagonistic action based on efficient competition, antibiosis and/or mycoparasitism. The ability of certain *Trichoderma* species to promote plant growth and induce systemic

Volume 63(1):69-81, 2019
Acta Biologica Szegediensis
http://abs.bibl.u-szeged.hu/index.php/abs

DOI:10.14232/abs.2019.1.69-81

resistance in plants can also be exploited within the frames of environmentally friendly agricultural practices.

The first step of the development of biocontrol means based on *Trichoderma* is generally the isolation of *Trichoderma* strains from agricultural soil samples derived from the fields of the crop plants to be protected. Isolated strains are screened in the laboratory for their antagonistic abilities towards the target pathogens, and properly characterized to select potential biocontrol agents (BCAs). The species-level identification of the selected BCA candidate *Trichoderma* strains by sequence-based molecular tools is a crucial step of the process, as besides the positive implications of the genus in biocontrol, certain *Trichoderma* species may be harmful as the causal agents of green mould infections affecting cultivated mushrooms, while others are able to cause opportunistic infections in humans. An exact and reliable identification of BCA candidates enables to avoid the development of potentially harmful members of the genus to biocontrol products, thus lowering the risks of *Trichoderma* biocontrol. Strain improvement by mutagenesis, protoplast fusion or genetic transformation can be performed to enhance the beneficial properties of the selected *Trichoderma* strains, however, the improvement by genetic manipulation may restrict the applicability of the resulting BCAs in several countries with strict GMO regulations. Subsequent steps are optimization of fermentation for the selected BCA and selection of the proper formulation and delivery. If the beneficial effects of the BCA candidate can be confirmed by greenhouse and field trials, registration and commercialization can follow. The development of proper, specific monitoring tools for the applied *Trichoderma* strains may provide important information about their population dynamics and performance in various agricultural systems.

The research was supported by the New National Excellence Program of the Ministry of Human Capacities (UNKP-18-4-SZTE-93).

E-mail: kredics@bio.u-szeged.hu

Molecular investigation of salt tolerance development in eukaryotic green algae

Gergely Maróti

Department of Biotechnology, Faculty of Science and Informatics, University of Szeged, Szeged, Hungary
Institute of Plant Biology, Biological Research Centre of the Hungarian Academy of Sciences, Szeged, Hungary

Enhancement of algal salt accumulation was the general aim of the study. Metabolic and genomic characterization of salt tolerance as well as the identification of novel efficient salt metabolizing eukaryotic green algae strains were the major tasks of this project. We have also tested the possibilities of experimental evolution of salt tolerance in selected green algal species. As a first step the biomass potential of a series of algal species in our collection was assessed under low salt conditions. Also, new algae isolates were recovered and purified from specific environments with high NaCl conditions (special soils and ponds). Biomass potential and initial salt tolerance were determined for the novel isolates as well.

Algae are thriving in complex communities in nature, they are in permanent interactions (mutualistic, neutral and parasitic) with a number of other microorganism, mostly with bacteria. Thus, we were interested in the effect of selected bacterial partners on the algal salt accumulation performance. We have tested the effects of natural bacterial partners and also designed fully synthetic algal-bacterial consortia. We have continuously monitored the algal and bacterial living cell number, morphology and photosynthetic efficiency. The salt accumulation performance of the algae was determined in selected stages of the adaptation process, salt tolerance of axenic algae was compared to algae associated with bacterial partners. Significant increase in salt tolerance was observed for certain algae strains (*Chlamydomonas reinhardtii* cc124 and *Chlorella* sp. MACC360). We suggest, that salt adaptation may occur through various ways as indicated by the highly different morphological changes of the applied algae strains. In order to get a better understanding of the underlying molecular changes, genome-level experiments were initiated, the whole transcriptome of the ancestor and adapted algae strains are under investigation either under axenic and bacterial associated conditions. The possible mutations (SNPs, deletions and insertions) will also be investigated beside the gene expression profiles.

Supported by the New National Excellence Program of the Ministry of Human Capacities (UNKP-18-4-SZTE-94).

E-mail: maroti.gergly@brc.mta.hu

Volume 63(1):69-81, 2018
Acta Biologica Szegediensis
http://abs.bibl.u-szeged.hu/index.php/abs

DOI:10.14232/abs.2018.1.69-81

Examination of the effects of zinc oxide nanoparticles on plants using proteomics

Árpád Molnár

Department of Plant Biology, Faculty of Science and Informatics, University of Szeged, Szeged, Hungary

Zinc oxide nanoparticles (ZnO NP) have broad range of radiation absorption, high chemical, mechanical, thermal and photostability and high electrochemical coupling coefficient. These rare properties make ZnO NP useful in *e.g.*, biomedicine, agriculture. NP can be synthetized in a wide variety of 3D structures and sizes, which have an impact on their toxicity. Their effects on plant species are mostly dose-dependent, lower concentrations are proven to be beneficial, while higher concentrations are toxic. In this study the involvement of nitrosative stress in ZnO toxicity was examined.

We studied the effect of 6 nm ZnO NP on two plant species, Indian mustard (*Brassica juncea* L. Czern. cv. Negro Caballo) and rapeseed (*Brassica napus* L. cv. GK Gabriella). Plants were grown for five days on sterile ½ MS media which contained control (0), 25 mg/l or 100 mg/l ZnO NP-s. We examined plant biomass production, cell viability, enzyme activities involved in superoxide radical homeostasis and protein tyrosine nitration.

25 mg/l ZnO NP concentration was beneficial to plants, indicated by increased tolerance index and biomass production. Cell viability in the root meristem decreased slightly, with changes in enzyme activities and protein tyrosine nitration pattern. On the other hand, 100 mg/l ZnO NP-s had toxic effect on both plant species, since it reduced biomass production, tolerance index and cell viability. Protein tyrosine nitration and enzyme activities were modified compared to control. *Brassica juncea* was more tolerant to ZnO NP toxicity.

Our data suggests, that ZnO NP toxicity is in strong correlation with protein tyrosine nitration, implying the importance of future studies in this research field.

Á. Molnár was supported by UNKP-18-3-IV-SZTE-34 New National Excellence Program of the Ministry of Human Capacities.

Supervisor: Zsuzsanna Kolbert
E-mail: molnara@bio.u-szeged.hu

Developing a novel protein-tagging, immundetection and purification system

Zsuzsánna Nagy

MTA-SZBK Lendület Laboratory of Cell Cycle Regulation, Institute of Biochemistry, Biological Research Centre of the Hungarian Academy of Sciences, Szeged, Hungary
Faculty of Science and Informatics, University of Szeged, Szeged, Hungary

Over the past years our laboratory has produced several monoclonal antibodies (mAb) that specifically recognize the p54 protein, the polyubiquitin receptor subunit of the 26S proteasome. We found that anti-p54 mAb1 recognizes the C-terminal region of the protein with unusually high specificity. Preliminary results suggested that the epitope of the antibody is relatively short, hence, it can be used to generate an epitope-tagging system for protein labelling, detection or purification. Therefore, I started to map the epitope of anti-p54 mAb1 and found that an 8-mer sequence localized in the C-terminus of the p54 protein serves as the epitope of anti-p54 mAb1. I aimed to compare the anti-p54 mAb1 with a commercially available immunoglobulin (anti-Flag M_2) that is widely used (however very expensive) in immunological applications due to its high specificity towards an artificial 8-mer epitope (tag) fused to the protein of interest. I did the comparison on whole cell lysates of *Drosophila* embryos or Chinese Hamster Ovary and human cells, respectively, representing different proteome complexities, using the same concentration of the two antibodies in Western-blot experiments. I found that anti-p54 mAb1 performed significantly better under the same conditions and did not produce any background at exposure when anti-Flag M_2 already generated non-specific bands. After that, I started to examine proteins, which were tagged with the anti-mAb1's 8-mer epitope on their N- or C-termini. When the 8-mer epitope was fused to either the N- or the C-terminus of the model proteins it always behaved as an immuno tag and the chimeric proteins were recognized by the anti-p54 mAb1 in Western-blot experiments. During this study I also generated plasmid vector systems in which any gene of interest can be fused to the 8-mer epitope (N- or C-terminally) and expressed in bacteria or Eukaryotic cells in a constitutive manner or under the regulation of inducible promoters. This would allow us to tag any proteins of interest with this 8-mer epitope for immuno-detection, staining or purification from bacteria to tissue culture cells.

Volume 63(1):69-81, 2019
Acta Biologica Szegediensis
http://abs.bibl.u-szeged.hu/index.php/abs

DOI:10.14232/abs.2019.1.69-81

This work was supported by grants from the Ministry of Human Capacities of Hungary (UNKP-18-2-I-SZTE-80) to ZsN, Ministry for National Economy of Hungary (GINOP-2.3.2-15-2016-00001 and GINOP-2.3.2-15-2016-00032) and Hungarian Academy of Sciences (Lendület Program Grant (LP2017-7/2017)) to ZL.

Supervisor : Zoltán Lipinszki
E-mail : zsuzsanna_nagy@yahoo.com

Nitric oxide signaling during nickel stress responses in plants

Zsuzsanna Kolbert, habil. PhD

Department of Plant Biology, Faculty of Science and Informatics, University of Szeged, Szeged, Hungary

Excess heavy metals may result in branched, shallow root systems due to primary root (PR) shortening and concomitant lateral root induction (LR). Although, nickel (Ni) can be a relevant environmental contaminant, its relationship with these special root morphological responses is largely unknown. Also, the putative involvement of nitric oxide (NO) signalling in plant nickel stress requires further research. Therefore, in the third year of my HAS János Bolyai Research Scholarship (2016-2019), I am currently studying the nickel stress-induced root system alterations with special attention to NO signalling. In connection with this research program, my goal was to disseminate the scientific topic and the experimental results.

Wide concentration-range (0, 25, 50, 75, 100 μM) nickel chloride treatments were applied to *Arabidopsis thaliana* L. (Col-0) and *Brassica juncea* L. Czern. (cv. Negro Caballo) and 50 μM Ni proved to induce altered root morphology (shorter PR and increased number of LRs compared to control). Moreover, the greater Ni tolerance of *B. juncea* was associated with smaller Ni-induced changes in its nitroproteome, as well as in the amount of S-nitrosoglutathione enzyme and in NO, hydrogen sulphide and reactive oxygen species levels.

These results were presented in the frame of a course (title: *Reactive nitrogen- and oxygen species in plants*) which is attended by both Biology Bsc. students and Biology Msc. students. Moreover, a poster (title: *Nitrosative stress in nickel-exposed Arabidopsis and Brassica*) will be presented at Straub Days organized by HAS Biological Research Centre in Szeged. I dealt with the topic in two seminar lectures. Additionally, two Bsc. theses were prepared (Kitti Sándor, Bsc.: Essentiality and toxicity of nickel in plants and Olivér Gaál, Bsc.: Nickel phytoremediation). Collectively, the dissemination of my research topic and experimental results has been realized by integrating them in university education and in research training, by presenting them to scientific community and by promoting them to a wider social circle (Researchers' Night 2018, Facebook page).

Supported by UNKP-18-4-SZTE-55 New National Excellence Program of the Ministry of Human Capacities.

E-mail: kolzsu@bio.u-szeged.hu

Investigation of nanoparticle-endothelial cell interactions in a microfluidic chip model of the blood-brain barrier

Gergő Porkoláb

Institute of Biophysics, Biological Research Centre of the Hungarian Academy of Sciences, Szeged, Hungary
Faculty of Science and Informatics, University of Szeged, Szeged, Hungary

The blood-brain barrier is a dynamic interface composed of brain microvascular endothelial cells that restrict the brain penetration of most neurotherapeutics. Thus, central nervous system diseases are especially challenging to treat pharmaceutically.

Our research group has been developing a novel and versatile microdevice, which enables the co-culture of two or three cell types, the flow of the culture medium, visualization of the cells by microscopy, monitoring of the transcellular electrical resistance and the measurement of monolayer permeability. Our integrated lab-on-a-chip device is suitable for modeling the blood-brain barrier and mimicking the cerebral blood flow. The aim of this study was to optimize this chip device developed in our laboratory for drug delivery experiments and to test the effect of fluid flow on nanoparticle-endothelial cell interactions.

hCMEC/D3 human cerebral microvascular endothelial cell monolayers were cultured in the device under static and dynamic flow conditions. The growth of cells and the integrity of the layer was monitored by phase contrast microscopy and

DOI:10.14232/abs.2018.1.69-81

transendothelial electrical resistance (TEER) measurements. Liposomes loaded with rhodamine B were prepared and tested for permeability across hCMEC/D3 monolayers. Cellular uptake of liposome-loaded rhodamine B in endothelial cells was also visualized by fluorescence microscopy.

We have successfully optimized our chip device for drug delivery experiments and showed that dynamic fluid flow plays an important role in the permeability and cellular uptake of the nanoparticle cargo. Our results indicate that the utilization of microfluidic chip devices could be an important step in drug delivery research.

The research was supported by the New National Excellence Program of the Ministry of Human Capacities (UNKP-18-2-II-SZTE-25).

Supervisors: Mária A. Deli, Szilvia Veszelka
E-mail: porkolab.gergo96@gmail.com

The role of autophagy in the regulation of axon degeneration during aging

Áron Szabó

Institute of Genetics, Biological Research Centre of the Hungarian Academy of Sciences, Szeged, Hungary
Department of Biochemistry and Molecular Biology, Faculty of Science and Informatics, University of Szeged, Szeged, Hungary

Structural integrity of neuronal processes is maintained by finely tuned protein degradation programmes. Macroautophagy is a compartmentalized form of both bulk degradation of cytoplasmic components and selective elimination of proteins and organelles. Autophagy is indispensable for the maintenance of normal cellular homeostasis and is especially active in the nervous system. During selective autophagy, selective autophagy receptors such as p62/Ref(2)P recognize several ubiquitin chain types on proteins followed by binding of the receptors to LC3/Atg8a that mediates the degradation of the whole complex. Loss of core autophagy genes in the mouse nervous system results in shortened lifespan, motor and behavioural problems due to apoptotic cell death and brain atrophy. Axon terminal dystrophy is also observed in these mice. We hypothesized that in the *Drosophila* wing nerve, late-onset axon degeneration could be induced by lack of proper autophagic processes. We knocked out or specifically downregulated in neurons core components of the autophagic machinery and examined aged animals. We found that while in young autophagy-deficient flies no change in axon structure could be observed, aged animals, earliest at 30 but mostly at 60 days of age developed axon fragmentation and loss. Currently no evidence exists concerning the death mechanisms that instruct axon destruction in lack of autophagy. To shine a light on this, we tested the role of caspases, mitochondrial oxidative stress and the injury-induced Wallerian degeneration pathway that have been implicated in diverse axon disintegration events. We found no role for caspases but curiously, overexpression of both Sod2, a mitochondrial superoxide dismutase and Wld^S, a potent inhibitor of Wallerian axon degeneration rescued axon fragmentation in *Syntaxin-17*-depleted animals. We validated our results using genetic mosaic analysis with autophagy gene null mutants and in a different axon model in the fly brain. In summary, we established a fly model for genetic dissection of late onset axon degeneration in autophagy deficiency and pinned down the downstream mechanisms mediating axon degeneration.

Supported by the New National Excellence Program of the Ministry of Human Capacities (UNKP-18-4-SZTE-98).

Supervisor: Prof. Dr. Gábor Juhász
E-mail: szabo.aron@brc.mta.hu

Investigation of immune activation and immune regulation in rodent models and human patient-derived blood

Gábor J. Szebeni

Department of Physiology, Anatomy and Neuroscience, Faculty of Science and Informatics, University of Szeged, Szeged, Hungary

The immune system is highly plastic owing to the complexity of cellular fates to execute the versatile polarization of lymphoid and myeloid cells. The activation and polarization evolve from the interactions in the network of immune cells with the surrounding soluble or anchored signals. The evolutionary advantage of this versatile polarization is the elimination of

Volume 63(1):69-81, 2019
Acta Biologica Szegediensis
http://abs.bibl.u-szeged.hu/index.php/abs

DOI:10.14232/abs.2019.1.69-81

pathogenic invaders and cancerous cells. However, due to genetic and environmental factors the polarization of leukocytes may be influenced and disturbed to render the immune system overwhelming or ineffective against pathologies.

To achieve high resolution measurement of cellular features, single cell mass cytometry has been used in our laboratory combining advantages of the single cell resolution of traditional fluorescence-based flow cytometry with the multiplexicity of inductively coupled plasma-mass cytometry. Instead of fluorophores detection for mass cytometry is based on stable heavy-metal isotope labeled antibodies. Thus, the autofluorescence and spectral overlapping are eliminated. This unique feature enables researchers to multiplex up to 45 different antibodies in one single tube. PBMCs of human systemic autoimmune diseases (RA, SLE, SSc), rat model of colitis and non-small cell lung cancer patients have been investigated by different antibody panels using mass cytometry. Plasma proteome profiling is also carried-out by Luminex and Legendplex technologies. Large data sets, disease associated patterns of cellular and plasma protein markers have been analyzed.

The combination of the analysis of cytokine production with the complex view of the heterogeneity of PBMCs at single cell resolution could potentially reveal novel pathways to identify therapeutic targets.

The research was supported by the New National Excellence Program of the Ministry of Human Capacities (UNKP-18-4-SZTE-73).

E-mail: szebeni.gabor@brc.mta.hu

Analysis of genes encoding possible spore coat-like proteins in opportunistic human pathogenic fungi

Csilla Szebenyi

Department of Microbiology, Faculty of Science and Informatics, University of Szeged, Szeged, Hungary
MTA-SZTE "Lendület" Fungal Pathogenicity Mechanisms Research Group, Közép fasor 52., H-6726 Szeged, Hungary

Members of the order Mucorales can be agents of life-threatening, opportunistic human infections, known as mucormycosis. Because of the devastating outcome of this disease, which has been observed despite the current treatment options, it is urgent to identify the possible virulence factors. It was previously shown that the spore coat CotH proteins played an important role in the pathogenesis of Mucorales, hence arise the main objective of our study to determinate the possible role of CotH5 protein in the pathogenesis of *M. circinelloides*.

In this experimental setup, a linearized deletion cassette was used along with the Cas9 enzyme and the gRNA complex for direct transfer without *in vitro* RNP formation and the use of plasmids to disrupt the *cotH5* gene in a homology directed repair mechanism. This approach resulted in stable transformants, in which gene disruption occurred by the integration of the selection marker at the expected position. The mutation was proven by PCR analysis and the lack of the appropriate transcripts was proven by qRT-PCR. Phenotypic characterization of mutant was performed and the possible role of the protein in the process of phagocytoses was also analyzed. We identified the CotH5 protein as a possible spore coat-like protein based on its amino acid sequence. Construction of strains, in which the *cotH5* gene is disrupted or overexpressed can provide a good tool to investigate its relevance in the pathogenicity and other biological mechanisms. Based on the results we think that the CotH5 protein may have a role in the sporulation of the fungus.

The study was supported by the grants UNKP-18-3-I-SZTE-89 New National Excellence Program of The Ministry of Human Capacities, LP2016-8/2016 and GINOP-2.3.2-15-2016-00035.

Supervisors: Tamás Papp, Gábor Nagy
E-mail: szebecsilla@gmail.com

Volume 63(1):69-81, 2018
Acta Biologica Szegediensis
http://abs.bibl.u-szeged.hu/index.php/abs

DOI:10.14232/abs.2018.1.69-81

Examining the efficiency of exercises aiming the development of oral health literacy and critical thinking

Ádám Szivós

Biology Methodology Group, Department of Physiology, Anatomy and Neuroscience, Faculty of Science and Informatics, University of Szeged, Szeged, Hungary

In our previous research, we examined the brushing habits of secondary school and university students and experienced that the ratio was high of those in both sample, who has problems with the evaluation and application of information. The development of oral health literacy may be connected to the development of critical thinking since the evaluation as a cognitive operation is a common feature of these two areas. The aim of our present research is to examine the efficiency of exercises aiming the development of oral health literacy and critical thinking in classrooms.

We tried two exercises in our research: one of them was an interview with false information in which they had to find the mistakes ("Interview with a dentist") and another was an article with questions ("Which brushing method is the best?"). After that, the students filled out a questionnaire about their motivation and the efficiency of the exercises.

According to 83.34% of the students (n=54, 35.2% of them female, 64.8% of them male) they could solve the tasks individually, and 90.74% of them could interpret the read text critically. Only 22.22% of the answering students agreed completely that the tasks demanded from them to apply their previous studies of health literacy taught in Biology classes. The 83.33% of the participants like reading in topics related to their health, and 74.07% likes critical thinking. Most of the students could not tell why plaque is dangerous, and they could not evaluate the significance of fluorides properly.

The results highlighted that students require to be concerned with the development of oral health literacy and critical thinking in classrooms. We set ourselves the target to develop more exercises in continuing our research.

Supported by the New National Excellence Program of the Ministry of Human Capacities (UNKP-18-2-I-SZTE-111).

Supervisor: Lászlóné Nagy Dr.
E-mail: szivosadam@gmail.com

Development and characterization of microbial lipase systems for industrial applications

Miklós Takó

Department of Microbiology, Faculty of Science and Informatics, University of Szeged, Szeged, Hungary

Lipases catalyze lipolytic reactions in which they release free fatty acids, diacylglycerols, monoacylglycerols and glycerol. Under certain conditions, lipases can synthesize lipid compounds through the catalysis of esterification processes. As a result of the above reactions, functional lipids, *i.e.* polyunsaturated fatty acids and alkyl esters, potentially applicable in different industries can be produced. Therefore, there is a need for identification of new lipases, and analysis of the background of reactions in specific conditions relevant for their practical application. With experiments from our laboratory a number of producer strains and enzymes have been characterized from the zygomycetes fungal group. Using these biocatalysts, and other enzymes from microbial sources, our aim was to develop and characterize lipase systems utilizable for future production of bioactive lipids. In line with this, immobilization and regiospecificity studies, as well as assays on lipases' hydrolytic potential against oils from various vegetable and animal sources were also planned.

For the investigations we selected the *Mortierella echinosphaera* and *Mucor corticolus* lipases that have been purified by our group prior to this assay. In addition, commercial forms of *Aspergillus niger*, *Rhizopus oryzae*, *Rhizopus niveus* and *Rhizomucor miehei* lipases were also included to the studies. In summary, the lipases of *M. echinosphaera*, *M. corticolus* and *R. oryzae* were successfully immobilized onto the polypropylene Accurel MP1000 carrier. The immobilized enzymes have shown great efficiency in catalysis of lipolytic reactions, and they exhibited improved biochemical properties, *e.g.*, storage and temperature stability, compared to the free enzymes. Moreover, the enzyme-support complexes proved to be reusable in several reaction cycles as well. Concerning regiospecificity, the studied enzymes exhibited different properties that affect (with potential) their hydrolytic behavior against oils substances. Finally, in a pilot experiment, a comparative analysis has also been initiated in which we examine the hydrolytic activity of selected lipases on vegetable and menhaden fish oils using a simple and fast chromogenic

Volume 63(1):69-81, 2019
Acta Biologica Szegediensis
http://abs.bibl.u-szeged.hu/index.php/abs

DOI:10.14232/abs.2019.1.69-81

test. Results so far showed high variability in the oil degradation potential of the catalysts tested.

The research was supported by the New National Excellence Program of the Ministry of Human Capacities (UNKP-18-4-SZTE-74).

E-mail: tako78@bio.u-szeged.hu

Interaction of neutrophil granulocytes with *Curvularia lunata*

Eszter Judit Tóth

Department of Microbiology, Faculty of Science and Informatics, University of Szeged, Szeged, Hungary
MTA-SZTE "Lendület" Fungal Pathogenicity Mechanisms Research Group, Szeged, Hungary

Emerging fungal pathogens, like *Curvularia lunata* represent a continuously increasing problem, because of the growing population with underlying conditions, the difficulties of diagnosis and the high antifungal resistance of certain fungal agents. This filamentous fungus is known as a trans-kingdom pathogen, which is able to cause infection both in plants and humans. The mycoses in humans can manifest as fungal keratitis, sinusitis, cutaneous lesions or invasive infections, depending on the immune status of the host. The aim of this study was to investigate the neutrophil response to hyphal form of *Curvularia lunata* and expose the fungal defence mechanisms.

In the present study, *C. lunata* SZMC 23759 and *A. fumigatus* SZMC 23245, both isolated from human eye infection were examined. Activation of neutrophils was measured in the presence and the absence of the supernatant of germinating conidia and after serum treatment. Effector mechanisms of the immune cells focused on oxidative burst and NET formation was studied. Melanin production and extracellular acidification by *C. lunata* was also analysed as a potential defence action of the fungus.

This research was supported by the grants „Lendület" LP2016-8/2016 and GINOP-2.3.2-15-2016-00035. EJT was granted by the UNKP-18-3-III-SZTE-28 New National Excellence Program of the Ministry of Human Capacities.

Supervisors: Dr. Tamás Papp, Dr. Csaba Vágvölgyi
E-mail: scedobipo@gmail.com

Cell division of microalgae investigated by protein derivatives

Bettina Ughy

Department of Biotechnology, Faculty of Science and Informatics, University of Szeged, Szeged, Hungary
Biological Research Centre of the Hungarian Academy of Sciences, Szeged, Hungary

Cell division is the most important process of living organisms. Bacterial cell division has been studied intensively for decades, but many fundamental questions remain unanswered. Cyanobacteria, which belong to microalgae, are biotechnologically important, photosynthetic Gram negative bacteria, the ancestors of plant plastids. Understanding the mechanisms of the bacterial cell division can lead to the development of new antibiotics, to biotechnology, and furthermore to the understanding of plant plastids development, division. In prokaryotes, and in the eukaryotic cell organelle plastids and mitochondria a tubulin homologue GTPase protein, the FtsZ initiates the cell division by the polymerization into a ring-like structure (Z-ring) at midcell. The Z-ring subsequently functions as a scaffold for recruitment of downstream factors that promotes the formation of the division septum. The positioning and timing of the Z-ring is crucial for the cells. It is believed that bacteria generally divide by binary fission producing two identical daughter cells, although in some cases asymmetrical division was also observed. Following the development of the division ring is possible by fluorescent microscopic techniques, when the FtsZ protein is fused with *e.g.*, green fluorescent protein (GFP). According to published information, the FtsZ-GFP chimeric gene cannot be completely segregated from the endogenous *ftsZ* gene, because the FtsZ-GFP chimera cannot form complete division rings without wild-type FtsZ (Buske PJ et al. 2015; Ma X et al. 1996). This might indicate that the presence of GFP can disturb the ring formation. At the same time the presence of chimera can cause alteration in the cell size influencing the proliferation time (Quin S et al. 1998). We have created new FtsZ-GFP chimeras in *Synechococcus* sp. PCC7942 cells with different linker between GFP and FtsZ to avoid possible interferences with the potential interactors. The reporter molecule made

DOI:10.14232/abs.2018.1.69-81

the FtsZ ring be visualized. The constructs allow us to examine the FtsZ protein interactions and to study the influence of the environmental factors on cell division.

The research was supported by the New National Excellence Program of the Ministry of Human Capacities (UNKP-18-4-SZTE-87).

E-mail: ughy.bettina@brc.mta.hu

Evolution of long-distance resource transport in complex multicellular fungi.

Torda Varga

Synthetic and Systems Biology Unit, Institute of Biochemistry, Biological Research Centre of the Hungarian Academy of Sciences, Szeged, Hungary.

With the evolution of complex multicellular life, organisms had to circumvent the limitation of diffusion, leading to the evolution of special animal and plant cells or tissues, which facilitate long-distance nutrient transport. Fungi can produce rhizomorphs, hyphal strands and cords (here Fungal Long-distance Transport Structure, FLTS) that enable the transportation of nutrients and water, have fundamental role in plant pathogenicity (*e.g.*, *Armillaria* spp.), the functioning of common mycorrhizal networks of plant communities and exploring and degrading wood material (*e.g.*, white rot fungi). Despite of the essential biological functions and the immense importance of FLTS, we have limited knowledge of its taxonomic distribution, macro-evolution and the genetic background of its development.

Therefore, we summarised more than 5.300 literature records on FLTS and performed macro-evolutionary analyses using a published mega-phylogeny (Varga et al. 2019, Nat. Ecol. Evol.) containing 5.284 species of mushroom-forming fungi (Agaricomycetes). We found that species in the phyla Ascomycota and Basidiomycota can develop FLTS, but the most complex morphologies can be found predominantly in Agaricomycetes, a class of Basidiomycota. In addition, FLTS is typical in most of the orders of Agaricomycetes, but it is most abundant in the Agaricales and Boletales. Furthermore, ancestral character state reconstructions showed that FLTS is possibly an ancient character state and first occurred in the most recent common ancestor of Phallomycetidae and Agaricales. To reveal genes responsible for FLTS development we want to compare transcriptomic data of species from two closely related FLTS orders, the Agaricales (*Armillaria ostoyae*) and the Boletales (*Serpula lacrymans*). Transcriptomic data are available for *A. ostoyae*, but the rhizomorph and fruiting body development of *S. lacrymans* is yet to be investigated. After examining the strain S7 on 11 different nutrient agars and in 12 different conditions, we found that culturing the strain on a complex media containing $NaNO_3$, KH_2PO_4, $MgSO_4$ and $FeSO_4$ in dark at 22 °C for one month resulted 1-2 mm wide rhizomorphs. Furthermore, using the same media, but exposing the culture to a sequence of temperature conditions in dark (22 °C, 4 °C, 18 °C) could induce fruiting body development.

Supported by the New National Excellence Program of the Ministry of Human Capacities (UNKP-18-3-IV-SZTE-52).

Supervisor: László G. Nagy
E-mail: varga.torda@gmail.com

Drug delivery by nanoparticles

Szilvia Veszelka

Institute of Biophysics, Biological Research Centre of the Hungarian Academy of Sciences, Szeged, Hungary, Hungary

The major obstacle of the pharmaceutical treatment of central nervous system disorders is the blood-brain barrier, which restricts the penetration of therapeutics to the brain. Nanocarriers hold great promise for drug delivery across the blood-brain barrier, but specific targeting is needed for the succesful brain delivery of nanoparticles, which is currently unsolved. Several clinically used drugs are known to be successfully cross the brain endothelial cells via the nutrient transporter solute carriers (SLC), however this pathway is not fully exploited for drug delivery. Ligands of SLC transporters at the blood-brain barrier are promising targeting vectors to increase the brain penetration of nanoparticles. The aims of this study were (i) to examine the mRNA expression levels of SLC transporters of different cell types, (ii) to compare the uptake of targeted nanoparticles in

Volume 63(1):69-81, 2019
Acta Biologica Szegediensis
http://abs.bibl.u-szeged.hu/index.php/abs

DOI:10.14232/abs.2019.1.69-81

primary pericytes, astroglia cells and neuroblastoma cells, (iii) to verify the uptake mechanisms in different cell types.

High mRNA expression levels for hexose and neutral amino acid transporting solute carriers (SLCs) were found in isolated astroglia cells and pericytes so we prepared, characterized and tested nanoparticles from non-ionic surfactants (niosomes) functionalized with alanine, ligands of SLC-transporters and glutathione, a reference ligand as blood-brain barrier targeting molecules.

The presence of targeting ligands on niosomes, especially the dual-labeling, increased the uptake of the cargo molecule in pericytes, astrocytes and neuroblastoma cells. This cellular uptake was temperature dependent and could be decreased with a metabolic inhibitor and endocytosis blockers filipin and cytochalasin D. Our data indicate that dual-labeling of nanoparticles with glutathione and alanine, a ligand of SLC transporters can be effective for blood-brain barrier targeting.

Supported by the New National Excellence Program of the Ministry of Human Capacities (UNKP-18-4-SZTE-89).

E-mail: veszelka.szilvia@brc.mta.hu

Role of the neurovascular unit and brain environment in the formation of central nervous system metastases

Imola Wilhelm[1,2], János Haskó[2], Kinga Molnár[2], István A. Krizbai[2]

[1]Department of Physiology, Anatomy and Neuroscience, Faculty of Science and Informatics, University of Szeged, Szeged, Hungary
[2]Institute of Biophysics, Biological Research Centre of the Hungarian Academy of Sciences, Szeged, Hungary

Brain metastases are devastating complications of cancer and an unmet challenge for clinicians. Therapeutic resistance of brain tumours largely depends on unique aspects linked to the cerebral environment and the neurovascular unit. Among cells of the neurovascular unit, endothelial cells and astrocytes are the most active in immediately responding to and continuously associating with invading tumour cells.

Here we used advanced microscopy techniques – including two-photon microscopy in living animals, confocal and super-resolution (stimulated emission depletion/STED) fluorescence imaging and transmission electron microscopy – to understand the mechanisms of interactions of triple negative breast cancer cells with cerebral endothelial cells and astrocytes. We followed reaction of brain resident cells to the tumour cells during the extravasation step and the metastatic growth phase in the brain parenchyma.

We observed that mammary carcinoma cells induce up-regulation of N-cadherin in cerebral endothelial cells; however, this mechanism is dispensable for the trans-endothelial migration. Breast cancer cells are able to migrate via the transcellular pathway through the endothelium, leaving the tight junctions intact. Metastatic cells breach the end-feet layer of astrocytes that cover the outer surface of cerebral vessels and accumulate along the capillaries attached to the vascular basement membrane. This process, called vascular co-option, is the main mechanism of tumour vascularization in the brain.

In conclusion, we identified new mechanisms involved in the reaction of brain resident cells to invading breast cancer cells. Our results contribute to a better understanding of the complex cross talk between metastatic cells and brain resident cells, which is essential for the identification of future therapeutic targets.

Supported by the New National Excellence Program of the Ministry of Human Capacities (UNKP-18-4-SZTE-100).

E-mail: wilhelm.imola@brc.mta.hu

Response of keratinocytes to pathogenic and skin commensalist *Candida* species

Erik Zajta

Department of Microbiology, Faculty of Science and Informatics, University of Szeged, Szeged, Hungary

Invasive *Candida* infections are prevalent worldwide and threaten especially those with compromised immunity. Besides these severe diseases, cutaneous infections caused by *Candida* species may also develop. *C. parapsilosis* regularly colonizes the human skin as a commensalist and only seldom leads to pathological conditions there. On the contrary, *C. albicans* is not a member of the normal flora of the human skin but it is the commonest agent of cutaneous candidiasis. Keratinocytes are able to mediate

DOI:10.14232/abs.2018.1.69-81

immunological activities, yet little is known about their response to related commensalist and pathogenic yeasts.

Therefore, our goal was to examine the interaction of *C. albican*s and the less harmful *C. parapsilosis* with human skin keratinocytes.

We infected HaCaT and HPK-KER cell lines with *C. albicans* and *C. parapsilosis* strains. Damage of skin epithelial cells was monitored through lactate dehydrogenase activity in supernatants of infected keratinocytes. Cytokine release from infected skin cells was determined by enzyme-linked immunosorbent assay from cell culture supernatants. We used imaging flow cytometry to reveal association of keratinocytes with green fluorescent protein expressing strains of the two *Candida* species and also to test if pHrodo™ Red stained yeasts are ingested by keratinocytes. Recently, we have initiated a survey on the occurrence of *Candida* species on healthy skin surfaces of Hungarian volunteers.

C. albicans caused remarkable damage to keratinocytes as opposed to *C. parapsilosis*. Pre-treatment of HaCaT cells with live or heat killed *Candida parapsilosis* did not reduce cellular damage triggered by *C. albicans*. IL-8 production was induced by *C. albicans* in both cell lines and also IL-6 secretion in HPV-KER cells. Release of these cytokines was hardly affected by *C. parapsilosis*. To a low extent, cells of both *Candida* species were able to adhere to keratinocytes and we observed occasional phagocytosis of both yeasts by skin cells. To date, only two *C. parapsilosis* and no *C. albicans* strains were isolated from skin surfaces.

This project contributes to a better understanding of skin immunity to pathogenic and commensalist yeasts. It was supported by the UNKP 18-3-IV-SZTE-55 New National Excellence Program of the Ministry of Human Capacities.

Supervisor: Attila Gácser
E-mail: writetotono@gmail.com